UNIVERSITAT POLITÈCNICA DE CATALUNYA BARCELONATECH

Synthesis and characterization of plasma-treated liquids and hydrogels for bone cancer therapy

Inès Hamouda

UNIVERSITAT POLITÈCNICA DE CATALUNYA BARCELONATECH

PhD program in Material Science and Engineering

Synthesis and Characterization of Plasma-Treated Liquids and Hydrogels for Bone Cancer Therapy

PhD. Thesis by:

Inès Hamouda

Thesis Advisors:

Dr. Cristina Canal

Dr. Cédric Labay

Department of Materials Science and Engineering

Barcelona

2020

BIOMATERIALS, BIOMECHANICS & TISSUE ENGINEERING

APACHE

erc European Research Council

Synthesis and Characterization of Plasma-Treated Liquids and Hydrogels for Bone Cancer Therapy

Barcelona

2020

AGRADECIMIENTOS

En este tramo final de la gran aventura de la tesis, quiero agradecer a las personas que me siguieron y/o formaron parte de esta aventura. No quiero olvidarme de nadie, por ello antes de nada, quiero disculparme si me olvido a alguien o si algún@ se siente excluid@.

Mis más sinceros agradecimientos van a mis directores de tesis *Cristina y Cédric*. *Cristina*, gracias por darme la oportunidad de aventurarme en la tesis doctoral y guiarme en este mundo que era desconocido para mí. Gracias por tu confianza, paciencia, y consejos a lo largo de estos tres años tanto a nivel profesional como personal. *Cédric*, gracias por haber estado siempre presente cuando necesitaba ayuda en el laboratorio y a la hora de escribir artículos. Gracias por tu gran implicación, dedicación y ayuda en todos los trabajos que forman parte de esta tesis.

Por otra parte, quiero agradecer a *Maria Pau*, por acogerme en su grupo de investigación BBT desde la estancia de máster hasta la elaboración de la tesis. Además, me gustaría dar las gracias a todos los miembros del BBT. En particular a *Carles*, por tu sonrisa siempre presente y por compartir discusiones interesantes. *Marta*, por tu alegría. *Montse*, por tu ayuda en los laboratorios. *José María*, por tus chistes! *Elisa*, por tu generosidad. *José Manuel*, por tus consejos. *Daniel,* por guiarme en mí primer congreso. *Meri&Txell*, por estar siempre sonrientes y por vuestra ayuda. A todos los del Plasma Medicine, *Juan*, por tus chistes, alegría general, tu gran ayuda en el laboratorio con las células y todo con mucha fantasía! *Miguel & Xavi*, por los momentos de estrés en el laboratorio! *Francesco*, por compartir tu experiencia conmigo, implicarte y ayudarme al laboratorio, grazie mille!

Luego, quiero agradecer desde lo más profundo del corazón a *Lazhar*, por acogerme de estancia corta en su grupo de investigación PCI en Le Mans. Quiero también dar las gracias a todos los miembros del grupo PCI, por toda la confianza depositada en mi. Entre todos me habéis enseñando el rigor del trabajo en

laboratorio para hacer buena ciencia. A cada una de mis visitas me hacéis sentir como una de vosotros y eso no tiene precio. *Erwan*, sin tu apoyo incondicional todo esto no hubiese sido posible. Gracias por estar aquí, ayudarme y guiarme en este largo camino que es la investigación.

Quiero dar un toque particular a mis compañeros de doctorado y de despacho, *Joanna*, juntas desde la práctica del máster, compartiendo mesa hasta empezar juntas la aventura de la tesis. *Mar*, por los buenos momentos compartidos. *Luisito péptidos*, por la alegría que aportas al despacho. *Yago*, cuando a ti te convienen las olas sin viento, a mí me conviene el mar plano y con viento ;). *Hossein, Marcel*, *Ana*, *Sergio*, *Joaquim*, *Victor*, *Claudia* y *Diego* por vivir y compartir juntos esta aventura de la tesis. A los post-docs, *Jordi*, *Osnat*, *Laura*, *Judit* e *Irene*, por vuestra ayuda en el laboratorio y por compartir vuestras experiencias. A los de empresas, *Miquel & Mònica* por vuestras sonrisas y por estar dispuestos a ayudar. *Sandra*, por empujarme adelante con nuevos proyectos y a ver si acabamos la ruta de los helados!

También quiero agradecer a todo el equipo del centro Multi-escala, por su disponibilidad y eficacia.

Esta aventura no sería igual sin algunas personas que me hicieron salir del entorno del laboratorio y hacer que disfrutara un poco más de la vida. *Jonathan*, por tu gran apoyo, las aventuras por Barcelona, y las salidas con todo el equipo; *Osy*, *Bela*, *David&Geo*, *Tobias*, *Nicolas* y *Lucia*. *Lourdes*, por tu apoyo, tu confianza, tus consejos, y tu alegría contagiosa, me has dado fuerzas para seguir yendo adelante. *El Guapo & el pequeño del mantenimiento*, por nuestras escapadas diarias de cafés y a todos los buenos momentos compartidos juntos. Mis compañeros de piso, quienes me han soportado en casa; *Gen*, más que una hermana. *Houyem*, la única probabilidad – posible – de compartir piso con una persona de Mahdia. *Edgar&Nekane*, por hacerme sentir como en casa, por la cuarentena juntos y por las series de Netflix que me obligasteis a ver para estar al día! Mis compañer@s e entrenadoras de sincro, las del KalliPolis, las ex-Kalli, y l@s del Mediterrani: *Elena, Amelia, Pol, Alicia, Marisa, Renata, Judit, Xenia, Ana, Eva, Irene, Claudia y Maite*. Gracias por todos los momentos buenos y cañeros dentro y fuera del agua.

Clémence & Emilie, las súper amigas, allí seguimos con más aventuras. *Stephen & Kristina, Hamid, Marine*, por vuestro interés y apoyo en esta tesis. Mis amigos y familia de Mahdia (*Khalti, Leïla, Dali*, *Hamza, Faten*, *Marwa*, *Hajer, Marine*) gracias por vuestro apoyo y por seguir compartiendo buenos momentos juntos.

Finalmente, todo esto no sería posible sin *Asma*, *chrikti*, por tus consejos, tu apoyo, por siempre estar a mi lado a pesar de la distancia. *Emna & Habib*, mis segundos padres, por vuestro apoyo incondicional. Mis *padres* por apoyarme en este camino desconocido y por empujarme siempre hacia adelante y a mis hermanos favoritos *Neïla & Nebil* por soportarme y seguirme en mis aventuras.

ABSTRACT

This PhD. Thesis tallies with the Starting Grant project funded by the European Research Council (ERC) entitled "Atmospheric Pressure plAsma meets biomaterials for bone Cancer HEaling" (APACHE) and has been carried out within the Biomaterials, Biomechanics and Tissue Engineering group (BBT) at the Barcelona East School of Engineering (EEBE) of the Universitat Politècnica de Catalunya (UPC). This project falls within in the area of *Plasma Medicine*, a new branch of medical technology encompassing physics, biology, medicine and chemistry. One of the main fields of interest in *Plasma Medicine* is cancer therapy. During the last decade, the anticancer capacity of cold plasmas has been illustrated in different cancer cell lines such as breast, skin, lung, pancreas, cervix or brain and has shown ability to kill cancer cells without damaging the surrounding tissues.

This PhD. Thesis is focused on investigating potential novel vehicles of plasma-treated liquids for bone cancer with the aim to provide an alternative to the current treatments (*i.e.* surgery, chemotherapy, radiation therapy and cryosurgery) that are not completely effective.

Cold plasma sources can be used to treat liquid media, thereby generating plasma-treated liquids, which can be applied to the cancer cells afterwards. Reactive oxygen and nitrogen species are generated from cold plasmas, which have been related to the biological effects of plasmas and plasma-treated liquids. Despite the exact mechanisms are not completely described yet, the reactive species generated are thought to be the main responsible of the biological effects of plasmas. Many of the radicals generated during the discharge can contribute to complex reactions in liquids: formation of other short and long-lived species in the solution. As plasma-treated liquids will probably be washed in the body through the blood flow when injected, another option for the reactive species transport should be employed.

Given the high capacity of hydrogels to store liquids, and their proven capacity as drug delivery agents, the use of biocompatible hydrogels is studied in this PhD. Thesis as novel vehicles for plasma-generated reactive species for bone cancer treatment. This may allow avoiding invasive surgery to the patient, as

hydrogels can be used to target tumours by injection. Within this context, in this PhD. Thesis the effect of the atmospheric pressure plasma jet is investigated in liquids and hydrogels to develop novel vehicles for plasma-based therapies (Figure 1).

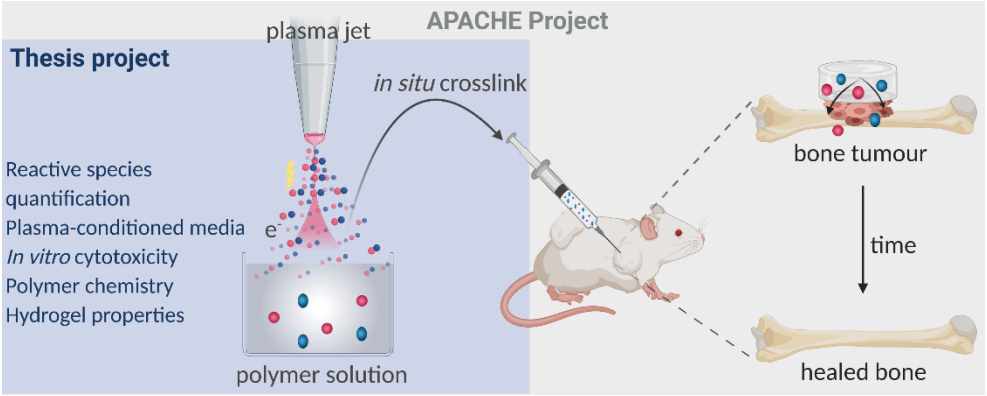

Figure 1.1: Representative scheme of the main objective of the Thesis (blue) in the framework of the ERC APACHE Project.

First, a literature review on plasma-treated polymers for biomedical applications is presented, with special emphasis on the future evolution and new possibilities arising in the treatment of polymer solutions or hydrogels by means cold plasmas for biomedical applications.

In a first experimental step, the efficiency of direct plasma treatment is compared to plasma treated or conditioned media with regard to their effects on healthy and cancer bone cells. The concentration of reactive species generated in cell culture media in different plasma treatment conditions is related to the biological effects observed.

Then, the effect of plasma treatment is carefully studied on the chemistry and physico-chemical properties of different hydrogel-forming polymers: natural (alginate), semi-synthetic (methacrylated gelatin) and synthetic (poly(oxide)ethylene based triblock copolymer) polymers. The generation, stability and release of reactive species generated in solution from plasma are discussed. This is done in different kinds of polymers with hydrogel-forming ability. The potential of polymer solutions

and hydrogels as reservoirs and vehicles of reactive species from cold plasmas are examined here.

RESUMEN

La presente tesis se enmarca dentro del proyecto europeo “Starting Grant” financiado por el Consejo Europeo de Investigación (ERC de sus siglas en inglés) titulado “Atmospheric Pressure plAsma meets biomaterials for bone Cancer HEaling” (APACHE) del grupo de investigación de Biomateriales, Biomecánica e Ingenieria de Tejidos (BBT) de la Escuela de Ingeniería de Barcelona Este (EEBE) de la Universidad Politécnica de Cataluña (UPC). Este proyecto se enmarca en el contexto del ámbito de la medicina de plasmas, una nueva área de tecnología médica que abarca física, biología, medicina y química. Uno de los principales temas de estudio en la medicina de plasmas es la terapia de cáncer. En los últimos años, la eficacia de los plasmas fríos contra el cáncer se demostró en varias líneas celulares como cáncer de mama, piel, pulmón, páncreas, cuello del útero o cerebro observando una selectividad hacia las células cancerígenas sin dañar a los tejidos circundantes.

Esta tesis está enfocada a la investigación de potenciales nuevos medios de líquidos tratados por plasma para la terapia de cáncer de hueso con el objetivo de dar una alternativa a los tratamientos actuales (*i.e.* cirugía, quimioterapia, radioterapia y crio-cirugía) que no son de todo eficaces.

Los equipos de plasmas fríos a presión atmosférica pueden usarse para el tratamiento de líquidos, generando un líquido activado por plasma, poniéndolo después en contacto con las células cancerígenas. Los plasmas fríos generados en el aire producen especies reactivas de oxígeno y nitrógeno que se han relacionado con los efectos celulares inducidos. Aunque los mecanismos involucrados no se han descrito completamente, las especies reactivas generadas son las principales responsables de los efectos biológicos provocados por plasma. Los radicales generados por plasma pueden contribuir a las complejas reacciones que tienen lugar en líquidos formando otras especies reactivas en solución de corta y larga vida. Una vez inyectados en el cuerpo, los líquidos se disiparán en la sangre, por lo que sería conveniente emplear otro tipo de vehículos para transportar las especies reactivas del plasma hasta el tumor.

Los hidrogeles presentan una gran capacidad para almacenar líquidos, y se han empleado a menudo como agentes de liberación de fármacos. Los hidrogeles se estudian en esta tesis como nuevos vehículos de especias reactivas generadas por plasma para terapia de cáncer de hueso, puesto que pueden ser inyectados y reticulados *in situ* en el paciente en el lugar de la terapia de forma mínimamente invasiva. En este contexto, en esta tesis, se investiga los efectos de los haces de plasma a presión atmosférica en líquidos e hidrogeles para desarrollar nuevos vehículos para terapias basadas en plasmas (Figura 1).

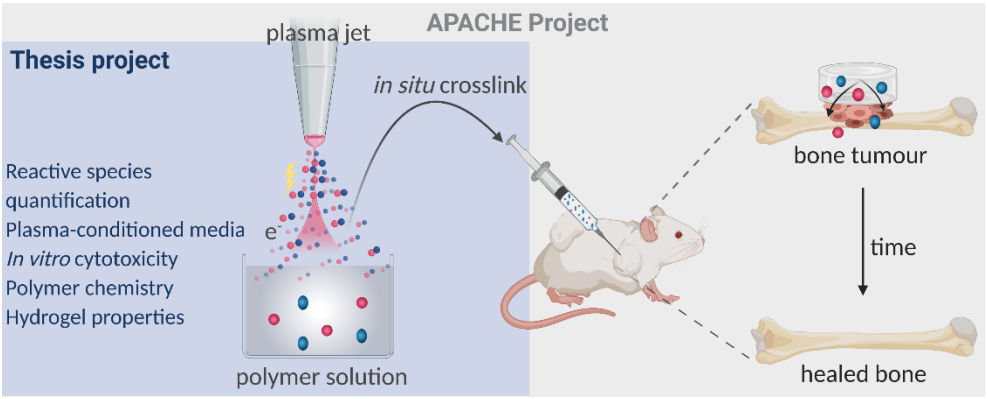

Figura 1: Representación esquemática del objetivo de la tesis (azul) dentro del proyecto ERC APACHE.

En esta Tesis se presenta, en primer lugar, un resumen sobre los polímeros tratados por plasma para aplicaciones biomédicas, con un enfoque especial a la evolución futura y a las nuevas posibilidades ofrecidas en el tratamiento de soluciones poliméricas o hidrogeles para aplicaciones biomédicas mediante plasmas fríos.

En un primer paso experimental, la eficacia del tratamiento directo de plasma es comparada al tratamiento indirecto mediante un líquido tratado por plasma, en cuanto a sus efectos en células sanas y cancerígenas de hueso. La concentración de especies reactivas generada en medios de cultivo en diferentes condiciones de tratamiento plasma se relaciona con los efectos biológicos observados.

A continuación, se estudia los efectos del tratamiento con plasma en la química y en las propiedades física-químicas de diferentes polímeros con habilidad para formar hidrogeles: natural (alginato), semi-natural (gelatina metacrilata) y sintético (poly(oxide)etileno tribloc copolimero). La generación, estabilidad, almacenamiento y la liberación de las especies reactivas generadas por plasma se discute en función de los diferentes polímeros estudiados y del método de reticulación empleado en cada caso. Se examina en esta tesis la posibilidad de emplear soluciones poliméricas e hidrogeles como reservorios y vehículos de especies reactivas generadas por plasma para aplicaciones en el área de medicina de plasmas.

TABLE OF CONTENTS

OBJECTIVES

The main goal of this PhD. Thesis is to investigate **the effects of atmospheric pressure plasma jets on liquids and hydrogels for bone cancer therapy**. In this context, the use of hydrogels in contact with atmospheric pressure plasma jets requires fundamental investigation on the most suitable polymers allowing to generate reactive species. Their biological effects, and any potential changes in the polymer structure must be investigated as it might alter the final biomaterial designed.

To achieve this general objective, different goals are proposed:

- Reviewing the main plasma-treated polymers for biomedical applications by cold plasmas and analysing their evolution for applications in the *Plasma Medicine* field (Chapter 1).

- Investigating the generation of reactive species in plasma-treated liquids (Chapters 2, 3 & 4) and their effects towards the selectivity of bone cancer cells against healthy cells (Chapter 2). Comparing the *in vitro* efficacy of both direct and indirect plasma treatment methods (Chapter 2).

- Examining the influence of the plasma settings (gas, gas flow and distance of the plasma nozzle) and experimental conditions (*i.e.* treatment time, surface/volume of the sample treated) on the generation of reactive species in liquids and polymer solutions (Chapter 2 & 3).

- Studying suitable hydrogels for the generation of reactive species and showing biological activity, in views of designing suitable carrier systems for reactive species from plasmas (Chapters 3 & 4).

- Investigating the effects of the atmospheric pressure plasma treatment on the chemistry and physic-chemical properties of natural, semi-synthetic and synthetic polymers and on its final hydrogel properties (Chapters 3, 4 & 5).

- Investigating the generation of reactive species and their stability in a polymer solution by plasma treatment. To assess the stability and release properties of the reactive species from the plasma-treated hydrogel (Chapters 3 & 4).

STRUCTURE

These objectives have been organized to constitute the different chapters of this PhD. Thesis, wherein each chapter is organized as an independent work. First, **Chapter 1** introduce the state of the art in plasma treatment of polymers for biomedical applications, and the different plasma sources employed therein. The evolution in the design and the methodology of plasma-treated polymers leading to new avenues for research in the *Plasma Medicine* field is discussed. Then, **Chapter 2** deals with the effects of plasma and plasma-treated media on bone cancer and healthy cells. The generation of reactive species in cell culture media is investigated and their cytotoxicity regarding different bone cancer and healthy cell lines analysed as a function of the concentration delivered. In **Chapter 3** the effects of atmospheric plasma treatment of a natural hydrogel on the generation of reactive species, on its properties and the biological effects related to it, is described. The generation of reactive species and their storage in a semi-synthetic polymer is addressed in **Chapter 4**. The release of reactive species from a plasma-treated gelatin-based hydrogel is discussed there. In **Chapter 5**, the fundamental study on the modification of the chemistry by plasma treatment of synthetic polymer is presented. In there, the influence of plasma treatment on the chemistry and the rheology of a poly(oxide) ethylene-based triblock copolymer hydrogel is reported.

LIST OF ABBREVIATIONS

3D: Three dimensional

APP: Atmospheric pressure plasma

APPJ: Atmospheric pressure plasma jet

bFGF: Basic fibroblast growth factor

CA: Contact angle

CAP: Cold atmospheric plasma

DBD: Dielectric barrier discharge

dMSCs: dog bone marrow stromal cells

BSA: Bovine serum albumin

DLS: Dynamic light scattering

FTIR-ATR: Fourier transform infra-red spectroscopy- Attenuated total reflectance

GelMA: Methacrylated gelatin

HDF: Human dermal fibroblast

hFF: human foreskin fibroblast

hMSCs: Human bone marrow mesenchymal

^{1}H-NMR: Proton nuclear magnetic resonance

hOB: Human osteoblasts

HOS: Human osteosarcoma cells

HPECs: Human prostatic epithelial cells

HUVEC: Human endothelial cell

LAP: lithium phenyl-2,4,6-trimethylbenzoylphosphinate

LPP: Low pressure plasma

MC3T3: mouse osteoblast like

MG63: osteosarcoma cells

NC: Non-crosslinked

OES: Optical emission spectroscopy

OS: Osteosarcoma

PCL: poly-caprolactone

PCM: Plasma conditioned media

PE: poly-ethylene

PET: poly-ethylene terephtalate

PEOT/PBT: poly(ethylene oxide terephthalate)/poly(butylene terephthalate)**PHB:** poly-hydroxybutyrate

PHBV: poly-hydroxybutyrate-co-hydroxyvalerate

PIS: Photo-initiating system

PDLLA: poly-D,L-lactic

PLA: poly-lactic acid

PLGA: poly-lactic-co-glycolide

PLLA: poly-Llactic acid

PMP:poly-4-methyl-1-pentene

PS: Polystyrene

RbMVEC: Rabbit microvascular endothelial cell

RONS: Reactive oxygen and nitrogen species

SaOs-2: Human osteosarcoma

SEM: Scanning electron microscopy

SLS: Static light scattering

tPOE: Poly(ethylene oxide)-based triblock copolymer

TE: Tissue engineering

UT: Untreated

VSMCs: rat vascular smooth muscle cell

CHAPTER 1

1. Evolution in Plasma Treatment of Polymers: Moving Towards Plasma Medicine Applications

ABSTRACT

Plasma sources have been widely investigated for surface modification of polymers to improve their surface properties. New plasma sources are constantly under development, so investigation has moved from low pressure plasmas to include also new developments in atmospheric pressure devices. Research on plasma-polymer interactions are of great interest in the biomedical field. This first chapter provides an updated overview on the state of the art of plasma-treated polymers for biomedical applications. The enhancement in biocompatibility induced in several polymers is developed with a focus on their biomedical applications. The different morphologies and physical state of the polymers investigated is discussed regarding the plasma source employed for its surface modification. This chapter is focused not only on conventional plasma treatment of solid-state polymer materials but also on new strategies emerged from the recent development of new versatile atmospheric pressure plasma devices. These have opened the door for the treatment of semi-solid polymers like hydrogels or even polymer solutions, showing very interesting avenues in the field of Plasma Medicine. New trends and future perspectives are discussed, with a special focus on plasma jets for biomedical purposes.

1.1. INTRODUCTION

Polymers represent the largest and most versatile class of biomaterials [1]. With appropriate chemical and physical properties, they have been extensively employed in a variety of biomedical applications [2,3]. In the biomedical field, good biocompatibility is required between the polymer surface and the living tissue which the material will be in contact with [4]. Although many biopolymers can potentially be suitable for tissue engineering (TE), a recurrent drawback is their high hydrophobicity [5]. This is related to their low surface energy which make these materials difficult for the cells to attach, spread and proliferate [6]. In order to enhance their hydrophilicity and their surface energy, the surface modification of polymers has been widely investigated [7]. Different methods have been explored to modify the chemistry on the surface of polymers [8–10]. New functional groups are introduced to enhance the hydrophilicity and improve the cell-polymer interactions [11–13]. Examples of these groups of biological interest are amino groups ($-NH_2$), carboxylic groups (-COOH) and hydroxyl groups (-OH). However, the surface modification through conventional wet chemical processes can induce some side effects; Irregularities on the polymer surface, decline in mechanical properties and faster degradation rate may occur. Moreover, the use of chemical products and big amounts of water or organic liquids during these processes generates hazardous chemical waste and costs [14–17]. In contrast, cold plasma treatment has raised great interest due its several advantages including their versatility allowing to tailor physico-chemical surface properties of the first nanometers of the surface without altering the bulk of the polymer [18], and therefore avoiding to alter their mechanical properties, being an environmentally-friendly dry method [19,20].

1.1.1. Cold plasmas

Plasma is a partially ionized neutral gas consisting of active species like radicals, ions, electrons, and photons [21]. Plasma has been described as the "fourth state of matter" (Figure 1.1) [22]. Traditionally, *cold plasmas*, also known as *non-thermal plasmas* or *low pressure plasmas* (LPP) have been produced at low pressures. LPP devices can be illustrated as an electrical discharge which occurs between two electrodes inserted in a glass tube under vacuum [23]. The tube can be filled by a gas or mixture of gases and is submitted to a voltage discharge (Scheme in Figure 1.2, left) [24]. A certain voltage must be applied to initiate a sufficient intensive electron avalanche which then propagates and sustains the plasma. Cold plasmas exhibit non-equilibrium energetic conditions where the electrons have high energy while the heavy particles (ions and neutral) maintain low energy. This way, the plasma, which is weakly ionized can have relatively low temperature, as low as room temperature [25]. LPP devices have traditionally been used for surface modification of polymers [26–28]. These sources are suitable for the treatment of polymer materials due to the low temperature of the plasma being close to room temperature and thus allowing treatment of heat-sensitive surfaces [29]. Cold plasmas have been widely employed to improve the biocompatibility of polymers designed to be in contact with biological tissues [30,31]. Plasma modification of polymers for biomedical applications has already been reported in excellent reviews [32,33,42,34–41]. In this chapter we wish to give a slightly different perspective, covering the evolution of the plasma treatment of polymers for biomedical purposes and the direction of the most recent developments, leading to novel applications in the *Plasma Medicine* field.

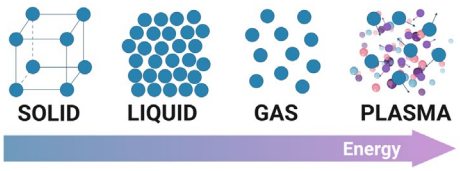

Figure 1.1: Scheme of the transition among the four states of matter (solid, liquid, gas and plasma) with the increasing of the energy supply to the system.

1.1.2. Cold plasma sources for polymer surface modification

As mentioned earlier, *cold plasmas* are of particular interest in surface modification of polymers. Different devices and configurations can be employed for the polymer-surface modification. Traditionally, LPP devices, working under vacuum were employed for the treatment of polymers in powder or in solid state [43]. The most usual configurations allow the treatment of bulky polymers such as 3-dimensional (3D) scaffolds, discs or films (Figure 1.2, left). In the last decades, plasma devices working at atmospheric pressure were developed in a variety of configurations, allowing to reduce costs, and often maintenance of vacuum facilities [44].

Atmospheric pressure plasma (APP) devices have allowed the treatment of different shapes and states of polymer materials, including liquids [45–48]. Dielectric barrier discharge (DBD) plasma sources are the most employed APP source for polymer treatment leading to comparable results than LPP devices [49–54]. However, their usual configurations (Figure 1.2, centre) with less space between the electrodes restrict the surface modification of some polymer materials. In fact, in most configurations only thin surfaces can be properly treated like films, membranes, fibers, or very thick scaffolds. The development of new atmospheric pressure plasma jets (APPJ) employed in biomedical applications [55], has already shown great potential in polymer surface modification [56–59]. In fact, APPJ devices, due to their simple system and compact design allow localized treatments (Figure 1.2, right). Moreover, these devices have the property to generate an extremely high concentration of chemically active species while maintaining the bulk temperature as low as at room temperature [45,60,61]. These properties make them suitable for the treatment of the surface of small scaffolds as well as large 3D structures and even liquids [46,47,62–65]. APPJ treatments have already shown their efficiency on 3D scaffolds for the attachment and proliferation of cells for TE applications [63,65,66].

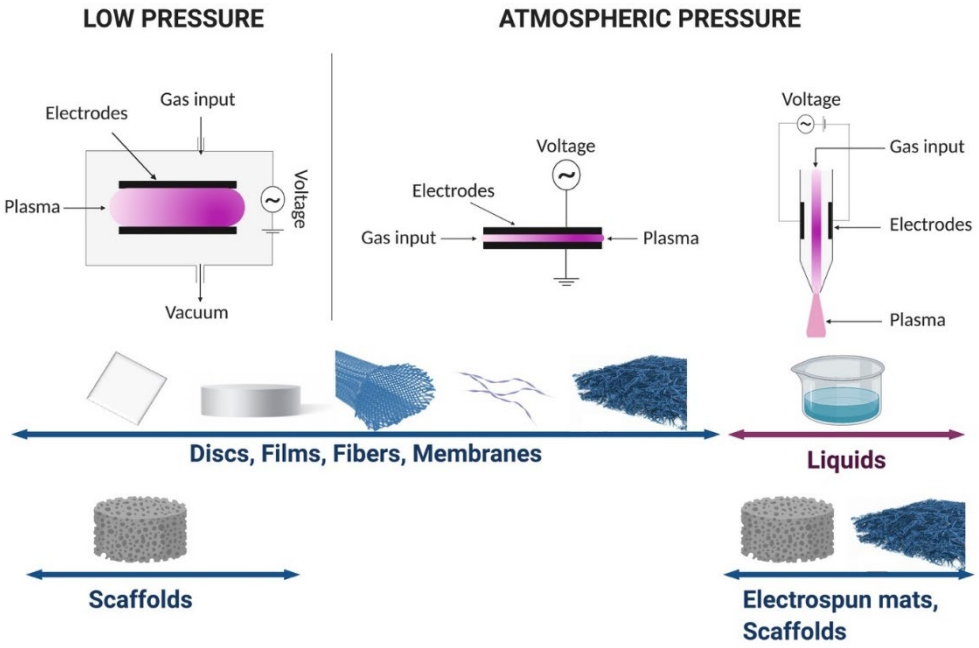

Figure 1.2: General scheme of cold plasma devices usually employed for the surface modification of different polymer morphologies and structures, at low pressure (left) or atmospheric pressure (right).

1.1.3. Plasma-solid polymer surface interaction

The appropriate selection of plasma sources and settings enables unique surface properties improving biocompatibility and functionality. The resulting polymer-surface modification can be tuned according to the conditions of the plasma device used (*e.g*. gas input, gas mixture, gas flow, energy input, reactor geometry). In addition to the process parameters, the physical characteristics of plasma are also influenced by the system parameters, such as electrodes (location, coupling mechanism, and surface area), reactor (shapes, materials, and inertness), frequency of power supply, gas inlets (position) and vacuum. Subsequently, changes in these parameters may affect the surface chemistry obtained by the plasma modification [67–69]. The polymer surface treatment is the resulting of a synergistic effect from the contribution of all the plasma components (*e.g*. atoms, radicals, excited species, charged particles, UV radiation…). In fact, the highly energetic electrons generated by plasma, and the variety of reactive species generated are the main responsible of the chemical reactions induced on the polymer surface [70]. These reactions can entail crosslinking, thin film deposition, grafting, functionalization or activation and etching as main process induced (Figure 1.3).

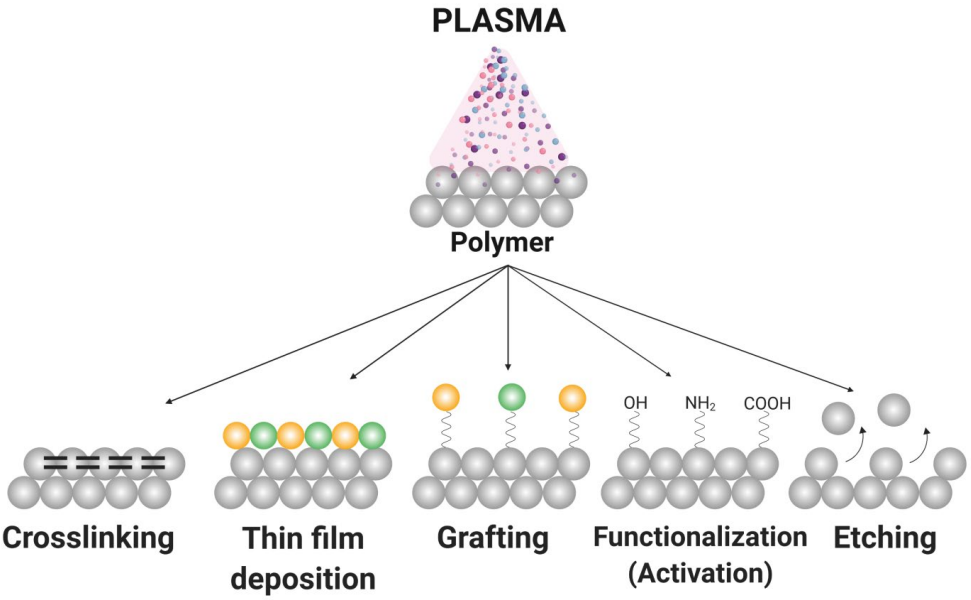

Figure 1.3: Main processes involved in the surface effects in plasma treatment of polymers.

1.2. POLYMERS FOR BIOMEDICAL APPLICATIONS

1.2.1. Surface modification of polymers

Plasma treatment of polymer surfaces has shown to be effective to improve the cell adhesion and proliferation as well as to control specific biological behaviour of cells on the treated-surface [71]. Biomedical applications of plasma-modified polymers have already been summarized in several excellent reviews [26,38,72–75]. Plasma surface modification will be here mainly focused on the functionalization or activation of polymeric materials which will be in contact with cells for potential use in biomedical purposes.

One of the most extensively studied effects of the plasma treatment of polymers aimed for biomedical applications is the modification of their wettability and adhesion characteristics. The modification of the wettability induced by plasma treatment depends on many parameters among them the plasma gas, power, treatment time, etc. By tuning the carrier gas employed, different functional groups are introduced on the treated surface. An increase of the gas pressure, discharge current or the plasma treatment time can also have an influence on the enhancement of the polymer surface wettability [76]. Air, oxygen, nitrogen and ammonia plasma carrier gas lead to increase the hydrophilicity of the polymer surface contrarily to the decrease observed when fluorine-containing gases are employed [77]. It is already well reported that oxygen containing gases (O_2 and CO_2) generate hydroxyl and carboxyl groups in the polymer surface [78]. Nitrogen and ammonia are employed to introduce amine groups while air is employed to generate both oxygen and amine containing moieties on the surface [79]. Helium and argon mainly generate oxygen groups on the treated-polymer surface, after exposition of the activated surface to ambient air [80]. Functional groups generated in the polymer surface are usually employed as anchoring sites for bioactive molecules such as proteins, or for using it as it is. The modification of roughness of the polymer surface through etching processes is also relevant for the cell-surface interaction behaviour.

1.2.2. Plasma treatment of polymers for applications in tissue engineering

The favorable surface modification of polymers just discussed has been applied on a variety of biocompatible polymers in views of TE for different organs. In this respect, a number of works have employed model surfaces such as films for characterize the effects obtained, both physic-chemically and biologically. Nevertheless, a significant corpse of study has investigated the polymers already in the final conformation to be employed, namely nanofiber mats or scaffolds obtained by electrospinning, 3D printing or by other methods (Table 1-1).

Various synthetic polymers presenting good structural and mechanical properties for biomedical applications have been investigated under plasma treatment [81]. Among them, poly(L-lactide acid) (PLLA), poly-Lactic acid (PLA), poly-D,L-Lactic acid (PDLLA) and Poly-D,L-Lactide-co-glycolide (PLGA) were intensively investigated as biomaterials for TE applications. The following sections and table 1-1 summarize some of the main findings in this regard.

Polylactides

Modification of polylactides by plasma has been mostly performed on films and employing LPP devices, although some studies have also explored different APP devices, highlighting their different advantages in views of TE. Chu et al. [82] modified PLLA films with NH_3 LPP and compared it to protein surface modification. Authors observed that Human endothelial cells (HUVEC) and rabbit microvascular endothelial cell (RbMVEC) adhesion and proliferation was two times higher after plasma treatment than in fibronectin-coated PLLA. The *in vitro* biocompatibility of PLLA films with rat vascular smooth muscle cells (VSMCs) was evaluated in [11] and in [83]. A decrease from 72° to 40° of the contact angle (CA) was recorded at the higher plasma treatment time due to the introduction of oxygen contents in both studies. An enhanced cell adhesion and proliferation (from $40 \cdot 10^3$ cells in PLLA to $180 \cdot 10^3$ cells in 400 s plasma-treated PLLA in 4 days) was

observed in [11] while plasma treatment have negligible effects on VSMCs cell proliferation in [83]. Khorasani et al., treated PLLA films with LPP using O_2 [84] and CO_2 [85] observing in both studies a decrease of the CA from 86° to 50° and 27° for CO_2 and O_2 gas, respectively, with the introduction of oxygen groups. Moreover, microscope images show that plasma-treated PLLA films promoted the cell affinity of nervous tissue B65 cells. Yang et al., [86] observed improved cell affinity of mouse 3T3 fibroblast cells on PDLLA films (from $3 \cdot 10^4$ to $7 \cdot 10^4$ cells/mL in 4 days) by using NH_3 LPP. The hydrophilicity (CA from 78° to 22°) of the plasma-treated films was improved due to introduction of oxygen and nitrogen functional groups that were responsible of the improved cell adhesion and proliferation. The atmospheric pressure devices investigated with regard to this polymer have been both DBDs and jets. Jacobs et al. [80] treated PLA foil using DBD device operating at medium pressure with different gases (dry air, Ar, and He). Mainly oxygen groups were introduced disregard the gas employed on the treated surface, that improved the initial attachment of human foreskin fibroblast cells (hFF). Although some differences were observed among the different gases, little influence seems to be found on the cell proliferation. Nagakawa et al. [49] and Teraoka et al. [87] recorded that APPJ treatment increased the hydrophilicity (CA from 77° to 40° after plasma treatment). The oxygen content on PLLA discs, increased twice the cell adhesion and proliferation of mouse osteoblast-like (MC3T3) after 3 days in [87] but its effects are negligible in [49].

In a closer approach to the application, 3D-printed PLA scaffolds were treated using APPJ by Wang et al. [66], to modify the nano-scale roughness and the chemical composition of the scaffold for bone TE. Cell adhesion and proliferation were enhanced in three cell line types: Human dermal fibroblast (hDF), Human osteoblasts (hOB) and bone marrow mesenchymal stem cells (hMSCs). Authors highlighted especially the successful nano-scale modifications, with a decrease of the CA from 70° to 24° and the introduction of oxygen groups that provided attachment sites to the cells. Moreover, authors observed a different behaviour on cell proliferation of OB and hMSCs in the plasma-treated scaffold probably due to

the changes in the chemistry of the treated-sample and also to the different cell metabolism characteristics. In another study, the same authors [65] employed APPJ to enhance the surface of electrospun core-shell nanofibrous PLLA scaffolds. The core contained Bovine Serum Albumin (BSA) to foster tissue regeneration, and the shell was made of PLLA. The BSA release was enhanced by the plasma treatment due to the enhanced wettability of the surface (decrease from 110° to 50° of the CA after plasma). The cell proliferation was enhanced preferently on Fibroblasts (twice higher than the control (32 000 cell/cm^2) after 5 days) rather than in Osteoblasts were the presence of BSA did not influence their proliferation (2 500 cell/cm^2 increase *vs.* the control in 5 days) in plasma-treated scaffold containing BSA. In contrast, the scaffolds with plasma treatment, and especially those combining with BSA revealed much fostered osteoinductive results on MSC differentiation.

Polylactide-co-glycolide

Copolymers of polylactic acid with polyglycolic acid, which have faster resorption rate *in vivo* related to their higher intrinsic wettability than PLA alone have also been investigated by plasma treatment, mainly in views of soft tissue substitution. Thus, PLGA films were treated using O_2 LPP in [84] and [88] recording increased wettability (decreased CA from 70° to 38° after plasma exposure) and introduction of oxygen functional groups. The plasma-treated PLGA films enhanced cell adhesion with neuronal and fibroblast cells, respectively. Plasma treatment using CO_2 as feed gas was employed by Shen et al. [78], on PLGA scaffolds in order to introduce acid carboxylic functional groups to enhance the immobilization and delivery of basic fibroblast growth factor (bFGF). The scaffold surface was successfully modified introducing anchorage sites leading to the immobilization and slow release of bFGF in the media. The adhesion and proliferation of mouse 3T3 fibroblast cells is improved on plasma-treated PLGA/bFGF scaffolds than in plasma-treated PLGA scaffolds. Park et al. [89], employed LPP with ammonia gas to investigate the protein expression in the culture

of mouse NIH3T3 fibroblast cells on electrospun PLGA. The hydrophilicity (decrease of CA from 140° to 50°) and the surface chemical composition (introduction of nitrogen groups) of PLGA nanofibers was altered by plasma treatment. Authors found a critical optimal concentration (2.25 %) of nitrogen contents for the adhesion and proliferation of NIH3T3 in the nanofiber matrix surface.

Polycaprolactone

Poly ε-caprolactone (PCL) is one of the most investigated biodegradable polymers in the biomedical field. Ghobeira et al. [90] investigated the APP treatment of PCL films with a DBD - using air or Ar as feed gas – to combine both surface modification and sterilization. First, APP treatment led to a decrease of the CA (from 74° to 55°) with the incorporation of oxygen contents without modifying the sample topography at short treatment times. However, none of the plasma conditions investigated was sufficient to allow efficient sterilization. A good biocompatibility for male Wistar rat cadavers' cells was obtained without altering more the surface topography by combining plasma with UV to sterilize. Nanofibrous scaffolds were modified by Prabhakaran et al. [91] using LPP working with air. They observed an enhancement of 17 % on the proliferation of Schwann cells in a PCL plasma-treated scaffold for neural applications compared to an untreated one in 8 days. Pappa et al. [92] also investigated electrospun nanofibrous PCL scaffold for cardiovascular implants using LPP device. Authors reported the surface modification (decrease of the CA from 90° to 20° and increase of oxygen contents) of the scaffold without altering bulk properties recording a stable elastic modulus (1-4 GPa) of both treated and untreated. All LPP treated samples using O_2 gas showed a good cytocompatibility towards mouse fibroblast L929 with an increase of cell viability and proliferation (10 % respecting the untreated sample after 7 days). Yildirim et al. [93] modified a 3D PCL scaffold by LPP with O_2 gas in order to introduce proteins afterwards to the scaffold surface to enhance osteoblastic differentiation. Authors

observed that the combination of plasma treatment and the addition of proteins into the scaffold surface doubled the proliferation and the differentiation rate of OB cells than in plasma-treated or in only protein modified ones or either untreated. Results obtained demonstrated that the plasma surface modification as well as the introduction of functional cues in the polymer surface highly improves the cellular functions. The influence of the carrier gas on the adhesion and proliferation of HUVEC cells was investigated in electrospun PCL scaffold by Recek et al. [77] using LPP working with O_2, NH_3 or SO_2 as a carrier gas. Authors obtained higher proliferation rate with respect to the untreated scaffold after 24 h when samples were treated with O_2 or NH_3 (60 %) than with SO_2 (40 %), consistently with the kind of functional groups grafted on the surface with each plasma treatment. Fisher et al. [94] introduced oxygen and nitrogen groups on 3D PCL scaffolds using LPP, rendering hydrophilic (CA = 50°) the hydrophobic (CA = 130°) PCL scaffold after 4 min of plasma treatment. Authors also observed a preference of Human osteosarcoma (SaOS-2) cells for the plasma-treated scaffolds rather than those untreated. In another study, Yildirim et al., [95] employed a DBD with O_2 as carrier gas to enhance mouse 7F2 osteoblast cells for bone TE on PCL scaffolds. Authors reported that 5 min of plasma treatment increased three times the surface roughness leading to an increase of the proliferation rate. Sardella et al., treated PCL scaffolds with LPP varying the composition of the N_2/H_2O gas mixture for the aim to introduce neutral, acidic or basic groups in order to drive the cell growth into scaffolds for TE and regenerative medicine purposes [96]. Oxygen and nitrogen contents are introduced to the scaffold surface as a function of the gas feed (0 to 100 % of N_2 and/or H_2O) leading to increase the oxygen contents when higher % feed of H_2O is used and more amino groups when N_2 feed % is increased. Authors found that at an optimal gas feed composition (50/50 N_2/H_2O) lead to the highest level of SaOs-2 cell growth due to the improvement of the plasma-treated scaffold surface hydrophilicity (CA from 130° for the untreated to 71°). Lee et al., [79] also investigated the influence of the combination of different carrier gases (Ar, H_2, N_2 and O_2) on PCL films using APP. In this study, the combination Ar + O_2 gas showed

a higher proliferation, a better cell distribution and growth of Human prostatic epithelial cells (HPECs) ($15 \cdot 10^5$ cells/mL) than Ar gas ($10 \cdot 10^5$ cells/mL) or the combination Ar + N_2 ($7.5 \cdot 10^5$ cells/mL) or Ar + H_2 ($1 \cdot 10^5$ cells/mL) at 3 days. De Valence et al., [99] reported that APP treatment using air on PCL scaffolds did not change the fibre morphology or its mechanical properties (stable elastic modulus of 7.5 MPa and same strain at rupture around 900 %). The scaffold hydrophilicity and wettability dramatically increased from a CA of 130° to 0° after 60 s of treatment. Moreover, authors observed a better cellularization of smooth muscle cells *in vivo* from the plasma-treated (48 %) scaffold compared to the untreated one (23 %). Trizio et al., treated PCL scaffolds by APPJ using He/O_2 gas mixtures [100]. The aim of this study was to achieve adequate chemical modification on the scaffold by means of plasma jet treatments to improve cell affinity. Authors reported that the increase of oxygen contents (from 25 % for the untreated scaffold to 35 % for the higher gas flow rate employed) on the plasma-treated scaffold improved their hydrophilicity resulting in a better clusterization and cytoskeleton morphology of the cultured cells on the scaffold.

Polyhydroxyalcanoates

Poly-hydroxybutyrate (PHB) and poly-hydroxybutyrate-co-hydroxyvalerate (PHBV) have also been modified with plasma for applications in TE of soft tissues (*i.e.* vascular and endothelial) bone and neural tissues). For instance, plasma treatment of PHB thick foils and non-woven fabrics using a LPP working with Ar was studied by Slepicka et al. in various works [11,101,102]. In all these studies, authors reported an increase of the surface energy and hydrophilicity (CA from 70° to 35°) of PHB samples following plasma treatment. Authors showed that plasma treatment led to the formation of oxygen groups on the polymer surface promoting the adhesion, proliferation and homogeneous spreading of NIH3T3 and VSMCs cells. Pompe et al. [103], modified the surface of PHB films comparing H_2O, NaOH and NH_3 LPP in order to control the adhesion of HUVEC cells. Better wettability

(from 80° to 70° for NaOH and NH_3 and 60° for H_2O plasma treatment) was recorded, related to the introduction of amine and carboxyl groups after plasma treatments. Authors also observed that the cell adhesion and the matrix reorganisation were dependent on the changes of the surface topography of the samples as a function of the treatment employed. In fact, even if NaOH plasma did not extensively change the surface characteristics, 75 % of cells were able to reorganize in the surface comparing to H_2O (70 %) or NH_3 (15 %) plasma. The effect of plasma exposure time, generation power and the chamber pressure of O_2 and N_2 LPP were investigated on PHBV films in [104]. New oxygen and/or nitrogen groups were introduced in function of the plasma treatment time and/or the generation power improving the adhesion of dog bone marrow stromal cells (dMSCs). PHBV nanofiber mats [105] and foams [106] were treated with LPP using O_2 and N_2 as a carrier gas respectively for potential bone TE applications. An increase of the hydrophilicity (CA from 123° to 45°) was observed and no changes in the bulk polymer were reported. SaOs-2 cell adhesion and proliferation with an initiation of mineralization were better using N_2 than O_2 plasma in [105]. In [106], O_2 plasma treatment lead to a 1.2 increase in cell number with respect to the untreated foam between 7 and 60 days of incubation as well as osteocalcin secretion. PHBV membranes were treated by O_2 and N_2 LPP to modify the polymer surface chemistry for potential cell growth in [107]. Authors reported that the plasma treatment altered the polymer surface by inducing roughness modifications (from 52 nm to 67 nm and 37 nm for N_2 and O_2 gas respectively) and increasing the surface hydrophilicity (CA decrease from 80° to 37° and 22° using N_2 and O_2 gas respectively). They observed that the plasma-treated membranes allowed better cell adhesion, proliferation and growth of the epithelial Vero cell lines than in untreated membranes especially in N_2 plasma treatments. PHBV scaffolds were investigated under O_2 LPP by Biazar et al. [108] for a potential use in nerve TE. Plasma treatment led to increase the hydrophilicity (CA from 107° to 48°) of the scaffolds with the introduction of oxygen functional groups. Plasma-treated samples showed

better adhesion, growth and proliferation of Schwann cells inside the scaffolds with a cell viability of 98 % towards 60 % for untreated sample at 48 h.

Natural polymers: chitosan

A few studies deal with the modification of natural polymers by plasma and have been tested in cell culture for a potential use in biomedical application. Luna et al. [109], treated chitosan membranes using N_2 and Ar LPP device in order to tune their surface properties for applications in TE. Authors reported an increase of the roughness (from 2.8 nm to 7.8 nm and 5.8 nm for N_2 and Ar plasma respectively at 40 min of treatment) but no significant changes in the CA following plasma treatment. The introduction of oxygen and nitrogen groups promoted the adhesion and proliferation of L929 mouse fibroblasts cells in plasma-treated membranes after 3 days compared to untreated sample. Chitosan scaffolds combined with hydroxyapatite nanoparticles were treated using APPJ in order to promote bone regeneration in [64]. Authors reported the formation of a more porous and hydrophilic (CA from 130° to 62° after 10 min of treatment) scaffold. Short plasma treatment times from 3 to 5 min were sufficient to promote hMSCs cell adhesion, migration and osteogenic differentiation. Electrospun hybrid scaffolds of PCL-chitosan-PCL were treated with APPJ using various mixtures of gases (Ar, Ar+O_2, Ar+O_2+N_2, and dry air) in [63]. Their aim was to modify the surface scaffold topography and functionality to improve human fibroblast MRC5 cells growth. Authors reported the effectiveness of the APPJ on the surface modification of scaffolds inducing hydrophilicity (CA from 126° to 80° and 75° for Ar+O_2+N_2 gas mixture (1 min) and dry air (9 min) respectively) and changes in topography leading to a better cell adhesion and proliferation (twice higher between day 5 and 7) for a further use in TE.

Other synthetic polymers

Plasma treatment was also investigated in thermoplastic polymers to induce changes in their surface topography for a potential use in TE. Sasmazel et al. [110], and Recek et al. [111], treated poly-ethylene terephtalate (PET) discs by LPP with the objective to induce biocompatibility. In both studies, plasma-treated PET showed good cell adhesion and proliferation of L929 mouse fibroblast (higher proliferation in 6 days than amine or protein grafted PET disc) and Human osteosarcoma (HOS) cells (200 % of cell viability in 6 days), respectively. Polystyrene (PS) foils and discs were treated by Recek et al. [112], and by Van Kooten et al. [113], respectively using LPP devices for TE applications. In both studies, oxygen groups were successfully introduced leading to a better cell adhesion and proliferation of HOS (> 200 % of cell viability in 6 days in [112]) and HUVEC (100 % of cell viability in 2 days in [113]) cells respectively. Polyethylene (PE) films were treated with Ar LPP in [114] for subsequent grafting of proteins able to enhance cell adhesion. Authors reported successful surface modification by plasma leading to enhance NIH3T3 cells (from $50 \cdot 10^3$ cell/cm^2 for untreated to $350 \cdot 10^3$ cell/cm^2 - the higher value obtained for 100 s of plasma treatment at 5 days of incubation). The addition of grafted proteins on the surface increased the cell adhesion and proliferation of NIH3T3 cells (higher cell density of $400 \cdot 10^3$ cell/cm^2 obtained for grafted-vitronectin in 300 s treated-PE at 5 days) that makes PE attractive for potential TE applications.

Biocompatible poly-4-methyl-1-pentene (PMP) polymer was treated using Ar LPP in [83]. Plasma treatment led to an increase of the hydrophilicity (CA from 105° to 20°), inducing roughness in the polymer surface without altering its morphology. Oxygen functional groups were generated on the surface related to better adhesion and proliferation of VSMCs cells (more than 10 times higher surface density of cells for 15 s plasma treated at higher plasma power after 7 days of incubation).

In a different approach involving plasma treatment of liquids, Grande et al. [47] employed APPJ to improve the electrospinnability of poly-ethylene oxide terephtalate/poly(butylene terephthalate) (PEOT/PBT) polymer solutions. Authors observed an increase on the polymer solution conductivity (from 0.75 to 1.05 $\mu S/cm^{-1}$) and viscosity (from 31 to 560 cP) after 16 min of plasma leading to a better electrospinnability. While a slight degradation of the polymer backbone was reported, plasma treatment of the solution induced slight modifications in the hydrophilicity depending on the solvent employed (CA from 137° to 141°, 130° and 113° for dimethylformamide, methanol and hexafluoroisopropanol solvents respectively) of the nanofibers, and an associated better cell adhesion of hFF cells in plasma-treated electrospun nanofibers (higher than 100 % of cell viability in the different conditions studied except for solutions treated in methanol (90 % of cell viability was recorded)).

Plasma treatments using APPJ devices are promising in the treatment of different shapes of polymers (discs, scaffolds, nanofibers, polymer solutions) allowing the immediate use as it is in TE. As the design of the atmospheric pressure devices such as jets allows the treatment of liquids; *i.e.* polymer solutions and hydrogels, new biomedical applications perspectives can be envisaged, which are succinctly described in the next section.

Table 1-1: Summary of the main polymers modified by plasma for biomedical purposes, their conformation and effects obtained.

Polymer	Polymer state	Plasma type and gas	Modifications	Biological effects	Applications in TE (cell type)	[Ref]
PLLA (poly(L-lactide acid))	Film	LPP (Ar)	↑ Hydrophilicity ↑ Roughness ↓ Surface energy Changes in surface morphology	→ Cell adhesion → Cell proliferation	Vascular TE (VSMCs)	[83]
	Film	LPP (O_2)	↑ Hydrophilicity	↑ Cell adhesion ↑ Cell proliferation	Nervous TE (B65)	[84]
	Film	LPP (CO_2)	↑ Hydrophilicity ↑ Oxygen groups	↑ Cell adhesion ↑ Cell proliferation	Nervous TE (B65)	[85]
	Film	LPP (NH_3)	↑ Hydrophilicity ↑ Amine & Amides groups	↑ Cell adhesion ↑ Cell proliferation	Vascular TE (HUVEC + RbMVEC)	[82]

	Thick foils	LPP (Ar)	↑ Hydrophilicity ↑ Oxygen groups	↑ Cell adhesion ↑ Cell proliferation ↑ Cell distribution & viability	Vascular TE (VSMCs)	[11]
	Discs	APP (Air, CO_2, C_3F_8)	↑ Hydrophilicity ↑ Roughness	↑ Cell adhesion ↑ Cell proliferation	Bone TE (MC3T3)	[49]
	Discs	APP (Air)	↑ Hydrophilicity ↑ Oxygen groups	↑ Cell adhesion ↑ Cell proliferation	Bone TE (MC3T3)	[87]
	Nanofibers	APPJ (He)	↑ Hydrophilicity ↑ Nanofiber pore size ↑ Specific surface area	↑ Cell adhesion ↑ Cell proliferation ↑ Osteoinductivity	Bone TE (HDF and OB)	[65]
PLA (Poly-Lactic acid)	Film	LPP (Dry Air, Ar, He)	↑ Hydrophilicity ↑ Oxygen groups	↑ Cell adhesion → Cell proliferation	TE (hFF)	[80]
	3D-printed scaffold	APPJ (He)	↑ Hydrophilicity ↑ Roughness ↑ Oxygen groups	↑ Cell adhesion ↑ Cell proliferation	Bone TE (hDF + OB + hMSCs	[66]

PDLLA (Poly-$_{D,L}$-Lactic acid)	Films	LPP (NH_3)	↑ Hydrophilicity ↑ Surface energy ↑ Oxygen & amines groups	↑ Cell adhesion ↑ Cell proliferation	TE (3T3 fibroblasts	[86]
PLGA (Poly-$_{D,L}$-Lactide co-glycolide)	Film	LPP (O_2)	↑ Hydrophilicity	↑ Cell adhesion ↑ Cell proliferation	Nervous TE (B65)	[84]
	Films	LPP (O_2)	↑ Hydrophilicity ↑ Roughness ↑ Oxygen groups	↑ Cell adhesion ↑ Cell proliferation	TE (3T3 fibroblasts)	[88]
	Foamed scaffold	LPP (CO_2)	↑ Hydrophilicity ↑ Roughness ↑ Oxygen groups	↑ Release of protein ↑ Cell proliferation ↑ Cell resistance to shear stress	TE (3T3 fibroblasts)	[78]
	Nanofibers	LPP (NH_3)	↑ Hydrophilicity ↑ Nitrogen groups → Morphology of nanofiber	↑ Cell adhesion ↑ Cell proliferation	TE (NIH3T3)	[89]

PCL (Poly ε-caprolactone)	Film	LPP (Air)	↑ Hydrophilicity ↑ Oxygen groups	↑ Cell adhesion ↑ Cell proliferation	TE (Schwann cells)	[79]
	Film	LPP (Air, Ar)	↑ Hydrophilicity ↑ Oxygen groups Altered surface morphology at long treatment times	↑ Cell adhesion ↑ Cell proliferation	TE (male Wistar rat cadavers' cells)	[90]
	Film	APP (Ar + He, O_2, N_2)	↑ Hydrophilicity ↑ Oxygen & Nitrogen groups	↑ Cell adhesion ↑ Cell proliferation ↑ Homogeneity of cell distribution & proliferation	TE (HPECs)	[115]
	Foamed scaffold	LPP (N_2/H_2O)	↑ Hydrophilicity ↑ Oxygen & Nitrogen groups	↑ Cell adhesion ↑Cell proliferation	TE (SaOS-2)	[94]

Electrospun nanofiber scaffold	LPP (Air)	↑ Hydrophilicity ↑ Oxygen + nitrogen groups	↑ Cell proliferation ↑ *In vivo* tissue regeneration	Vascular TE (Primary porcine smooth muscle cells)	[91]
3D-printed scaffold	LPP (O_2)	↑ Hydrophilicity ↑ Roughness	↑ Cell adhesion → Cell proliferation	TE (7F2 osteoblast)	[93]
Electrospun Nanofiber scaffolds	LPP (O_2, NH_3, SO_2)	↑ Hydrophilicity ↑ Oxygen, Nitrogen & Sulfur groups ↓ Topography	↑ Cell adhesion ↑ Cell proliferation	TE (HUVEC)	[77]
Electrospun Nanofiber scaffold	LPP (O_2)	↑ Hydrophilicity ↑ Roughness	↑ Cell adhesion ↑ Cell proliferation ↑ Homogeneity of cell distribution & proliferation	TE (L929 fibroblasts)	[92]

	Scaffold	LPP (N_2/H_2O)	↑ Hydrophilicity ↑ Oxygen & Nitrogen groups	↑ Cell adhesion ↑ Cell growth	TE Regenerative Medicine (SaOs-2)	[96]
	Scaffold	APP (O_2)	↑ Hydrophilicity ↑ Surface energy ↑ Roughness	↑ Cell adhesion ↑ Cell proliferation	TE (7F2 osteoblast)	[95]
	Scaffold	APPJ (He/O_2)	↑ Hydrophilicity ↑ Oxygen groups No changes in bulk of scaffold	↑ Cell adhesion ↑ Cell colonization ↑ Cell-surface interactions	TE Regenerative Medicine (SaOs-2)	[100]
PHB (Poly-hydroxybutyrate)	Film	LPP (NH_3, H_2O)	↑ Hydrophilicity ↑ Oxygen & amine groups	↑ Cell adhesion Matrix re-organisation	TE (HUVECs)	[103]
	Thick foil	LPP (Ar)	↑ Hydrophilicity ↑ Surface energy ↑ Oxygen groups	↑ Cell adhesion ↑ Cell proliferation ↑ Homogeneity of cell distribution & proliferation	TE (NIH3T3)	[101]

	Thick foil	LPP (Ar)	↑ Hydrophilicity ↑ Roughness	↑ Cell adhesion ↑ Cell proliferation	TE (VSMCs)	[11]
	Thick foil	LPP (Ar)	↑ Hydrophilicity ↑ Surface energy ↑ Oxygen groups	↑ Cell adhesion ↑ Cell proliferation ↓ Bacterial colonies	TE (NIH3T3)	[102]
	Non-woven fabric	LPP (Ar)	↑ Hydrophilicity ↑ Surface energy ↑ Oxygen groups	↑ Cell adhesion ↑ Cell proliferation ↓ Bacterial colonies	TE (NIH3T3)	[102]
PHBV (Poly(3-hydroxybutyrate-co-hydroxyvalerate))	Film	LPP (O_2, N_2)	↑ Hydrophilicity ↑ Oxygen & Nitrogen groups	↑ Cell adhesion ↑ Cell proliferation	Cartilage TE (BMSCs)	[104]
	Membrane	LPP (O_2, N_2)	↑ Hydrophilicity ↑ Roughness	↑ Cell adhesion ↑ Cell proliferation	TE (Vero cells)	[107]

	Foam	LPP (O_2)	↑ Hydrophilicity Changes in surface chemistry	↑ Cell adhesion ↑ Cell proliferation Initiation of mineralization	Bone TE (Stromal osteoblastic cells)	[106]
	Electrospun thin scaffold	LPP (O_2)	↑ Hydrophilicity ↑ Oxygen groups	↑ Cell adhesion ↑ Cell proliferation	Nerve TE (Schwann cells)	[108]
	Nanofiber	LPP (O_2, N_2)	↑ Hydrophilicity → Nanofiber morphology	↑ Cell adhesion ↑ Cell proliferation Initiation of mineralization	Bone TE (SaOs-2)	[105]
PS (Polystyrene)	Foil	LPP (O_2)	↑ Oxygen groups	↑ Cell adhesion ↑Cell proliferation	TE (HOS)	[112]
	Disc	LPP (Ar)	↑ Hydrophilicity ↑ Oxygen groups	↑ Cell adhesion ↑Cell proliferation	TE (HUVEC)	[113]

PET (Polyethylene Terephthalate)	Disc	LPP (H_2O/O_2)	↑ Carboxyl groups	↑ Cell adhesion ↑Cell proliferation	TE (L929 fibroblasts)	[110]
	Disc	LPP (O_2, CF_4)	↑ Hydrophilicity / hydrophobicity ↑ Oxygen or Fluorine groups	↑ Cell adhesion ↑Cell proliferation	TE (HOS)	[111]
PE (Polyethylene)	Film	LPP (Ar)	↑ Hydrophilicity ↑ Roughness Changes in surface morphology	↑ Cell adhesion ↑ Cell proliferation ↑ Homogeneity of cell distribution & proliferation	TE (NIH3T3)	[114]
PMP (poly-4-methyl-1-pentene)	Film	LPP (Ar)	↑ Hydrophilicity ↑ Roughness ↑ Oxygen groups → Surface morphology	↑ Cell adhesion ↑Cell proliferation	TE (VSMCs)	[83]

PEOT/PBT (poly(ethylene oxide terephthalate)/poly(butylene terephthalate))	solution	APPJ (Ar)	↑ Electrospinability Uniform fiber diameter No changes in the bulk ↑ Oxygen groups	Non-cytotoxic	TE (hFF)	[47]
Chitosan	Membrane	LPP (Ar, N_2)	↑ Roughness ↑ Oxygen & Nitrogen groups	↑ Cell adhesion ↑Cell proliferation	TE (L929 fibroblasts)	[109]
Hydroxyapatite-Chitosan	Foamed scaffold	APPJ (He)	↑ Hydrophilicity ↑ Roughness	↑ Cell adhesion ↑Osteogenic differentiation	Bone TE (hMSCs)	[64]
PCL/Chitosan/PCL	Electrospun scaffold	APPJ (Ar, Ar+O_2, Ar+O_2+N_2, dry air)	↑ Hydrophilicity ↑ Oxygen groups ↓ Fiber diameter	↑ Cell adhesion ↑Cell proliferation	TE (Human fibroblast MRC5 cells)	[63]

1.3. MOVING TOWARDS PLASMA MEDICINE APPLICATIONS

The development of plasma sources at atmospheric pressure like APPJ has paved the way for applications in medicine creating a new branch of medical technology called *Plasma Medicine*. This multidisciplinary field regroups the interactions between the different species of plasmas and the complex biochemistry involved with tissues or biological samples [116]. Today, *Plasma Medicine* raises great interest and includes three main fields of concern; sterilization, wound healing and cancer therapy [117–119].

1.3.1. Reactive species in cancer therapy

In this regard, it has been demonstrated that APPJ treatments can lead to tumour cells cycle arrest, and induction of cell death [120]. Although the mechanism involved in cancer cell death is not yet fully understood, reactive oxygen and nitrogen species (RONS) from plasmas have been pointed out to as one of the main responsible of the biological effects of plasmas [121]. In fact, oxidative stress has been demonstrated to play an important role in cell signalling pathways as a key player of the cell function in health and disease [122]. It is known that an increase of the RONS concentration above a certain threshold, leads to disrupting the cellular homeostasis through oxidative stress mechanisms [123–125].

In plasma-based anticancer therapies, selectivity of the treatment towards tumour cells has been claimed. This can be attributed to the intrinsic oxidative stress levels in tumour *vs.* healthy cells; In contrast to healthy cells, tumour cells contain higher steady state concentrations of RONS and often bear malfunctioning anti-oxidant mechanisms. An excess of exogenous oxidative stress (*i.e.* from plasmas) causes a disturbance of the oxidative balance in these cells, which can exceed the cellular anti-oxidative defence, and lead to cell death by activating intra-cellular signalling pathways [126,127]. Besides, it has been shown that the biological effects

triggered by plasmas can also be mediated by plasma-treated liquids, thereby opening possibilities for local delivery of these liquids parenterally.

1.3.2. Plasma-treated liquids

As discussed earlier, APPJ devices generate in liquids a large variety of RONS. Among them radicals ($O_2^{\bullet-}$, $O_2^{\bullet 2-}$, $^{\bullet}OH$), molecules, peroxides (ROOR) and ions (*i.e.* ^{-}OH, NO_2^-, NO_3^-), also freely moving charges and strong electric fields which are the key parameters of the APPJ sources application. The interaction of APPJs with liquids derives in the diffusion and reaction of these RONS to create secondary reactive species.

Many parameters affect the generation of RONS in solutions, the differences in chemical composition being critical to that aim. Mechanisms induced by APPJ treatment in liquids have already been reported in several excellent reviews [128–135]. It is important to keep in mind that the kind and concentrations of RONS generated in liquids can differ regarding the plasma device employed and the settled parameters (*i.e.* carrier gas, gas flow, distance of treatment, discharge electrode, plasma length, shape, voltage, current, etc.) [136–138]. RONS are created through a cascade of reaction which starts from the mixture of the gas discharge with the ambient air generating more species and solvated electrons at the near-surface of the plasma-treated liquid. More RONS are produced at the plasma-liquid interface when these excited species enter in contact with the treated liquid and then transported into the intermediate liquid before to reach the target site.

Long-lived species such as H_2O_2 and NO_2^- are by far the species mostly characterized, followed by NO_3^-. The methodology/equipment for detection of short-lived species such as hydroxyl (^{-}OH), peroxo- (HOO^-), O_2^-, or peroxinitrite ($ONOO^-$) radicals is more challenging so it is less often measured in literature. In this regard, it has been shown that not a single species is responsible for the anticancer effect observed, and that the interplay of a number of reactive species is crucial.

1.3.3. Plasma-treated polymers in Plasma Medicine

In this sense, the interactions between plasmas and liquids (*i.e.* polymer solutions) and semi-solid polymer state have opened new pathways to better understand interactions between plasma and biological tissues [139] and opened the avenue for designing novel delivery systems. RONS from APPJ are generated in liquids which can be employed in local delivery as a non-invasive therapy [135,140–142]. In that direction, investigation on APPJ-treated polymers can be of great interest by combining both properties: polymers and RONS from plasma for biomedical applications.

Despite extensive literature devoted to plasma modification of polymers for TE already described, the research regarding plasma treatment of hydrated polymers, polymer solutions or hydrogels at atmospheric pressure is scarce. Table 1-2 summarizes the few polymers investigated in solution or hydrogel state using APPJ in views of *Plasma Medicine* applications. Szili and co-workers recently started to investigate interactions between APPJ and hydrogels employed as tissue model [139,143] in order to understand effects previously observed in biological tissues. The investigation on the delivery and transport of RONS through synthetic tissue is important for the future development of APPJ medical therapies as well as to improve the understanding of APPJ interactions with soft tissues. Theoretical modelling of the delivery of RONS from atmospheric plasmas to liquids and living tissues has been already studied [144,145]. As mentioned different hydrogels have been employed as models of real biological tissues and cells (Figure 1.4) ; Agarose [143,146–148] and gelatine [149–152] thin film hydrogels were used as a substitutes for the tissue barrier in order to understand potential mechanisms involved during plasma treatment of the skin.

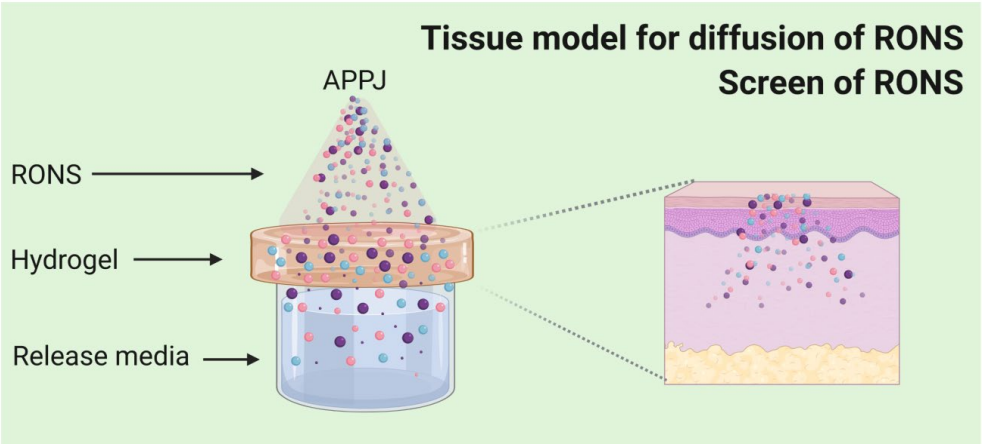

Figure 1.4: Current strategies related to treatment of hydrogels for applications in *Plasma Medicine*: Hydrogels are used as surrogates of tissues to investigate the penetration depth of plasmas, or also as screens for certain RONS during plasma treatment.

Table 1-2: Polymers investigated by APPJ in *Plasma Medicine* field.

Polymer	Polymer state	Plasma type	Objective	Effects	[Refs]
Gelatin	Hydrogel (mm thick)	APPJ (He)	Investigation of plasma-induced phenomena within real tissues	Dehydratation of the gelatin RONS transportation	[149,152] [150,151]
Agarose	Hydrogel (mm thick)	APPJ (He)	Monitoring APPJ interactions with real tissues	RONS accumulation in the hydrogel Release from the hydrogel	[143,147,148]

An APPJ working with He was employed where RONS such as hydrogen peroxide, nitrite, nitrate and molecular oxygen generated in liquid and in the hydrogel target after plasma treatment were quantified through chemical probes and UV absorption [146]. Results revealed that the concentration of RONS generated in the liquid below the hydrogel films and the rate of generation can be tuned with the plasma exposure time, the hydrogel film thickness, the type of gas used for plasma generation, the gas flow and the distance between the plasma source and the target [143]. The amount of RONS is also dependant of the hydrogel concentration and composition. The penetration of RONS into the hydrogels and their quantification into liquid media were allowed after plasma treatment [149]. It was observed that RONS can be accumulated in the hydrogel up to a certain threshold concentration, at which point they can be released into the aqueous phase through a slow diffusion molecular process [143]. It has been shown that in the hydrogel films the distribution of RONS generated is not uniform [149]. A part of a slight dehydration, APPJ did not induce visual damage to the hydrogel film. A delay in the apparition of RONS in deionised water in presence of the hydrogel film on the top of the well plate is noticed due to the penetration depth from the hydrogel thickness [146]. A linear time dependence in the increase of RONS is observed up to 40 min when the jet is switched off after plasma treatment traducing potential chemical reactions that can occur post plasma treatment in liquid media. The results obtained from these studies confirmed the generation and the transport of RONS from the APPJ through the hydrogel film to the liquid media [148], [150].

In that direction, in this PhD. Thesis, a new approach related to the treatment of polymer solutions using APPJ is investigated to develop hydrogels which may act as reservoir of plasma-generated RONS and thus be used as local delivery systems of RONS (Figure 1.5).

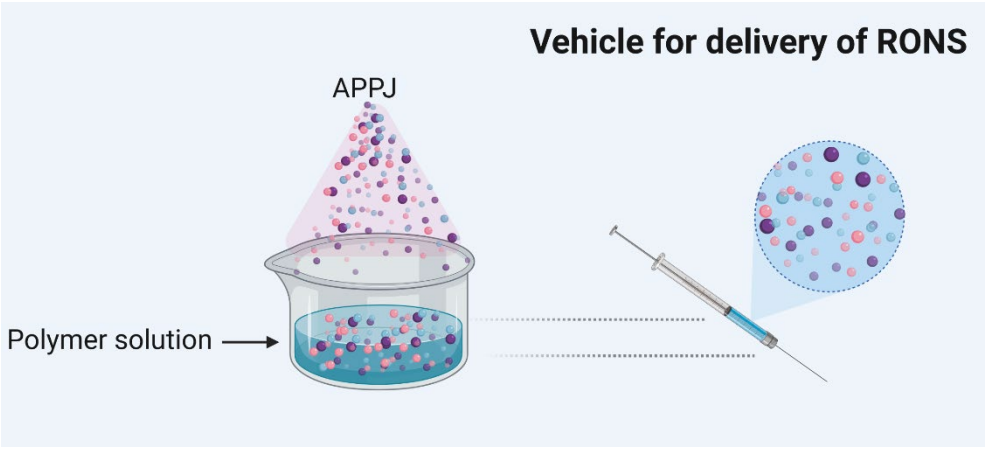

Figure 1.5: Novel strategy investigated in this PhD. Thesis: Treatment of biocompatible polymeric solutions with ability to crosslink, to generate and deliver RONS locally to the diseased site.

1.4. CONCLUSION

Despite plasma treatment of polymers has been known for some decades, their ability improving biocompatibility by an environmentally friendly technique still raises great interest, especially in views of tissue engineering. In this sense, the enhanced biological behaviour of plasma-treated scaffolds of several polymers is promising.

Moreover, the evolution of plasma devices, with the advent of more simple and compact plasma devices working at atmospheric pressure opens new avenues in the field. The field has moved from treating solid polymers, with the main aim of grafting new chemical moieties on the surface, to delivering and entrapping the reactive species from plasmas to biological tissues.

This is reflected in the translation of this area towards *Plasma Medicine*, wherein treatment of hydrogels with atmospheric plasmas is emerging as useful in a variety of areas, including investigation of the behaviour of plasmas in the treatment of real tissues and as will be the focus of this thesis, their use as delivery systems for RONS. In summary, these novel areas of research are certainly paving the way for exciting discoveries.

REFERENCES

1. Park, J.L.R.S. *Biomaterials: An Introduction*; Springer, Ed.; 3rd Editio.; Springer Science+Business Media, LLC: New York, 2007;
2. Griffith, L.G. Polymeric biomaterials. *Acta Mater.* **2000**, *48*, 263–277.
3. Shoichet, M.S. Polymer scaffolds for biomaterials applications. *Macromolecules* **2010**, *43*, 581–591.
4. Elbert, D.L.; Hubbell, J.A. Surface treatments of polymers for biocompatibility. *Annu. Rev. Mater. Sci.* **1996**, *26*, 365–394.
5. Hezi-Yamit, A.; Sullivan, C.; Wong, J.; David, L.; Chen, M.; Cheng, P.; Shumaker, D.; Wilcox, J.N.; Udipi, K. Impact of polymer hydrophilicity on biocompatibility: Implication for DES polymer design. *J. Biomed. Mater. Res. Part A* **2009**, *90A*, 133–141.
6. Thurston, R.M.; Clay, J.D.; Schulte, M.D. Effect of Atmospheric Plasma Treatment On Polymer Surface Energy and Adhesion. *J. Plast. Film Sheeting* **2007**, *23*, 63–78.
7. Schonhorn, H.; Hansen, R.H. Surface treatment of polymers for adhesive bonding. *J. Appl. Polym. Sci.* **1967**, *11*, 1461–1474.
8. Nedela, O.; Slepicka, P.; Švorcík, V. Surface modification of polymer substrates for biomedical applications. *Materials (Basel).* 2017, *10*.
9. Bu, Y.; Ma, J.; Bei, J.; Wang, S. Surface Modification of Aliphatic Polyester to Enhance Biocompatibility. *Front. Bioeng. Biotechnol.* **2019**, *7*.
10. Katti, D.; Vasita, R.; Shanmugam, K. Improved Biomaterials for Tissue Engineering Applications: Surface Modification of Polymers. *Curr. Top. Med. Chem.* **2008**, *8*, 341–353.
11. Slepičková Kasálková, N.; Slepička, P.; Bačáková, L.; Sajdl, P.; Švorčík, V. Biocompatibility of plasma nanostructured biopolymers. *Nucl. Instruments Methods Phys. Res. Sect. B Beam Interact. with Mater. Atoms* **2013**, *307*, 642–646.
12. Ma, Z.; Mao, Z.; Gao, C. Surface modification and property analysis of biomedical polymers used for tissue engineering. *Colloids Surfaces B Biointerfaces* **2007**, *60*, 137–157.
13. Bauser, H.; Chmiel, H. Improvement of the Biocompatibility of Polymers Through Surface Modification. In *Polymers in Medicine*; Springer US: Boston, MA, 1983; pp. 297–309.
14. Montanari, L.; Costantini, M.; Signoretti, E.C.; Valvo, L.; Santucci, M.; Bartolomei,

M.; Fattibene, P.; Onori, S.; Faucitano, A.; Conti, B.; et al. Gamma irradiation effects on poly(dl-lactictide-co-glycolide) microspheres. *J. Control. Release* **1998**, *56*, 219–229.

15. Loo, S.C.J.; Ooi, C.P.; Boey, Y.C.F. Radiation effects on poly(lactide-co-glycolide) (PLGA) and poly(l-lactide) (PLLA). *Polym. Degrad. Stab.* **2004**, *83*, 259–265.
16. Koo, G.-H.; Jang, J. Surface modification of poly(lactic acid) by UV/Ozone irradiation. *Fibers Polym.* **2008**, *9*, 674–678.
17. Desai, S.M.; Singh, R.P. Surface Modification of Polyethylene. In; Springer, Berlin, Heidelberg; pp. 231–294.
18. Stoffels, E.; Flikweert, A.J.; Stoffels, W.W.; Kroesen, G.M.W. Plasma needle: a non-destructive atmospheric plasma source for fine surface treatment of (bio)materials. *Plasma Sources Sci. Technol.* **2002**, *11*, 383–388.
19. Goddard, J.M.; Hotchkiss, J.H. Polymer surface modification for the attachment of bioactive compounds. *Prog. Polym. Sci.* **2007**, *32*, 698–725.
20. Desmet, T.; Morent, R.; De Geyter, N.; Leys, C.; Schacht, E.; Dubruel, P. Nonthermal Plasma Technology as a Versatile Strategy for Polymeric Biomaterials Surface Modification: A Review. *Biomacromolecules* **2009**, *10*, 2351–2378.
21. Langmuir, I. Oscillations in Ionized Gases. *Proc. Natl. Acad. Sci. U. S. A.* **1928**, *14*, 627–37.
22. Langmuir, I.; Jones, H.A. Collisions Between Electrons and Gas Molecules. *Phys. Rev.* **1928**, *31*, 357–404.
23. Langmuir, I. Electric discharges in gases at low pressures. *J. Franklin Inst.* **1932**, *214*, 275–298.
24. Bittencourt, J.A. *Fundamentals of Plasma Physics*; Springer, Ed.; 3rd ed.; Springer-Verlag New York, 2004;
25. Keidar, M. *Plasma Cancer Therapy*; Springer, 2020;
26. Ikada, Y. Surface modification of polymers for medical applications. *Biomaterials* **1994**, *15*, 725–736.
27. Tanaka, H.; Ishikawa, K.; Mizuno, M.; Toyokuni, S.; Kajiyama, H.; Kikkawa, F.; Metelmann, H.-R.; Hori, M. State of the art in medical applications using non-thermal atmospheric pressure plasma. *Rev. Mod. Plasma Phys.* **2017**, *1*, 3.
28. Chu, P..; Chen, J..; Wang, L..; Huang, N. Plasma-surface modification of biomaterials. *Mater. Sci. Eng. R Reports* **2002**, *36*, 143–206.

29. Hori, M. General introduction. In *Plasma Medical Science*; Elsevier, 2018; pp. 1–4 ISBN 9780128150047.
30. Yasuda, H.; Gazicki, M. Biomedical applications of plasma polymerization and plasma treatment of polymer surfaces. *Biomaterials* 1982, *3*, 68–77.
31. Graves, D.B. Low temperature plasma biomedicine: A tutorial review. *Phys. Plasmas* **2014**, *21*, 080901.
32. Favia, P.; Sardella, E.; Gristina, R.; D'Agostino, R. Novel plasma processes for biomaterials: micro-scale patterning of biomedical polymers. *Surf. Coatings Technol.* **2003**, *169–170*, 707–711.
33. d'Agostino, R.; Favia, P.; Oehr, C.; Wertheimer, M.R. Low-Temperature Plasma Processing of Materials: Past, Present, and Future. *Plasma Process. Polym.* **2005**, *2*, 7–15.
34. Liston, E.M.; Martinu, L.; Wertheimer, M.R. Plasma surface modification of polymers for improved adhesion: a critical review. *J. Adhes. Sci. Technol.* **1993**, *7*, 1091–1127.
35. Loh, J.H. Plasma surface modification in biomedical applications. *Med. Device Technol. 10*, 24–30.
36. Chu, P.K. Plasma-Treated Biomaterials. *IEEE Trans. Plasma Sci.* **2007**, *35*, 181–187.
37. Morent, R.; De Geyter, N.; Desmet, T.; Dubruel, P.; Leys, C. Plasma Surface Modification of Biodegradable Polymers: A Review. *Plasma Process. Polym.* **2011**, *8*, 171–190.
38. Gomathi, N.; Sureshkumar, A.; Neogi, S. RF plasma-treated polymers for biomedical applications. *Curr. Sci. 94*, 1478–1486.
39. Poncin-Epaillard, F.; Legeay, G. Surface engineering of biomaterials with plasma techniques. *J. Biomater. Sci. Polym. Ed.* **2003**, *14*, 1005–1028.
40. Desmet, T.; Morent, R.; De Geyter, N.; Leys, C.; Schacht, E.; Dubruel, P. Nonthermal Plasma Technology as a Versatile Strategy for Polymeric Biomaterials Surface Modification: A Review. *Biomacromolecules* **2009**, *10*, 2351–2378.
41. Cheruthazhekatt, S.; Černák, M.; Slavíček, P.; Havel, J. Gas plasmas and plasma modified materials in medicine. *J. Appl. Biomed.* **2010**, *8*, 55–66.
42. Trizio, I.; Trulli, M.G.; Lo Porto, C.; Pignatelli, D.; Camporeale, G.; Palumbo, F.; Sardella, E.; Gristina, R.; Favia, P. Plasma Processes for Life Sciences. In *Reference*

Module in Chemistry, Molecular Sciences and Chemical Engineering; Elsevier, 2018.

43. Canal, C.; Molina, R.; Bertran, E.; Erra, P. Wettability, ageing and recovery process of plasma-treated polyamide 6. *J. Adhes. Sci. Technol.* **2004**, *18*, 1077–1089.
44. Schutze, A.; Jeong, J.Y.; Babayan, S.E.; Jaeyoung Park; Selwyn, G.S.; Hicks, R.F. The atmospheric-pressure plasma jet: a review and comparison to other plasma sources. *IEEE Trans. Plasma Sci.* **1998**, *26*, 1685–1694.
45. Penkov, O. V.; Khadem, M.; Lim, W.-S.; Kim, D.-E. A review of recent applications of atmospheric pressure plasma jets for materials processing. *J. Coatings Technol. Res.* **2015**, *12*, 225–235.
46. Grande, S.; Van Guyse, J.; Nikiforov, A.Y.; Onyshchenko, I.; Asadian, M.; Morent, R.; Hoogenboom, R.; De Geyter, N. Atmospheric Pressure Plasma Jet Treatment of Poly-ε-caprolactone Polymer Solutions To Improve Electrospinning. *ACS Appl. Mater. Interfaces* **2017**, *9*, 33080–33090.
47. Grande, S.; Cools, P.; Asadian, M.; Van Guyse, J.; Onyshchenko, I.; Declercq, H.; Morent, R.; Hoogenboom, R.; De Geyter, N. Fabrication of PEOT/PBT Nanofibers by Atmospheric Pressure Plasma Jet Treatment of Electrospinning Solutions for Tissue Engineering. *Macromol. Biosci.* **2018**, 1800309.
48. Shi, Q.; Vitchuli, N.; Nowak, J.; Lin, Z.; Guo, B.; Mccord, M.; Bourham, M.; Zhang, X. Atmospheric plasma treatment of pre-electrospinning polymer solution: A feasible method to improve electrospinnability. *J. Polym. Sci. Part B Polym. Phys.* **2011**, *49*, 115–122.
49. Nakagawa, M.; Teraoka, F.; Fujimoto, S.; Hamada, Y.; Kibayashi, H.; Takahashi, J. Improvement of cell adhesion on poly(L-lactide) by atmospheric plasma treatment. *J. Biomed. Mater. Res. Part A* **2006**, *77A*, 112–118.
50. Shenton, M.J.; Stevens, G.C. Surface modification of polymer surfaces: atmospheric plasma versus vacuum plasma treatments. *J. Phys. D. Appl. Phys.* **2001**, *34*, 2761–2768.
51. Kusano, Y. *Atmospheric pressure plasmas for polymer surface modification: Alternating current gliding arcs and ultrasound enhanced plasmas*; DTU Wind Energy, 2019; ISBN 978-87-93549-49-4.
52. Kusano, Y. Atmospheric Pressure Plasma Processing for Polymer Adhesion: A Review. *J. Adhes.* **2014**, *90*, 755–777.

53. Kostov, K.G.; Nishime, T.M.C.; Castro, A.H.R.; Toth, A.; Hein, L.R.O. Surface modification of polymeric materials by cold atmospheric plasma jet. *Appl. Surf. Sci.* **2014**, *314*, 367–375.

54. Geßner, C.; Bartels, V.; Betker, T.; Matucha, U.; Penache, C.; Klages, C.-P. Surface modification for biomedical purposes utilizing dielectric barrier discharges at atmospheric pressure. *Thin Solid Films* **2004**, *459*, 118–121.

55. Laroussi, M.; Lu, X. Room-temperature atmospheric pressure plasma plume for biomedical applications. *Appl. Phys. Lett.* **2005**, *87*, 113902.

56. Winter, J.; Brandenburg, R.; Weltmann, K.-D. Atmospheric pressure plasma jets: an overview of devices and new directions. *Plasma Sources Sci. Technol.* **2015**, *24*, 064001.

57. Laroussi, M.; Akan, T. Arc-Free Atmospheric Pressure Cold Plasma Jets: A Review. *Plasma Process. Polym.* **2007**, *4*, 777–788.

58. Cheng, C.; Liye, Z.; Zhan, R.-J. Surface modification of polymer fibre by the new atmospheric pressure cold plasma jet. *Surf. Coatings Technol.* **2006**, *200*, 6659–6665.

59. Stoffels, E.; Flikweert, A.J.; Stoffels, W.W.; Kroesen, G.M.W. Plasma needle: a non-destructive atmospheric plasma source for fine surface treatment of (bio)materials. *Plasma Sources Sci. Technol.* **2002**, *11*, 383–388.

60. Laroussi, M.; Lu, X. Room-temperature atmospheric pressure plasma plume for biomedical applications. *Appl. Phys. Lett.* **2005**, *87*, 113902.

61. Lu, X.; Xiong, Z.; Zhao, F.; Xian, Y.; Xiong, Q.; Gong, W.; Zou, C.; Jiang, Z.; Pan, Y. A simple atmospheric pressure room-temperature air plasma needle device for biomedical applications. *Appl. Phys. Lett.* **2009**, *95*, 181501.

62. Tucker, B.S.; Baker, P.A.; Xu, K.G.; Vohra, Y.K.; Thomas, V. Atmospheric pressure plasma jet: A facile method to modify the intimal surface of polymeric tubular conduits. *J. Vac. Sci. Technol. A* **2018**, *36*, 04F404.

63. Surucu, S.; Masur, K.; Turkoglu Sasmazel, H.; Von Woedtke, T.; Weltmann, K.D. Atmospheric plasma surface modifications of electrospun PCL/chitosan/PCL hybrid scaffolds by nozzle type plasma jets for usage of cell cultivation. *Appl. Surf. Sci.* **2016**, *385*, 400–409.

64. Wang, M.; Cheng, X.; Zhu, W.; Holmes, B.; Keidar, M.; Zhang, L.G. Design of Biomimetic and Bioactive Cold Plasma-Modified Nanostructured Scaffolds for

Enhanced Osteogenic Differentiation of Bone Marrow-Derived Mesenchymal Stem Cells. *Tissue Eng. Part A* **2014**, *20*, 1060–1071.

65. Wang, M.; Zhou, Y.; Shi, D.; Chang, R.; Zhang, J.; Keidar, M.; Webster, T.J. Cold atmospheric plasma (CAP)-modified and bioactive protein-loaded core–shell nanofibers for bone tissue engineering applications. *Biomater. Sci.* **2019**.
66. Wang, M.; Favi, P.; Cheng, X.; Golshan, N.H.; Ziemer, K.S.; Keidar, M.; Webster, T.J. Cold atmospheric plasma (CAP) surface nanomodified 3D printed polylactic acid (PLA) scaffolds for bone regeneration. *Acta Biomater.* **2016**, *46*, 256–265.
67. Poncin-Epaillard, F.; Legeay, G. Surface engineering of biomaterials with plasma techniques. *J. Biomater. Sci. Polym. Ed.* 2003, *14*, 1005–1028.
68. Van Deynse, A.; Cools, P.; Leys, C.; Morent, R.; De Geyter, N. Surface modification of polyethylene in an argon atmospheric pressure plasma jet. *Surf. Coatings Technol.* **2015**, *276*, 384–390.
69. Mozetič, M.; Primc, G.; Vesel, A.; Zaplotnik, R.; Modic, M.; Junkar, I.; Recek, N.; Klanjšek-Gunde, M.; Guhy, L.; Sunkara, M.K.; et al. Application of extremely non-equilibrium plasmas in the processing of nano and biomedical materials. *Plasma Sources Sci. Technol.* **2015**, *24*, 015026.
70. Biederman, H.; Osada, Y. Plasma chemistry of polymers. In; Springer, Berlin, Heidelberg, 1990; pp. 57–109.
71. Nelea, V.; Luo, L.; Demers, C.N.; Antoniou, J.; Petit, A.; Lerouge, S.; R. Wertheimer, M.; Mwale, F. Selective inhibition of type X collagen expression in human mesenchymal stem cell differentiation on polymer substrates surface-modified by glow discharge plasma. *J. Biomed. Mater. Res. Part A* **2005**, *75A*, 216–223.
72. Chu, P..; Chen, J..; Wang, L..; Huang, N. Plasma-surface modification of biomaterials. *Mater. Sci. Eng. R Reports* **2002**, *36*, 143–206.
73. Liston, E.M.; Martinu, L.; Wertheimer, M.R. Plasma surface modification of polymers for improved adhesion: a critical review. *J. Adhes. Sci. Technol.* **1993**, *7*, 1091–1127.
74. Nageswaran, G.; Jothi, L.; Jagannathan, S. Plasma Assisted Polymer Modifications. *Non-Thermal Plasma Technol. Polym. Mater.* **2019**, 95–127.
75. Cvelbar, U.; Canal, C.; Hori, M. Plasma-inspired biomaterials. *J. Phys. D. Appl. Phys.* **2017**, *50*, 040201.

76. Fridman, A. *Plasma Chemistry*; Press, C.U., Ed.; Cambridge.; New York, USA, 2008;

77. Recek, N.; Resnik, M.; Motaln, H.; Lah-Turnšek, T.; Augustine, R.; Kalarikkal, N.; Thomas, S.; Mozetič, M. Cell Adhesion on Polycaprolactone Modified by Plasma Treatment. *Int. J. Polym. Sci.* **2016**, *2016*, 1–9.

78. Shen, H.; Hu, X.; Bei, J.; Wang, S. The immobilization of basic fibroblast growth factor on plasma-treated poly(lactide-co-glycolide). *Biomaterials* **2008**, *29*, 2388–2399.

79. Lee, H.-U.; Jeong, Y.-S.; Jeong, S.-Y.; Park, S.-Y.; Bae, J.-S.; Kim, H.-G.; Cho, C.-R. Role of reactive gas in atmospheric plasma for cell attachment and proliferation on biocompatible poly ε-caprolactone film. *Appl. Surf. Sci.* **2008**, *254*, 5700–5705.

80. Jacobs, T.; Declercq, H.; De Geyter, N.; Cornelissen, R.; Dubruel, P.; Leys, C.; Beaurain, A.; Payen, E.; Morent, R. Plasma surface modification of polylactic acid to promote interaction with fibroblasts. *J. Mater. Sci. Mater. Med.* **2013**, *24*, 469–478.

81. Ikada, Y.; Tsuji, H. Biodegradable polyesters for medical and ecological applications. *Macromol. Rapid Commun.* **2000**, *21*, 117–132.

82. Chu, C.F.L.; Lu, A.; Liszkowski, M.; Sipehia, R. Enhanced growth of animal and human endothelial cells on biodegradable polymers. *Biochim. Biophys. Acta - Gen. Subj.* **1999**, *1472*, 479–485.

83. Slepička, P.; Trostová, S.; Slepičková Kasálková, N.; Kolská, Z.; Sajdl, P.; Švorčík, V. Surface Modification of Biopolymers by Argon Plasma and Thermal Treatment. *Plasma Process. Polym.* **2012**, *9*, 197–206.

84. Khorasani, M.T.; Mirzadeh, H.; Irani, S. Plasma surface modification of poly (l-lactic acid) and poly (lactic-co-glycolic acid) films for improvement of nerve cells adhesion. *Radiat. Phys. Chem.* **2008**, *77*, 280–287.

85. Khorasani, M.T.; Mirzadeh, H.; Irani, S. Comparison of fibroblast and nerve cells response on plasma treated poly (L-lactide) surface. *J. Appl. Polym. Sci.* **2009**, *112*, 3429–3435.

86. Yang, J.; Bei, J.; Wang, S. Improving cell affinity of -poly(<scp>D,L</scp> -lactide) film modified by anhydrous ammonia plasma treatment. *Polym. Adv. Technol.* **2002**, *13*, 220–226.

87. TERAOKA, F.; NAKAGAWA, M.; HARA, M. Surface Modification of Poly(L-lactide) by Atmospheric Pressure Plasma Treatment and Cell Response. *Dent. Mater.*

J. **2006**, *25*, 560–565.

88. Hasirci, N.; Endogan, T.; Vardar, E.; Kiziltay, A.; Hasirci, V. Effect of oxygen plasma on surface properties and biocompatibility of PLGA films. *Surf. Interface Anal.* **2010**, *42*, 486–491.
89. Park, H.; Lee, J.W.; Park, K.E.; Park, W.H.; Lee, K.Y. Stress response of fibroblasts adherent to the surface of plasma-treated poly(lactic-co-glycolic acid) nanofiber matrices. *Colloids Surfaces B Biointerfaces* **2010**, *77*, 90–95.
90. Ghobeira, R.; Philips, C.; Declercq, H.; Cools, P.; De Geyter, N.; Cornelissen, R.; Morent, R. Effects of different sterilization methods on the physico-chemical and bioresponsive properties of plasma-treated polycaprolactone films. *Biomed. Mater.* **2017**, *12*, 015017.
91. Prabhakaran, M.P.; Venugopal, J.; Chan, C.K.; Ramakrishna, S. Surface modified electrospun nanofibrous scaffolds for nerve tissue engineering. *Nanotechnology* **2008**, *19*, 455102.
92. Pappa, A.M.; Karagkiozaki, V.; Krol, S.; Kassavetis, S.; Konstantinou, D.; Pitsalidis, C.; Tzounis, L.; Pliatsikas, N.; Logothetidis, S. Oxygen-plasma-modified biomimetic nanofibrous scaffolds for enhanced compatibility of cardiovascular implants. *Beilstein J. Nanotechnol.* **2015**, *6*, 254–262.
93. Yildirim, E.D.; Besunder, R.; Pappas, D.; Allen, F.; Güçeri, S.; Sun, W. Accelerated differentiation of osteoblast cells on polycaprolactone scaffolds driven by a combined effect of protein coating and plasma modification. *Biofabrication* **2010**, *2*, 014109.
94. Fisher, E.R. Challenges in the characterization of plasma-processed three-dimensional polymeric scaffolds for biomedical applications. *ACS Appl. Mater. Interfaces* **2013**, *5*, 9312–9321.
95. Yildirim, E.D.; Ayan, H.; Vasilets, V.N.; Fridman, A.; Guceri, S.; Sun, W. Effect of Dielectric Barrier Discharge Plasma on the Attachment and Proliferation of Osteoblasts Cultured over Poly(ε-caprolactone) Scaffolds. *Plasma Process. Polym.* **2008**, *5*, 58–66.
96. Sardella, E.; Fisher, E.R.; Shearer, J.C.; Garzia Trulli, M.; Gristina, R.; Favia, P. N 2 /H 2 o Plasma Assisted Functionalization of Poly(ε-caprolactone) Porous Scaffolds: Acidic/Basic Character versus Cell Behavior. *Plasma Process. Polym.* **2015**, *12*, 786–798.

97. Intranuovo, F.; Gristina, R.; Brun, F.; Mohammadi, S.; Ceccone, G.; Sardella, E.; Rossi, F.; Tromba, G.; Favia, P. Plasma Modification of PCL Porous Scaffolds Fabricated by Solvent-Casting/Particulate-Leaching for Tissue Engineering. *Plasma Process. Polym.* **2014**, *11*, 184–195.

98. Domingos, M.; Intranuovo, F.; Gloria, A.; Gristina, R.; Ambrosio, L.; Bártolo, P.J.; Favia, P. Improved osteoblast cell affinity on plasma-modified 3-D extruded PCL scaffolds. *Acta Biomater.* **2013**, *9*, 5997–6005.

99. Valence, S. De; Tille, J.C.; Chaabane, C.; Gurny, R.; Bochaton-Piallat, M.L.; Walpoth, B.H.; Möller, M. Plasma treatment for improving cell biocompatibility of a biodegradable polymer scaffold for vascular graft applications. *Eur. J. Pharm. Biopharm.* **2013**, *85*, 78–86.

100. Trizio, I.; Intranuovo, F.; Gristina, R.; Dilecce, G.; Favia, P. He/O 2 Atmospheric Pressure Plasma Jet Treatments of PCL Scaffolds for Tissue Engineering and Regenerative Medicine. *Plasma Process. Polym.* **2015**, *12*, 1451–1458.

101. Slepička, P.; Stýblová, S.; Kasálková, N.S.; Rimpelová, S.; Švorčík, V. Cytocompatibility of polyhydroxybutyrate modified by plasma discharge. *Polym. Eng. Sci.* **2014**, *54*, 1231–1238.

102. Slepička, P.; Malá, Z.; Rimpelová, S.; Slepičková Kasálková, N.; Švorčík, V. Plasma treatment of the surface of poly(hydroxybutyrate) foil and non-woven fabric and assessment of the biological properties. *React. Funct. Polym.* **2015**, *95*, 71–79.

103. Pompe, T.; Keller, K.; Mothes, G.; Nitschke, M.; Teese, M.; Zimmermann, R.; Werner, C. Surface modification of poly(hydroxybutyrate) films to control cell-matrix adhesion. *Biomaterials* **2007**, *28*, 28–37.

104. Wang, Y.; Lu, L.; Zheng, Y.; Chen, X. Improvement in hydrophilicity of PHBV films by plasma treatment. *J. Biomed. Mater. Res. Part A* **2006**, *76A*, 589–595.

105. Unalan, I.; Colpankan, O.; Albayrak, A.Z.; Gorgun, C.; Urkmez, A.S. Biocompatibility of plasma-treated poly(3-hydroxybutyrate-co-3-hydroxyvalerate) nanofiber mats modified by silk fibroin for bone tissue regeneration. *Mater. Sci. Eng. C* **2016**, *68*, 842–850.

106. Torun Köse, G.; Korkusuz, F.; Korkusuz, P.; Purali, N.; Özkul, A.; Hasirci, V. Bone generation on PHBV matrices: An in vitro study. *Biomaterials* **2003**, *24*, 4999–5007.

107. Lucchesi, C.; Ferreira, B.M.P.; Duek, E.A.R.; Santos, A.R.; Joazeiro, P.P. Increased response of Vero cells to PHBV matrices treated by plasma. *J. Mater. Sci. Mater.*

Med. **2008**, *19*, 635–643.

108. Biazar, E.; Keshel, S.H.; Sahebalzamani, A.; Heidari, M. Design of oriented porous PHBV scaffold as a neural guide. *Int. J. Polym. Mater. Polym. Biomater.* **2014**, *63*, 753–757.
109. Luna, S.M.; Silva, S.S.; Gomes, M.E.; Mano, J.F.; Reis, R.L. Cell adhesion and proliferation onto chitosan-based membranes treated by plasma surface modification. *J. Biomater. Appl.* **2011**, *26*, 101–116.
110. Sasmazel, H.T.; Manolache, S.; Gümüşderelioğlu, M. Functionalization of Nonwoven Pet Fabrics by Water/O2 Plasma for Biomolecule Mediated Cell Cultivation. *Plasma Process. Polym.* **2010**, *7*, 588–600.
111. Recek, N.; Jaganjac, M.; Kolar, M.; Milkovic, L.; Mozetič, M.; Stana-Kleinschek, K.; Vesel, A. Protein Adsorption on Various Plasma-Treated Polyethylene Terephthalate Substrates. *Molecules* **2013**, *18*, 12441–12463.
112. Recek, N.; Mozetič, M.; Jaganjac, M.; Milkovič, L.; Žarkovic, N.; Vesel, A. Improved proliferation of human osteosarcoma cells on oxygen plasma treated polystyrene. *Vacuum* **2013**, *98*, 116–121.
113. Van Kooten, T.G.; Spijker, H.T.; Busscher, H.J. Plasma-treated polystyrene surfaces: Model surfaces for studying cell-biomaterial interactions. *Biomaterials* **2004**, *25*, 1735–1747.
114. Rimpelová, S.; Kasálková, N.S.; Slepička, P.; Lemerová, H.; Švorčík, V.; Ruml, T. Plasma treated polyethylene grafted with adhesive molecules for enhanced adhesion and growth of fibroblasts. *Mater. Sci. Eng. C* **2013**, *33*, 1116–1124.
115. Jin Ho Lee; Jong Woo Park; Hai Bang Lee Cell adhesion and growth on polymer surfaces with hydroxyl groups prepared by water vapour plasma treatment. *Biomaterials* **1991**, *12*, 443–448.
116. Laroussi, M.; Laroussi; Mounir Plasma Medicine: A Brief Introduction. *Plasma 2018, Vol. 1, Pages 47-60* **2018**, *1*, 47–60.
117. Fridman, G.; Friedman, G.; Gutsol, A.; Shekhter, A.B.; Vasilets, V.N.; Fridman, A. Applied Plasma Medicine. *Plasma Process. Polym.* **2008**, *5*, 503–533.
118. Keidar, M. Plasma for cancer treatment. *Plasma Sources Sci. Technol.* **2015**, *24*, 033001.
119. Laroussi, M. Low-Temperature Plasma Jet for Biomedical Applications: A Review. *IEEE Trans. Plasma Sci.* **2015**, *43*, 703–712.

120. Keidar, M.; Shashurin, A.; Volotskova, O.; Ann Stepp, M.; Srinivasan, P.; Sandler, A.; Trink, B. Cold atmospheric plasma in cancer therapy. *Phys. Plasmas* **2013**, *20*, 057101.

121. Graves, D.B. The emerging role of reactive oxygen and nitrogen species in redox biology and some implications for plasma applications to medicine and biology. *J. Phys. D. Appl. Phys.* **2012**, *45*, 263001.

122. Trachootham, D.; Alexandre, J.; Huang, P. Targeting cancer cells by ROS-mediated mechanisms: a radical therapeutic approach? *Nat. Rev. Drug Discov.* **2009**, *8*, 579–591.

123. Zhao, S.; Xiong, Z.; Mao, X.; Meng, D.; Lei, Q.; Li, Y.; Deng, P.; Chen, M.; Tu, M.; Lu, X.; et al. Atmospheric Pressure Room Temperature Plasma Jets Facilitate Oxidative and Nitrative Stress and Lead to Endoplasmic Reticulum Stress Dependent Apoptosis in HepG2 Cells. *PLoS One* **2013**, *8*.

124. Diehn, M.; Cho, R.W.; Lobo, N.A.; Kalisky, T.; Dorie, M.J.; Kulp, A.N.; Qian, D.; Lam, J.S.; Ailles, L.E.; Wong, M.; et al. Association of reactive oxygen species levels and radioresistance in cancer stem cells. *Nature* **2009**, *458*, 780–783.

125. Ray, A.; Ranieri, P.; Karamchand, L.; Yee, B.; Foster, J.; Kopelman, R. Real-Time Monitoring of Intracellular Chemical Changes in Response to Plasma Irradiation. *Plasma Med.* **2017**, *7*, 7–26.

126. Barekzi, N.; Laroussi, M. Effects of Low Temperature Plasmas on Cancer Cells. *Plasma Process. Polym.* **2013**, *10*, 1039–1050.

127. Graves, D.B. Reactive Species from Cold Atmospheric Plasma: Implications for Cancer Therapy. *Plasma Process. Polym.* **2014**, *11*, 1120–1127.

128. Wende, K.; Williams, P.; Dalluge, J.; Van Gaens, W.; Aboubakr, H.; Bischof, J.; von Woedtke, T.; Goyal, S.M.; Weltmann, K.-D.; Bogaerts, A.; et al. Identification of the biologically active liquid chemistry induced by a nonthermal atmospheric pressure plasma jet. *Biointerphases* **2015**, *10*.

129. Bruggeman, P.J.; Kushner, M.J.; Locke, B.R.; Gardeniers, J.G.E.; Graham, W.G.; Graves, D.B.; Hofman-Caris, R.C.H.M.; Maric, D.; Reid, J.P.; Ceriani, E.; et al. Plasma–liquid interactions: a review and roadmap. *Plasma Sources Sci. Technol.* **2016**, *25*, 053002.

130. Uchida, G.; Nakajima, A.; Takenaka, K.; Koga, K.; Shiratani, M.; Setsuhara, Y. Gas Flow Rate Dependence of the Discharge Characteristics of a Plasma Jet Impinging

onto the Liquid Surface. *IEEE Trans. Plasma Sci.* **2015**, *43*, 4081–4087.

131. Lu, X.; Naidis, G.V.; Laroussi, M.; Reuter, S.; Graves, D.B.; Ostrikov, K. Reactive species in non-equilibrium atmospheric-pressure plasmas: Generation, transport, and biological effects. *Phys. Rep.* **2016**, *630*, 1–84.
132. Adamovich, I.; Baalrud, S.D.; Bogaerts, A.; Bruggeman, P.J.; Cappelli, M.; Colombo, V.; Czarnetzki, U.; Ebert, U.; Eden, J.G.; Favia, P.; et al. The 2017 Plasma Roadmap: Low temperature plasma science and technology. *J. Phys. D. Appl. Phys.* **2017**, *50*, 323001.
133. Samukawa, S.; Hori, M.; Rauf, S.; Tachibana, K.; Bruggeman, P.; Kroesen, G.; Whitehead, J.C.; Murphy, A.B.; Gutsol, A.F.; Starikovskaia, S.; et al. The 2012 Plasma Roadmap. *J. Phys. D. Appl. Phys.* **2012**, *45*, 253001.
134. Verlackt, C.C.W.; Van Boxem, W.; Bogaerts, A. Transport and accumulation of plasma generated species in aqueous solution. *Phys. Chem. Chem. Phys.* **2018**, *20*, 6845–6859.
135. Yan, D.; Sherman, J.H.; Keidar, M. The Application of the Cold Atmospheric Plasma-Activated Solutions in Cancer Treatment. *Anticancer. Agents Med. Chem.* **2017**, *17*.
136. Norberg, S.A.; Tian, W.; Johnsen, E.; Kushner, M.J. Atmospheric pressure plasma jets interacting with liquid covered tissue: touching and not-touching the liquid. *J. Phys. D. Appl. Phys.* **2014**, *47*.
137. Khlyustova, A.; Labay, C.; Machala, Z.; Ginebra, M.-P.; Canal, C. Important parameters in plasma jets for the production of RONS in liquids for plasma medicine: A brief review. *Front. Chem. Sci. Eng.* **2019**, *13*, 238–252.
138. Dobrynin, D.; Fridman, A.; Starikovskiy, A.Y. Reactive Oxygen and Nitrogen Species Production and Delivery Into Liquid Media by Microsecond Thermal Spark-Discharge Plasma Jet. *IEEE Trans. Plasma Sci.* **2012**, *40*, 2163–2171.
139. Szili, E.J.; Hong, S.H.; Oh, J.S.; Gaur, N.; Short, R.D. Tracking the Penetration of Plasma Reactive Species in Tissue Models. *Trends Biotechnol.* **2017**.
140. Sato, Y.; Yamada, S.; Takeda, S.; Hattori, N.; Nakamura, K.; Tanaka, H.; Mizuno, M.; Hori, M.; Kodera, Y. Effect of Plasma-Activated Lactated Ringer's Solution on Pancreatic Cancer Cells In Vitro and In Vivo. *Ann. Surg. Oncol.* **2018**, *25*, 299–307.
141. Takeda, S.; Yamada, S.; Hattori, N.; Nakamura, K.; Tanaka, H.; Kajiyama, H.; Kanda, M.; Kobayashi, D.; Tanaka, C.; Fujii, T.; et al. Intraperitoneal Administration

of Plasma-Activated Medium: Proposal of a Novel Treatment Option for Peritoneal Metastasis From Gastric Cancer. *Ann. Surg. Oncol.* **2017**, *24*, 1188–1194.

142. Van Boxem, W.; Van der Paal, J.; Gorbanev, Y.; Vanuytsel, S.; Smits, E.; Dewilde, S.; Bogaerts, A. Anti-cancer capacity of plasma-treated PBS: effect of chemical composition on cancer cell cytotoxicity. *Sci. Rep.* **2017**, *7*, 16478.
143. Szili, E.J.; Oh, J.-S.; Hong, S.-H.; Hatta, A.; Short, R.D. Probing the transport of plasma-generated RONS in an agarose target as surrogate for real tissue: dependency on time, distance and material composition. *J. Phys. D. Appl. Phys.* **2015**, *48*, 202001.
144. Chen, C.; Liu, D.X.; Liu, Z.C.; Yang, A.J.; Chen, H.L.; Shama, G.; Kong, M.G. A Model of Plasma-Biofilm and Plasma-Tissue Interactions at Ambient Pressure. *Plasma Chem. Plasma Process.* **2014**, *34*, 403–441.
145. Tian, W.; Kushner, M.J. Atmospheric pressure dielectric barrier discharges interacting with liquid covered tissue. *J. Phys. D. Appl. Phys.* **2014**, *47*, 165201.
146. Oh, J.-S.; Szili, E.J.; Gaur, N.; Hong, S.-H.; Furuta, H.; Kurita, H.; Mizuno, A.; Hatta, A.; Short, R.D. How to assess the plasma delivery of RONS into tissue fluid and tissue. *J. Phys. D. Appl. Phys.* **2016**, *49*.
147. Oh, J.; Szili, E.J.; Gaur, N.; Hong, S. In-situ UV Absorption Spectroscopy for Monitoring Transport of Plasma Reactive Species through Agarose as Surrogate for Tissue. *J. Photopolym. Sci. Technol.* **2015**, *28*.
148. Oh, J.-S.; Szili, E.J.; Hong, S.-H.; Gaur, N.; Ohta, T.; Hiramatsu, M.; Hatta, A.; Short, R.D.; Ito, M. Mass Spectrometry Analysis of the Real-Time Transport of Plasma-Generated Ionic Species Through an Agarose Tissue Model Target. *J. Photopolym. Sci. Technol.* **2017**, *30*, 317–323.
149. Marshall, S.E.; Jenkins, A.T.A.; Al-Bataineh, S.A.; Short, R.D.; Hong, S.-H.; Thet, N.T.; Oh, J.-S.; Bradley, J.W.; Szili, E.J. Studying the cytolytic activity of gas plasma with self-signalling phospholipid vesicles dispersed within a gelatin matrix. *J. Phys. D. Appl. Phys.* **2013**, *46*.
150. Gaur, N.; Szili, E.J.; Oh, J.-S.; Hong, S.-H.; Michelmore, A.; Graves, D.B.; Hatta, A.; Short, R.D. Combined effect of protein and oxygen on reactive oxygen and nitrogen species in the plasma treatment of tissue. *Appl. Phys. Lett.* **2015**, *107*, 103703.
151. Endre, J.S.; James, W.B.; Robert, D.S. A â€˜tissue modelâ€™™ to study the plasma

delivery of reactive oxygen species. *J. Phys. D. Appl. Phys.* **2014**, *47*, 152002.

152. Szili, E.J.; Gaur, N.; Hong, S.-H.; Kurita, H.; Oh, J.-S.; Ito, M.; Mizuno, A.; Hatta, A.; Cowin, A.J.; Graves, D.B.; et al. The assessment of cold atmospheric plasma treatment of DNA in synthetic models of tissue fluid, tissue and cells. *J. Phys. D. Appl. Phys.* **2017**, *50*, 274001.

CHAPTER 2

2. Selectivity of Plasma Jet Treatment and of Plasma-Conditioned Media on Bone Cancer Cell Lines

ABSTRACT

Atmospheric pressure plasma jets already demonstrated selectivity in several cancer cell lines both *in vitro* and *in vivo.* Their effects are essentially based on the biochemistry of the reactive oxygen and nitrogen species generated by plasmas in physiological liquids, also known as plasma-conditioned liquids. Plasma conditioned media are efficient in the generation of reactive species inducing selective cancer cell death. However, fewer studies reported on the selectivity of bone cancer cell lines using plasma conditioned media, so further investigation is needed. Here, 2 different volumes of cell culture media with or without cells with those were treated with plasma jet to compare the effects of direct treatment or of plasma-conditioned media. Biological effects were correlated with the concentrations of reactive species generated in the liquid by plasma treatment. A linear increase of reactive species in cell culture medium was obtained with plasma treatment time independently of the volume treated. Values up to 700 µM for H_2O_2 and 140 µM of NO_2^- were reached in 2 mL after 15 min of plasma treatment in AdvDMEM cell culture media. Selectivity towards bone cancer cells was observed after both direct and indirect plasma treatment, leading to a decrease cell viability of bone cancer cells down to 30 % for the longest plasma treatment, while maintaining the survival of healthy cells. Plasma conditioned media demonstrated its efficiency as a potential non-invasive technique for bone cancer therapy.

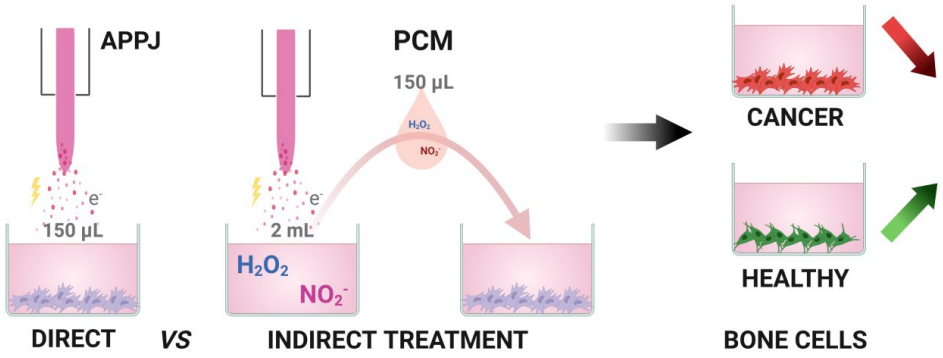

Figure 2.1: Representative scheme of Chapter 2; Effect of direct plasma treatment with an atmospheric pressure plasma jet (APPJ) and indirect treatment with Plasma Conditioned Media (PCM) on bone cancer and healthy bone cells.

2.1.INTRODUCTION

Primary bone cancers such as osteosarcoma are, in general, developmental diseases affecting primarily children and adolescents. Osteosarcoma is an aggressive malignant neoplasm that arises from primitive transformed cells of mesenchymal origin that exhibits osteoblastic differentiation, and thus produces malignant osteoid. Current therapies for osteosarcoma are not completely effective, and patients are prone to relapse. In this context, atmospheric pressure plasma jet (APPJ) treatments have arisen as a potential new therapy for cancer [1–3]. The emergent field of Plasma Medicine employs APPJ devices for cancer therapies [4,5]. In fact, APPJ have the potential to affect cells through complex biochemical processes with the ability to selectively kill cancer cells without affecting healthy cells, *i.e.* in the surrounding tissues [6–8]. This effect is mainly attributed to the reactive oxygen and nitrogen species (RONS) generated by APPJ, responsible to disturb the cell metabolism environment [9,10]. However, it is known that other components from plasmas such as electromagnetic fields and UV radiation also affect the cells; so many researchers rely preferably on direct plasma treatments.

Healthy cells already present a certain level of RONS for their metabolism regulation while cancer ones have abnormal high levels. Addition of exogenous RONS can surpass the toxicity threshold levels and overwhelm the cellular defense mechanisms, leading to cell death [11–14]. Promising directions have emerged by targeting cancer cells through their metabolism for oncological therapies [15], and APPJ-based therapies have already demonstrated its selectivity towards variety of cancer cell lines [16–22].

The efficiency of APPJ has been demonstrated in vitro and in vivo by directly treating cells or tumors with the plasma jet [21,23]. As mentioned, direct treatment of cells with APPJ leads to selective killing of cancer cells without affecting healthy cells. As cells are covered with biological media, *i.e.* blood in *in vivo* situations or cell culture media in *in vitro* studies, interactions between APPJ and liquids occur during treatment, leading to biological effects. In that direction, plasma-conditioned media (PCM) was investigated as potential vehicle of RONS

from APPJ to avoid the effects of UV radiation and electric fields which can disturb the cell environment. The efficiency on the generation of RONS from APPJ depends on the device configuration, the selected parameters such as carrier gas, gas flow and the distance of treatment. Furthermore, the chemical composition of the treated liquid, its volume or the cell line type employed are important to determine the biological effects of plasmas. It is of great interest to suitably quantify the RONS generated in cell culture media in different conditions and their effects on cells for the understanding of the suitable dose of RONS needed to reach the selectivity toward cancer cells. As osteosarcoma is of difficult access, a therapy dealing with plasma conditioned liquids could be adapted to a minimally invasive approach. Few studies reported the direct plasma treatment of three types of osteosarcoma cell lines (U2-OS, MNNG/OS and SaOS-2) [24–26]. Indirect treatment using different cell culture media, in accordance to the cell line employed was evaluated on the selectivity of SaOS-2 cell line versus healthy cells [27,28]. However, treating different cell culture media implies generating different amount of RONS by plasmas, and thus, the effects previously reported need to be verified in equality of conditions. Plasma conditioned liquids, *i.e.* saline solutions, also demonstrated their selectivity towards SaOS-2, U2-OS and MG63 bone cancer cell lines versus hMSC cell line [29]. In this context, we aim to further extend the investigation of direct and indirect APPJ treatment methods on different bone healthy and cancer cell lines. Here, the same cell culture media is employed in direct plasma treatment and to generate plasma-conditioned media in indirect treatment on different cells to compare both treatments ensuring the same concentration of reactive species. The potential of the use of PCM is studied here as a potential tool for a non-invasive therapy for bone cancer.

2.2.MATERIALS & METHODS

2.2.1. Materials

Sarcoma Osteogenic (SaOS-2, ATCC, USA), passages 10-24, and human Osteosarcoma (MG63, CRL-1427, ATCC, USA), passages 20-34, were used as cancer cell lines. Human osteoblast primary cells (hOB, 406-05A, Sigma-Aldrich, USA), passages 2-3, and human Bone Marrow-derived Mesenchymal Stem Cells (hMSC; Tebu-bio, France) from passage 4 were used as primary healthy cell lines. For *in vitro* cell culture, Advanced Dulbecco's Modified Eagle Medium (AdvDMEM), SILAC™ AdvDMEM (without phenol Red), Dulbecco's Modified Eagle Medium (DMEM), Growth Osteoblast medium, Annexin V and propidium iodide were purchased from Gibco Life technologies (Thermo Fisher Scientific). McCoy's 5A culture medium was purchased from Sigma-Aldrich. Mammalian Protein Extraction Reagent (M-PER) was purchased from Thermo-Scientific. Fetal bovine serum (FBS), L-glutamine, penicillin, streptomycin, sodium pyruvate 100X, trypsin (TrypLE) and Alexa Fluor (AF 488) were purchased from Invitrogen. Lactate dehydrogenase activity (LDH, Cytotoxicity Detection Kit) was purchased from Roche Applied Science. Sulphanilamide (purity ≥ 99 %, M.W.: 172.20 g/mol, powder form), N-(1-naphtyl) ethylenediamine (purity > 98 %, M.W.: 259.17 g/mol; powder form), sodium nitrite ($NaNO_2$) (purity of 99.999 %, M.W: 69.00 g/mol; powder form), Amplex™ Red reagent (M.W.: 257.25 g/mol, powder form), horseradish peroxidase enzyme type VI (HRP) and hydrogen peroxide solution (30 % $_{w/w}$ in H_2O, M.W.: 34.01 g/mol; liquid form) were purchased from Sigma-Aldrich. Phosphate-buffered saline tablets (PBS) was purchased from Thermo Fisher Scientific. All the reagents used for reactive species detection were prepared using MilliQ water (Millipore, Merck). All reagents were used as received in their chemical grade. Helium (He 5.0) for plasma treatments was purchased from PRAXAIR, Spain.

2.2.2. Plasma treatment of liquid media

Plasma-conditioned media (PCM) was obtained by treating supplemented AdvDMEM cell culture media or water as control by using an atmospheric pressure plasma jet (APPJ) made of a single electrode (Figure 2.2), as described elsewhere [30]. Helium flow, used as plasma carrier gas, was employed at 5 L/min by using a Bronkhorst MassView flow controller (Bronkhorst, Netherlands) and the working distance between the capillary of plasma device and the interface of the liquid medium was fixed at 20 mm. Different volumes of liquids were investigated; For indirect treatment, a volume of 2 mL of liquid was treated during 5, 10 and 15 min with APPJ in 24-well plates (ϕ = 15.6 mm). For a volume of 150 µL, APPJ treatments were of 0.5, 1 and 1.5 min in 96-well plates (ϕ = 6.9 mm).

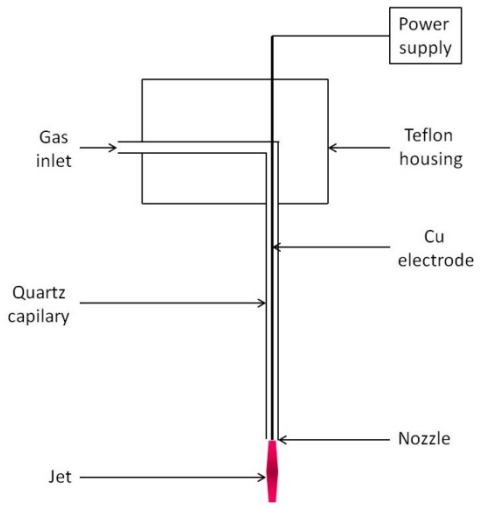

Figure 2.2: Schematic representation of the APPJ.

2.2.3. Optical emission spectroscopy

Optical Emission Spectroscopy (OES) was employed to give information of the main excited species emitted by the plasma. The equipment used was a spectrometer F600-UVVIS-SR (StellarNet Inc., USA), which was connected to an Ocean Insight QP600-2-SR optical fiber (Ocean Insight, USA) with lens collecting

information from the measure point near the plasma jet (10 mm). Influence of gas flow between 0 and 8 L/min was evaluated on the generation of reactive species in gas phase. All results were obtained with an integration time of 1000 ms and an average of 10 scans. Data were processed using the SpectraWiz software (StellarNet Inc., USA).

2.2.4. Detection of reactive species

Reactive species were quantified in water as control liquid, in SILAC™ AdvDMEM and in supplemented SILAC™ AdvDMEM (without Phenol Red) cell culture media following APPJ treatment in different volumes as described in section 2.2.2.

Concentration of nitrites (NO_2^-) was determined by Griess reaction method [31–33]. Griess reagent was obtained by dissolving 1 % $_{wt/v}$ of sulphanilamide, 0.1 % $_{wt/v}$ of N-(1-naphtyl) ethylenediamine and 5 % $_{wt/v}$ of phosphoric acid in MilliQ water. 50 µL of Griess reagent were added on 50 µL of plasma-treated sample in 96-well plates. The plates were incubated for 10 min at room temperature protected from light. The absorbance was measured at λ_{abs}= 540 nm using a Synergy Hybrid Multi Mode Microplate Reader (Biotek, USA). Calibration curve of [NO_2^-] was prepared by diluting $NaNO_2$ in the corresponding medium.

Concentration of hydrogen peroxides (H_2O_2) was evaluated by fluorescence spectroscopy using Amplex™ Red Reagent (AR) and horseradish peroxidase (HRP) enzyme, following supplier's protocol. H_2O_2 generation with APPJ was measured through the detection of resorufin, a fluorescent compound, final product of the reaction of H_2O_2 with AR with HRP as catalyst [34]. The samples were incubated in the dark at 37 ºC during 30 min. Fluorescence intensity was measured using a Synergy Hybrid Multi Mode Microplate Reader (Biotek, USA) with excitation and emission wavelengths of 560/20 nm and 590/20 nm, respectively. A calibration curve was prepared from a 30 % $_{w/w}$ in H_2O hydrogen peroxide solution in the corresponding medium.

2.2.5. In vitro cell experiments

2.2.5.1. Cell culture

McCoy's was used for the growth of SaOS-2, DMEM for MG63 and AdvDMEM for hMSC, all supplemented with 10 % of FBS, 1 % of L-glutamine and 1 % of penicillin (50 U/mL)/streptomycin (50 µg/mg). 1 % of sodium pyruvate was also added in McCoy's culture medium. Each cell type was cultured in its own cell culture media. All plasma treatments were performed in supplemented AdvDMEM with 10 % of FBS, 1 % of L-glutamine and 1 % of penicillin (50 U/mL)/streptomycin (50 µg/mg). In all the experiments, cell culture media in contact with cells was replaced by fresh supplemented AdvDMEM before plasma treatment or by plasma-treated supplemented AdvDMEM.

2.2.5.2.Direct treatment

For direct treatment, subconfluent cells were detached from the flask using trypsin, centrifuged and seeded with a density of $1 \cdot 10^4$ cells by well in 96-well plates with 150 µL of their corresponding complete cell medium. After 24-hour incubation (37 ºC, 95 % humidity, 5 % CO_2) to allow cell adhesion, fresh supplemented AdvDMEM cell culture media was replaced before treatment. APPJ treatment was performed subsequently on the wells containing the adhered cells covered by the cell culture media, according to the plasma treatment condition described previously (20 mm distance and 5 L/min gas flow). Influence of plasma treatment time on cell viability was evaluated for direct treatment from 0.5 to 1.5 min and for incubation times from 24 to 72 h.

2.2.5.3.Indirect treatment

The indirect treatment refers to replacing cell culture medium with PCM in the seeded cells. Briefly, $1 \cdot 10^4$ cells were seeded into 96-well plates with 150 µL of their corresponding media and allowed to adhere for 24 hours. Then, 2 mL of fresh supplemented AdvDMEM cell culture media was treated by APPJ and cell culture medium was replaced by 150 µL of this PCM in the wells containing the adhered

cells. Influence of plasma treatment time on cell viability was evaluated for indirect treatment from 5 to 15 min. The control refers to untreated cells where the cell culture media was replaced by untreated media. The plates were incubated at 37 °C under 5 % of CO_2 and 95 % humidity atmosphere for 24 h, 48 h and 72 h for further evaluation of cell viability.

2.2.5.4. Cell viability

After each incubation period, cells were lysed with 100 µL of M-PER. The lysates were analyzed to quantify the number of cells by measuring the LDH following manufacturer's protocols. This allows quantifying and measuring the number of cells. For both direct and indirect treatments, a negative control with no cells and only untreated culture medium as well as a positive control with the corresponding cell type in untreated medium were evaluated as well. This positive control was employed as reference for 100 % cell viability. Absorbance was measured at a λ = 492 nm using a Synergy HTX multi-mode microplate reader (BioTek, USA) and the cell viability was normalized with respect to cells only.

2.2.5.5.Flow cytometry

To determine the cell death mechanism of SaOS-2 and MG63 cells, flow cytometry was carried out after indirect treatment of the cells. $8 \cdot 10^4$ cells were seeded into 24-well plates with 1.2 mL of their corresponding media and let in incubation for 24-hour adhesion. Then, 2 mL of fresh supplemented AdvDMEM cell culture media were treated by APPJ during 15 min in the conditions described in section 2.2. Cell culture medium was then replaced by 1.2 mL of this PCM in the wells containing the adhered cells. After 72 h of incubation, the supernatants were collected, cells were detached using trypsin and centrifuged. The collected cells were then stained with Alexa Fluor 488, Annexin V, a biochemical marker of apoptosis and propidium iodide (PI), a marker of cell membrane integrity following the supplier's instructions (Vybrant apoptosis assay kit, Molecular probes). Annexin V marker has good affinity with phosphatidylserine (PS), located on the cytoplasmic

surface membrane of normal viable cell. When a cell is in an apoptotic state, PS is translocated from the inner to the outer leaflet of the plasma membrane, exposing PS the external environment. PI is a marker for necrosis state as it is impermeant to live and apoptotic cells. It penetrates to the damaged membranes of necrotic cells, binding tightly to the nucleic acids in the cell, which stain for red fluorescence. Apoptotic, necrotic and healthy cells state were analyzed in a Gallios multi-color flow cytometer instrument (Beckman Coulter, Inc, Fullerton, CA) set up with the 3-lasers 10 colors standard configuration. Excitation was done using a blue (488 nm) laser. Forward scatter, side scatter, green fluorescence (525/40 nm) from AF 488, Annexin V and red fluorescence (695/30 nm) emitted by PI were collected using logarithmic scales. Forward scatter was used as discriminating parameter.

2.2.6. Statistics

All the experiments were done on triplicate. Statistical differences were determined using one-way ANOVA with Tukey's post-hoc tests using Minitab 18 software (Minitab Inc., USA). Statistical significance was considered when $p < 0.05$. Data are presented as mean ± standard deviation.

2.3.RESULTS

2.3.1. Generation of reactive species by APPJ

2.3.1.1. Gas phase

The excited species generated by the atmospheric pressure plasma jet (APPJ) in the gas phase were recorded in air using Optical Emission Spectroscopy (Figure 2.3). Different peaks appeared that can be attributed to He (carrier gas) (λ = 706 nm), O^* (λ = 777 nm), $^*OH$ (λ = 316 nm), N_2^+ 1st positive (λ = 380 nm) and N_2 2nd+. An increase of the intensity of these peaks was observed with the increase of the gas flow employed up to 6 L/min. The intensity of the spectral lines of these species decreases below and above these gas flows.

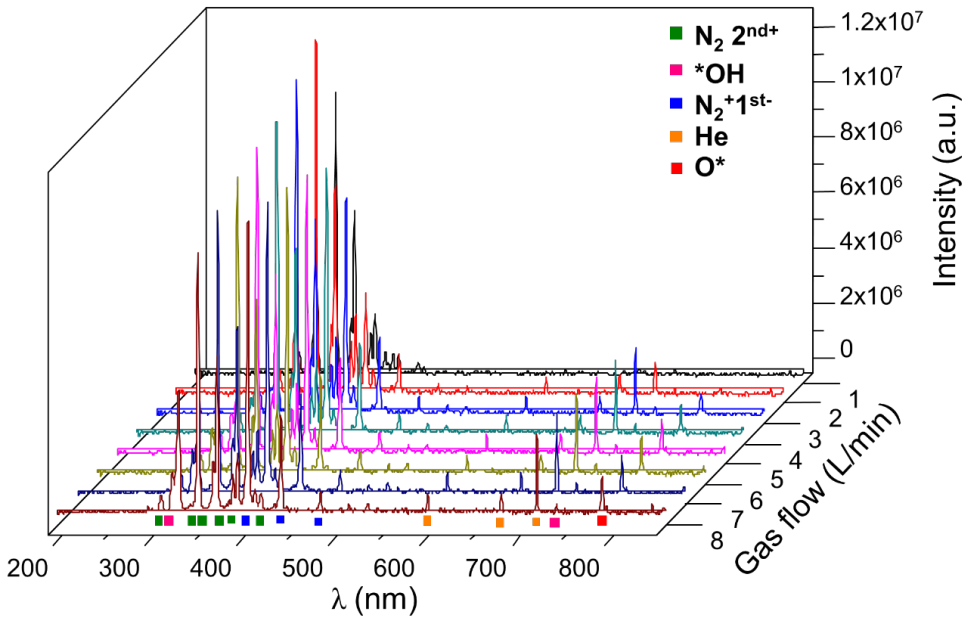

Figure 2.3: Optical emission spectra of the plasma jet operated with He at different flow rates in air.

2.3.1.2. Liquid phase

The generation of two major reactive species from the APPJ was quantified in water, in AdvDMEM and in the supplemented AdvDMEM, as used for cell culture. The concentrations of two of the main species generated, hydrogen peroxides (H_2O_2) and nitrites (NO_2^-) were investigated in different volumes following APPJ treatments (Figure 2.4). A linear increase of both H_2O_2 and NO_2^- following APPJ treatment in all liquids was clearly observed disregard the volume treated as a function of the plasma treatment time. As a general trend, higher concentrations of both H_2O_2 and NO_2^- were obtained in the supplemented AdvDMEM with respect to AdvDMEM and water. The concentration of these generated species highly depends on the APPJ treatment time, volume and chemical composition of the treated liquid. In 2 mL, higher concentrations of H_2O_2 and NO_2^- (700 µM and 170 µM respectively in supplemented AdvDMEM at 15 min) were reached due to longer treatment time employed. In a volume of 150 µL, lower concentrations were obtained with shorter treatment time (350 µM and 60 µM of H_2O_2 and NO_2^- respectively in supplemented AdvDMEM at 1.5 min).

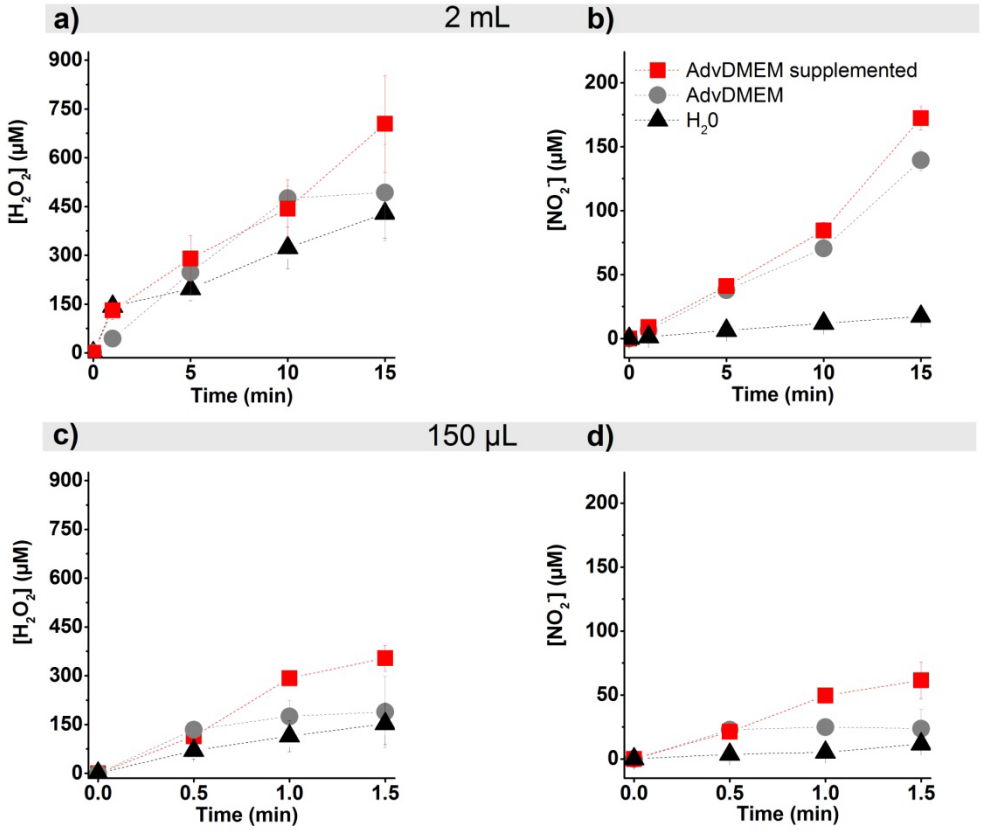

Figure 2.4: Generation in water (triangle), AdvDMEM (circle) and supplemented AdvDMEM (square) of a) H_2O_2 and b) NO_2^- in a volume of 2 mL and of c) H_2O_2 and d) NO_2^- in 150 µL of volume as a function of APPJ treatment time.

2.3.2. Cell cytotoxicity

2.3.2.1.Direct treatment

APPJ treatment was directly applied on cells seeded in 96 well-plates (WP) covered with 150 µL of fresh supplemented AdvDMEM cell culture media. Two healthy primary bone and two osteosarcoma cell lines were compared at different APPJ treatment times. The cell viability of human osteoblast primary cells (hOB), Human bone marrow-derived mesenchymal stem cells (hMSC), bone healthy cells and Sarcoma osteogenic human cells (SaOS-2), Osteosarcoma (MG63) cancer cells is presented in Figure 2.5 at three different times of incubation after the plasma treatment. Results clearly show that both healthy cells remain fully viable (Figure 2.5 a and b), as viability of hMSC was above 80 % at all treatment times. Furthermore, hOB exposed to direct plasma displayed enhanced cell proliferation (Figure 2.5 a) following APPJ treatment after 24 hours of incubation (135 ± 2 % for 1.5 min) followed by a slight decrease (110 ± 10 % for 1.5 min at 72 h). hMSC cells were more sensitive to direct plasma treatment, showing a small reduction in viability to values between 85 and 100 % (Figure 2.5 b).

For osteosarcoma cells, cell viability below 80 % was obtained in all cases. Both APPJ treatment time and incubation times clearly decrease the viability of SaOS-2 cells from 73 ± 10 % for 0.5 min at 24 h down to 25 ± 10 % for 1.5 min at 72 h (Figure 2.5 c). MG63 cells were less sensitive to plasma treatment, showing viability decrease from 75 ± 5 % at 24 h to 55 ± 3 % after 1.5 min of APPJ treatment at 72 h (Figure 2.5 d).

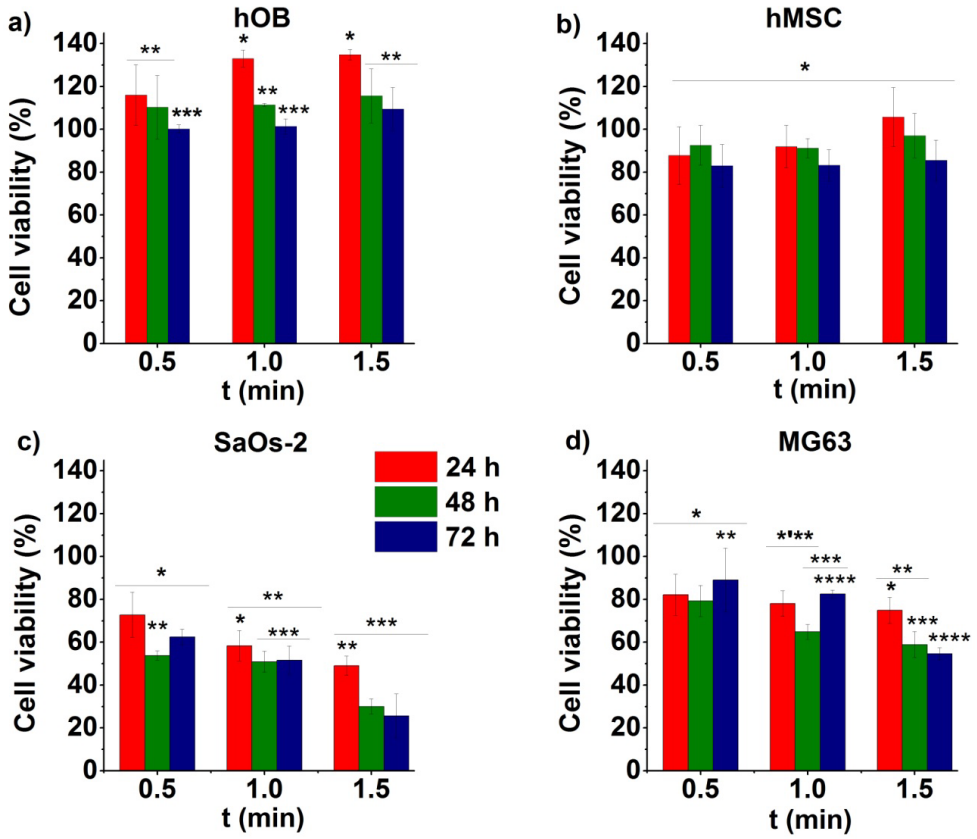

Figure 2.5: Effects of direct APPJ treatment at different times on cell viability of a) hOB, b) hMSC, c) SaOS-2 and d) MG63 cells at three different incubation times of 24, 48 and 72 hours.

2.3.2.2.Indirect treatment

To evaluate the indirect treatment, supplemented AdvDMEM was treated between 5 and 15 min with APPJ as described in the experimental part, to obtain PCM. This PCM was put in contact with cells seeded in the same conditions as described above. The trends obtained with the indirect treatment (Figure 2.6) were similar to those with direct treatment, except for hOB. The indirect treatment with PCM shows a minor reduction in cell viability for both types of healthy cells with cell viability usually between 80 and 90 % (Figure 2.6 a). A minor decrease in the

viability was observed in hMSCs treated with for 15 min-PCM from 90 ± 10 % at 24 h to 70 ± 5 % at 72 h (Figure 2.6 b).

Cell viability of bone cancer cells decreased with the plasma treatment time as well with the incubation time. SaOS-2 cells were more sensitive to plasma treatment, with values around 50 % for PCM treated for 10 min or 30 % for 15 min-treated PCM (at 72 h of incubation). MG63 cells can initially withstand the effects of PCM fairly well (70 % viability with 10 min PCM) but after a certain threshold with 15 min-PCM, values also decreased down to 30 %.

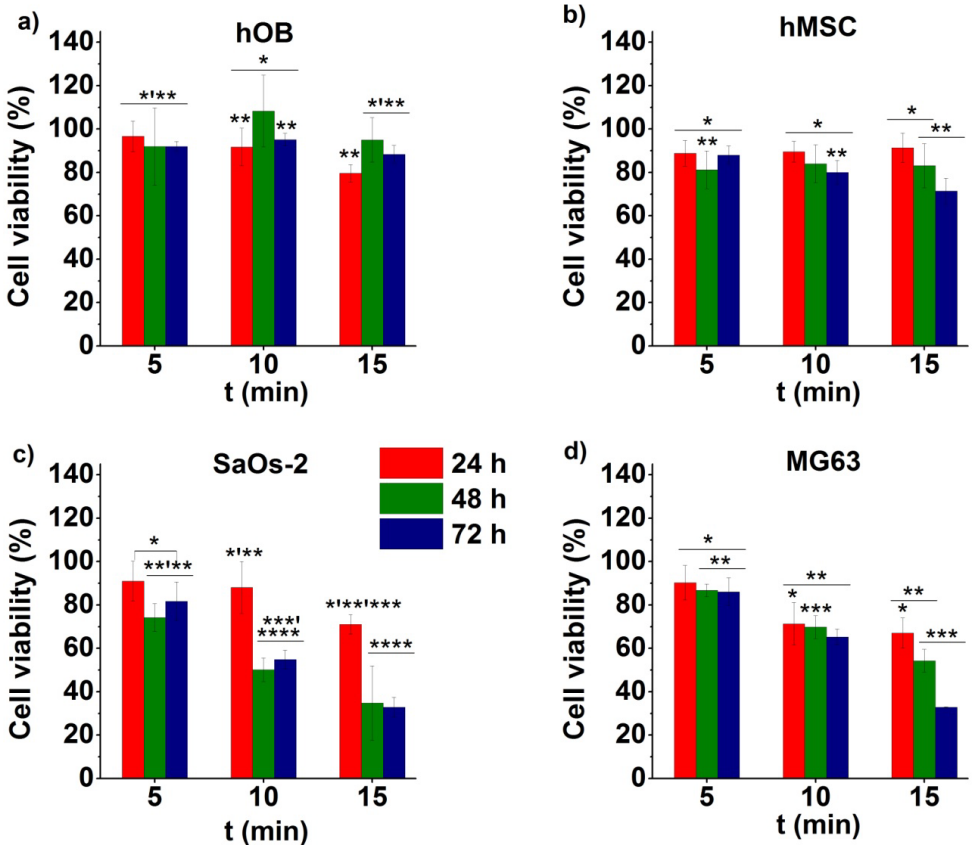

Figure 2.6: Effects of indirect APPJ treatment with PCM at different times on cell viability of a) hOB, b) hMSC, c) SaOS-2 and d) MG63 cells at three different incubation times 24, 48 and 72 hours.

To discern the mechanism of cancer cell death related to the cell viability observed in Figure 2.6, flow cytometry was performed on SaOS-2 and MG63 osteosarcoma cells (Figure 2.7). Indirect plasma treatment of SaOS-2 and MG63 cells with PCM induced apoptosis of the bone cancer cells, with all cells in the pre-apoptotic or apoptotic stage. Incubation of 72 h after 15 min of indirect plasma treatment of SaOS-2 cells lead to 24 % of pre-apoptotic and 65 % of apoptotic stage comparing to the untreated (8.3 % and 9.5 % for pre-apoptotic and apoptotic, respectively). Similar trends were observed with MG63 cells where 6.7 % of cells were in pre-apoptotic and 16.5 % in apoptotic stage while the values were more than 3 times lower for the untreated MG63 cells (1.5 % and 7.8 % for pre-apoptotic and apoptotic stage respectively).

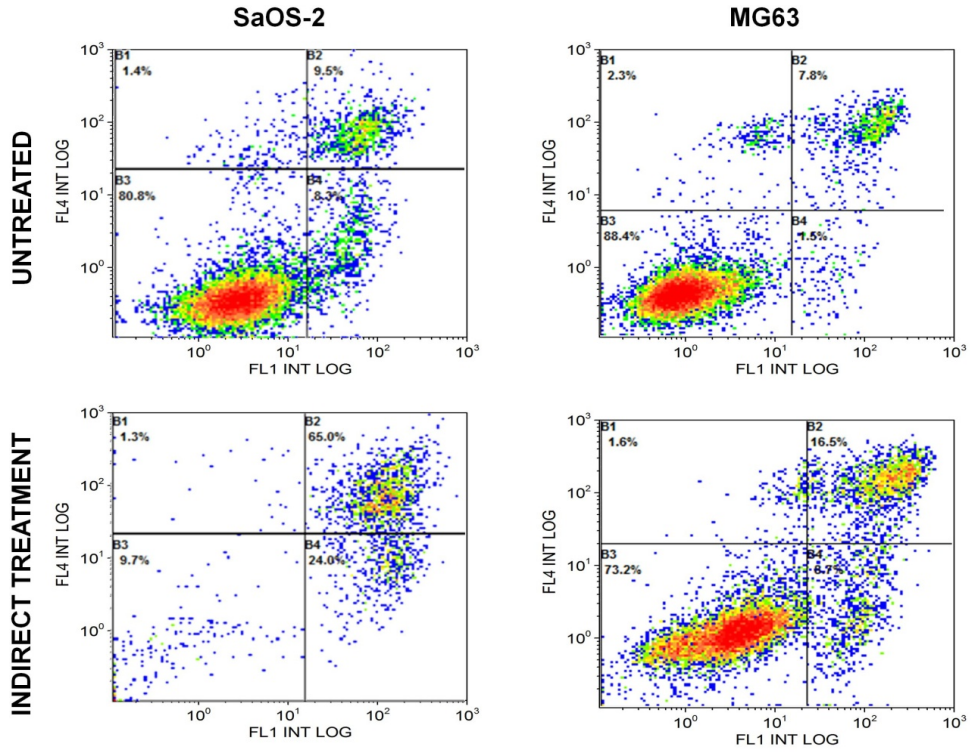

Figure 2.7: Flow cytometry of SaOS-2 and MG63 cells after 15 min of indirect APPJ treatment and 72 h of incubation.

2.4.DISCUSSION

Osteosarcoma (OS) is a primary bone tumor with low rate survival (between 5 and 60 % depending on the stage of the tumor at diagnosis), so alternative therapies to the current surgery + chemotherapy are an urgent need. In this sense, recent studies [24,27,35–38] have investigated the direct effects of cold atmospheric pressure plasma jets on OS cells (essentially U2-OS and MNNG/OS) recording a decrease in cell proliferation of the OS cells. While in general it is claimed that cold plasmas are selective, not affecting healthy cells, few works have devoted efforts to this aspect.

Here we investigate the effects of a helium APPJ on the cytotoxicity (Figures 2.5 & 2.6) and cell death mechanism (Figure 2.7) of two OS cell lines (SaOS-2 and MG63) and two healthy primary cells (hMSC and HOBs). The results clearly show that the direct APPJ treatment proposed is selective, allowing survival of the healthy cells with cell viability of 100 % and higher (Figure 2.5 a & b), while reflecting a progressive decrease of cell viability for concern cells (down to 30 % for SaOS-2 cells and 55 % for MG63 in just 1.5 min of treatment – Figure 2.5 c & d). This confirms the findings for other cancer types [39] and, translated to a future clinical scenario, this might imply avoiding the undesirable side effects of current therapies (*i.e.* chemotherapy).

Moreover, enhanced cell death in SaOS-2 and MG63 was recorded with increasing APPJ treatment time (thus increasing the concentration of detected species in liquids), and the effects were fostered with incubation time, in agreement with previous works [27,28].

Bone is an organ which requires surgery to be reached by APPJ, so taking advantage of the similar cytotoxic effects attributed to plasma-treated liquids [9] can be an interesting asset in views of providing a minimally invasive therapy to be injected in the tumor site. Here we compare the effects of direct APPJ treatment (Figure 2.5) with those of plasma-conditioned media (PCM) (Figure 2.6), obtained from treatment of cell culture media with APPJ, and then transferring this PCM onto the cells. Similar effects (cytotoxicity and selectivity) as those observed with direct

plasma treatment were found. In this regard, the chemistry of the plasma-treated liquid is of critical importance [40–42], as it determines the kind and concentration of reactive species. In normal conditions of cell culture, each cell line is grown in its particular cell culture medium, so some works have investigated the plasma treatment with different PCM for each cell line, hampering comparison [27]. Here, AdvDMEM has been employed (composition detailed in supplementary table S2-2) that includes proteins, amino-acids, sugars, salts, etc. The wide variety of molecules in the liquid justify the higher concentration of RONS generated by APPJ in comparison to water (Figure 2.4). As observed in other works, the concentration of peroxides generated by this APPJ is higher than that of nitrites. However, due to the presence of pyruvate - a scavenger of H_2O_2 - in this cell culture medium, the concentration here is lower than in other works [28].

The gas phase of this Helium - APPJ was characterized by several radical and ionic species, mainly $^*O$, $^*OH$, and N_2^+ (Figure 2.3), as described elsewhere [27]. Figure 2.8 schematically summarizes some of the reactions taking place between the species detected in the plasma gas phase and a liquid (water), leading to a variety of species, among them NO_2^- and H_2O_2 that have been quantified here.

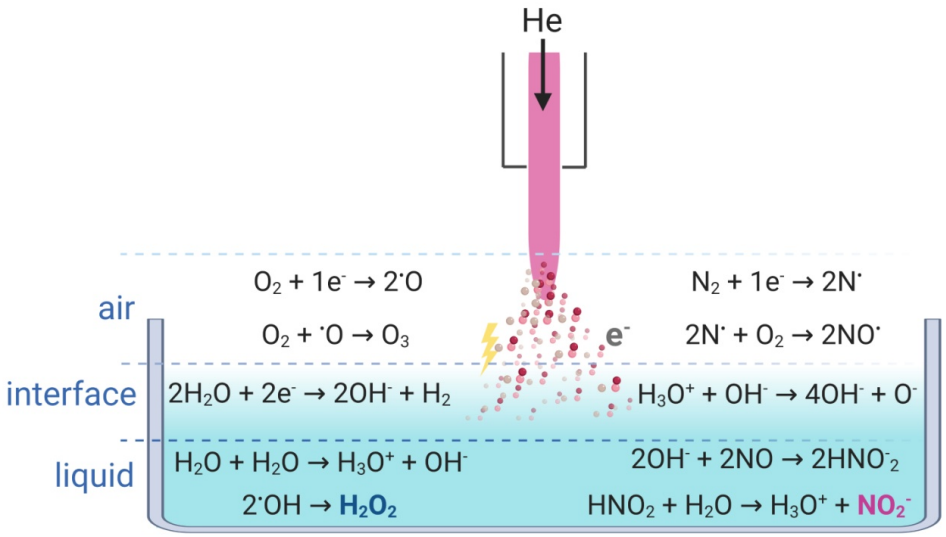

Figure 2.8: Schematic representation of some of the main chemical reactions which may occur from APPJ in aqueous liquids leading to H_2O_2 and NO_2^- formation [40,43].

Usually, plasma treatment of liquids leads to important acidification (*i.e.* down to pH=2 in water [44]), although for cell culture media like here the pH of PCM only decreases less than 0.5 points in 15 minutes, due to the buffering effect of the proteins and amino-acids present in the cell culture media (no buffer was added to the cell culture media used in this work).

It might seem surprising that the cell viability values obtained here with direct APPJ treatment (Figure 2.5) and indirect treatment with PCM (Figure 2.6) are so close (Table 2-1) (*i.e.* for SaOS-2 at 72 h and the longest time is around 25-30 % with both treatments, and for MG63 of 55 % for direct and 33 % for indirect treatment).

On the one hand, it is known that direct treatment with APPJ contains, in addition to the RONS already discussed, a number of additional stimuli that can affect the cells, namely UV-Vis and electromagnetic radiation, photons, electrons, etc. On the other hand, analysis of the concentration of RONS in each of both kinds of treatments (Table 2-1) shows that the concentration of H_2O_2 and NO_2^- is nearly double in the PCM employed in the indirect treatment with regard to that of the one of the direct APPJ treatment. This difference of concentration is due to the much longer treatment times employed to treat the bigger volume required for the indirect treatment (Table 2-1).

Table 2-1 : Compilation of the concentration of H_2O_2 and NO_2^- for the corresponding cytotoxicity in SaOS-2 and MG63 cells at the three treatment times investigated for either direct APPJ treatment or indirect treatment with PCM.

	Direct treatment				**Indirect treatment**			
	[RONS] (µM)		Cell Viability (%) *		[RONS] (µM)		Cell Viability (%) *	
	H_2O_2	**NO_2^-**	**SaOS-2**	**MG63**	**H_2O_2**	**NO_2^-**	**SaOS-2**	**MG63**
T1	*114 ± 37*	*21 ± 5*	*62 ± 4*	*89 ± 15*	*290 ± 70*	*40 ± 5*	*82 ± 5*	*86 ± 6*
T2	*290 ± 6*	*50 ± 1*	*52 ± 7*	*83 ± 2*	*444 ± 90*	*85 ± 6*	*55 ± 4*	*62 ± 4*
T3	*350 ± 40*	*60 ± 14*	*26 ± 10*	*55 ± 3*	*704 ± 150*	*170 ± 9*	*33 ± 5*	*33 ± 0.3*

T1 = 0.5 min for direct or 5 min for indirect treatment. T2 = 1 min for direct or 10 min for indirect treatment. T3 = 1.5 min for direct or 15 min for indirect treatment. *Cell viability at 72 h of incubation.

We observed here that equivalent biological results were obtained in both direct and indirect treatment, triggering cell death of bone cancer cells, related to the higher concentration of RONS in the PCM with longer APPJ treatment times (Figure 2.9). Cell death was triggered by apoptotic mechanisms in agreement with previous papers [43–45]. Other works have investigated direct and indirect plasma treatments, although the different experimental conditions make it difficult to establish comparisons [46-48]. Thus could provide an interesting alternative for treatment of bone tumors with a minimally invasive approach employing plasma-conditioned liquids.

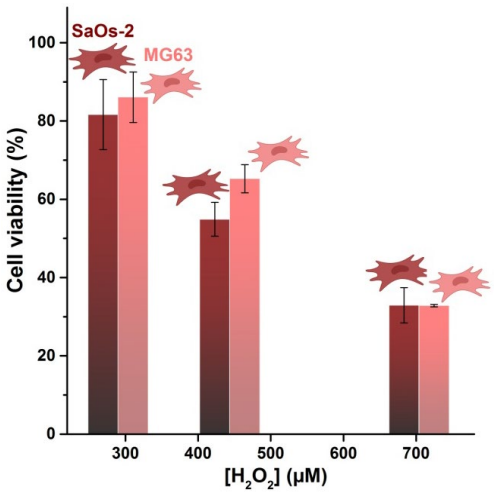

Figure 2.9 : Schematic representation of the H_2O_2-dose dependence on the cell viability of SaOs-2 and MG63 at 72 h of incubation in indirect treatment.

2.5.CONCLUSION

APPJ treatments are investigated here as potential alternative to current bone cancer treatments. The anti-cancer capacity of direct APPJ treatment and indirect treatment with plasma-conditioned media are both effective in vitro to diminish viability of cancer cells. The viability of cancer cells decreases down to 30 % at 72 hours with the increase of treatment time while healthy cells maintain their viability higher than 80 %. The effective selectivity of bone cancer cell lines versus healthy cell lines is dependent on the dose of reactive species generated in the media. In our experimental conditions, higher concentrations of H_2O_2 and NO_2^- are generated in bigger volume with longer APPJ treatment time leading to similar biological results as direct treatment which also involves UV-Vis radiation, electromagnetic fields, among others. Therefore, employing plasma conditioned liquids could provide a promising alternative for minimally invasive bone cancer therapy.

REFERENCES

1. Weltmann, K.-D.; Polak, M.; Masur, K.; von Woedtke, T.; Winter, J.; Reuter, S. Plasma Processes and Plasma Sources in Medicine. *Contrib. to Plasma Phys.* **2012**, *52*, 644–654.
2. Park, G.Y.; Park, S.J.; Choi, M.Y.; Koo, I.G.; Byun, J.H.; Hong, J.W.; Sim, J.Y.; Collins, G.J.; Lee, J.K. Atmospheric-pressure plasma sources for biomedical applications. *Plasma Sources Sci. Technol.* **2012**, *21*, 43001.
3. Kajiyama, H.; Utsumi, F.; Nakamura, K.; Tanaka, H.; Toyokuni, S.; Hori, M.; Kikkawa, F. Future perspective of strategic non-thermal plasma therapy for cancer treatment. *J. Clin. Biochem. Nutr.* **2017**, *60*, 33–38.
4. Laroussi, M.; Laroussi; Mounir Plasma Medicine: A Brief Introduction. *Plasma 2018, Vol. 1, Pages 47-60* **2018**, *1*, 47–60.
5. Tanaka, H.; Ishikawa, K.; Mizuno, M.; Toyokuni, S.; Kajiyama, H.; Kikkawa, F.; Metelmann, H.-R.; Hori, M. State of the art in medical applications using non-thermal atmospheric pressure plasma. *Rev. Mod. Plasma Phys.* **2017**, *1*, 3.
6. Bauer, G.; Graves, D.B. Mechanisms of Selective Antitumor Action of Cold Atmospheric Plasma-Derived Reactive Oxygen and Nitrogen Species. *Plasma Process. Polym.* **2016**, *13*, 1157–1178.
7. Laroussi, M. Low-Temperature Plasma Jet for Biomedical Applications: A Review. *IEEE Trans. Plasma Sci.* **2015**, *43*, 703–712.
8. Graves, D.B. Low temperature plasma biomedicine: A tutorial review. *Phys. Plasmas* **2014**, *21*, 80901.
9. Graves, D.B. Reactive Species from Cold Atmospheric Plasma: Implications for Cancer Therapy. *Plasma Process. Polym.* **2014**, *11*, 1120–1127.
10. Volotskova, O.; Hawley, T.S.; Stepp, M.A.; Keidar, M. Targeting the cancer cell cycle by cold atmospheric plasma. *Sci. Rep.* **2012**, *2*, 636.
11. Trachootham, D.; Alexandre, J.; Huang, P. Targeting cancer cells by ROS-mediated mechanisms: a radical therapeutic approach? *Nat. Rev. Drug Discov.* **2009**, *8*, 579–591.
12. Schumacker, P.T. Reactive oxygen species in cancer cells: Live by the sword, die by the sword. *Cancer Cell* **2006**, *10*, 175–176.
13. Sardella, E.; Mola, M.G.; Gristina, R.; Piccione, M.; Veronico, V.; De Bellis, M.; Cibelli, A.; Buttiglione, M.; Armenise, V.; Favia, P.; et al. A Synergistic Effect of

Reactive Oxygen and Reactive Nitrogen Species in Plasma Activated Liquid Media Triggers Astrocyte Wound Healing. *Int. J. Mol. Sci.* **2020**, *21*, 3343.

14. Azzariti, A.; Iacobazzi, R.M.; Di Fonte, R.; Porcelli, L.; Gristina, R.; Favia, P.; Fracassi, F.; Trizio, I.; Silvestris, N.; Guida, G.; et al. Plasma-activated medium triggers cell death and the presentation of immune activating danger signals in melanoma and pancreatic cancer cells. *Sci. Rep.* **2019**, *9*, 1–13.
15. Fruehauf, J.P.; Meyskens, F.L. Reactive oxygen species: a breath of life or death? *Clin. Cancer Res.* **2007**, *13*, 789–94.
16. Ratovitski, E.A.; Cheng, X.; Yan, D.; Sherman, J.H.; Canady, J.; Trink, B.; Keidar, M. Anti-Cancer Therapies of 21st Century: Novel Approach to Treat Human Cancers Using Cold Atmospheric Plasma. *Plasma Process. Polym.* **2014**, *11*, 1128–1137.
17. Hirst, A.M.; Frame, F.M.; Arya, M.; Maitland, N.J.; O'Connell, D. Low temperature plasmas as emerging cancer therapeutics: the state of play and thoughts for the future. *Tumor Biol.* **2016**, *37*, 7021–7031.
18. Keidar, M.; Shashurin, A.; Volotskova, O.; Ann Stepp, M.; Srinivasan, P.; Sandler, A.; Trink, B. Cold atmospheric plasma in cancer therapy. *Phys. Plasmas* **2013**, *20*, 57101.
19. Keidar, M. Plasma for cancer treatment. *Plasma Sources Sci. Technol.* **2015**, *24*, 33001.
20. Keidar, M.; Yan, D.; Beilis, I.I.; Trink, B.; Sherman, J.H. Plasmas for Treating Cancer: Opportunities for Adaptive and Self-Adaptive Approaches. *Trends Biotechnol.* **2018**, *36*, 586–593.
21. Yan, D.; Sherman, J.H.; Keidar, M. Cold atmospheric plasma, a novel promising anti-cancer treatment modality. *Oncotarget* **2017**, *8*, 15977–15995.
22. Keidar, M.; Walk, R.; Shashurin, A.; Srinivasan, P.; Sandler, A.; Dasgupta, S.; Ravi, R.; Guerrero-Preston, R.; Trink, B. Cold plasma selectivity and the possibility of a paradigm shift in cancer therapy. *Br. J. Cancer* **2011**, *105*, 1295–301.
23. Keidar, M.; Shashurin, A.; Volotskova, O.; Ann Stepp, M.; Srinivasan, P.; Sandler, A.; Trink, B. Cold atmospheric plasma in cancer therapy. *Phys. Plasmas* **2013**, *20*, 57101.
24. Gümbel, D.; Gelbrich, N.; Weiss, M.; Napp, M.; Daeschlein, G.; Sckell, A.; Ender, S.A.; Kramer, A.; Burchardt, M.; Ekkernkamp, A.; et al. New Treatment Options for Osteosarcoma - Inactivation of Osteosarcoma Cells by Cold Atmospheric Plasma.

Anticancer Res. **2016**, *36*, 5915–5922.

25. Gümbel, D.; Bekeschus, S.; Gelbrich, N.; Napp, M.; Ekkernkamp, A.; Kramer, A.; Stope, M.B. Cold Atmospheric Plasma in the Treatment of Osteosarcoma. *Int. J. Mol. Sci.* **2017**, *18*.
26. Guembel, D.; Gelbrich, N.; … M.N.-A.; 2017, undefined Peroxiredoxin expression of human osteosarcoma cells is influenced by cold atmospheric plasma treatment. *ar.iiarjournals.org* **2017**, *37*, 1031–1038.
27. Canal, C.; Fontelo, R.; Hamouda, I.; Guillem-Marti, J.; Cvelbar, U.; Ginebra, M.-P. Plasma-induced selectivity in bone cancer cells death. *Free Radic. Biol. Med.* **2017**, *110*.
28. Tornin, J.; Mateu-Sanz, M.; Rodríguez, A.; Labay, C.; Rodríguez, R.; Canal, C. Pyruvate Plays a Main Role in the Antitumoral Selectivity of Cold Atmospheric Plasma in Osteosarcoma. *Sci. Rep.* **2019**, *9*.
29. Mateu-Sanz, M.; Tornín, J.; Brulin, B.; Khlyustova, A.; Ginebra, M.-P.; Layrolle, P.; Canal, C. Cold Plasma-Treated Ringer's Saline: A Weapon to Target Osteosarcoma. *Cancers (Basel).* **2020**, *12*, 227.
30. Zaplotnik, R.; Bišćan, M.; Kregar, Z.; Cvelbar, U.; Mozetič, M.; Milošević, S. Influence of a sample surface on single electrode atmospheric plasma jet parameters. *Spectrochim. Acta - Part B At. Spectrosc.* **2015**, *103–104*, 124–130.
31. Green, L.C.; Wagner, D.A.; Glogowski, J.; Skipper, P.L.; Wishnok, J.S.; Tannenbaum, S.R. Analysis of nitrate, nitrite, and [15N]nitrate in biological fluids. *Anal. Biochem.* **1982**, *126*, 131–138.
32. Giustarini, D.; Rossi, R.; Milzani, A.; Dalle-Donne, I. Nitrite and Nitrate Measurement by Griess Reagent in Human Plasma: Evaluation of Interferences and Standardization. *Methods Enzymol.* **2008**, *440*, 361–380.
33. Guevara, I.; Iwanejko, J.; Dembińska-Kieć, A.; Pankiewicz, J.; Wanat, A.; Anna, P.; Gołąbek, I.; Bartuś, S.; Malczewska-Malec, M.; Szczudlik, A. Determination of nitrite/nitrate in human biological material by the simple Griess reaction. *Clin. Chim. Acta* **1998**, *274*, 177–188.
34. Mishin, V.; Gray, J.P.; Heck, D.E.; Laskin, D.L.; Laskin, J.D. Application of the Amplex red/horseradish peroxidase assay to measure hydrogen peroxide generation by recombinant microsomal enzymes. *Free Radic. Biol. Med.* **2010**, *48*, 1485–1491.
35. Jacoby, J.M.; Strakeljahn, S.; Nitsch, A.; Bekeschus, S.; Hinz, P.; Mustea, A.;

Ekkernkamp, A.; Tzvetkov, M. V; Haralambiev, L.; Stope, M.B. An Innovative Therapeutic Option for the Treatment of Skeletal Sarcomas: Elimination of Osteo- and Ewing's Sarcoma Cells Using Physical Gas Plasma. *Int. J. Mol. Sci. Artic. Int. J. Mol. Sci 2020*, 4460.

36. Haralambiev, L.; Nitsch, A.; Muzzio, D. The Effect of Cold Atmospheric Plasma on the Membrane Permeability of Human Osteosarcoma Cells Role of S1P and LP1 during pregnancy View project. *ar.iiarjournals.org* **2020**, *40*, 841–846.
37. Haralambiev, L.; Wien, L.; Gelbrich, N.; Kramer, A. Effects of Cold Atmospheric Plasma on the Expression of Chemokines, Growth Factors, TNF Superfamily Members, Interleukins, and Cytokines in Human Osteosarcoma Cells Cold atmospheric Plasma in tumor therapy View project Meaning of prophylactic measures to prevent Surgical Site Infections (SSI) in surgical infectious prevention. View project. *ar.iiarjournals.org*.
38. Guembel, D.; Suchy, B.; Wien, L.; … N.G.-A.; 2017, undefined Comparison of cold atmospheric plasma Devices' efficacy on osteosarcoma and fibroblastic in vitro cell models. *ar.iiarjournals.org* **2017**, *37*, 5407–5414.
39. Dubuc, A.; Monsarrat, P.; Virard, F.; Merbahi, N.; Sarrette, J.P.; Laurencin-Dalicieux, S.; Cousty, S. Use of cold-atmospheric plasma in oncology: a concise systematic review. *Ther. Adv. Med. Oncol.* **2018**, *10*.
40. Khlyustova, A.; Labay, C.; Machala, Z.; Ginebra, M.-P.; Canal, C. Important parameters in plasma jets for the production of RONS in liquids for plasma medicine: A brief review. *Front. Chem. Sci. Eng.* **2019**, *13*, 238–252.
41. Wende, K.; Williams, P.; Dalluge, J.; Van Gaens, W.; Aboubakr, H.; Bischof, J.; von Woedtke, T.; Goyal, S.M.; Weltmann, K.-D.; Bogaerts, A.; et al. Identification of the biologically active liquid chemistry induced by a nonthermal atmospheric pressure plasma jet. *Biointerphases* **2015**, *10*.
42. Adamovich, I.; Baalrud, S.D.; Bogaerts, A.; Bruggeman, P.J.; Cappelli, M.; Colombo, V.; Czarnetzki, U.; Ebert, U.; Eden, J.G.; Favia, P.; et al. The 2017 Plasma Roadmap: Low temperature plasma science and technology. *J. Phys. D. Appl. Phys.* **2017**, *50*, 323001.
43. Bruggeman, P.J.; Kushner, M.J.; Locke, B.R.; Gardeniers, J.G.E.; Graham, W.G.; Graves, D.B.; Hofman-Caris, R.C.H.M.; Maric, D.; Reid, J.P.; Ceriani, E.; et al. Plasma–liquid interactions: a review and roadmap. *Plasma Sources Sci. Technol.*

2016, *25*, 53002.

44. Labay Cédric, Roldan Marcel, Tampieri Francesco, Stancampiano Augusto, Escot Bocanegra Pablo, Ginebra Maria Pau, C.C. Enhanced generation of reactive species in gelatin hydrogel solutions for selective cancer therapy. *Submitt. ACS Mater. Interfaces* **2020**.
45. Saito, K.; Asai, T.; Fujiwara, K.; Sahara, J.; Koguchi, H.; Fukuda, N.; Suzuki-Karasaki, M.; Soma, M.; Suzuki-Karasaki, Y. Tumor-selective mitochondrial network collapse induced by atmospheric gas plasma-activated medium. *Oncotarget* **2016**, *7*, 19910–27.
46. Adachi, T.; Tanaka, H.; Nonomura, S.; Hara, H.; Kondo, S.I.; Hori, M. Plasma-activated medium induces A549 cell injury via a spiral apoptotic cascade involving the mitochondrial-nuclear network. *Free Radic. Biol. Med.* **2015**, *79*.
47. Biscop; Lin; Boxem; Loenhout; Backer; Deben; Dewilde; Smits; Bogaerts Influence of Cell Type and Culture Medium on Determining Cancer Selectivity of Cold Atmospheric Plasma Treatment. *Cancers (Basel).* **2019**, *11*, 1287.
48. Van Boxem, W.; Van der Paal, J.; Gorbanev, Y.; Vanuytsel, S.; Smits, E.; Dewilde, S.; Bogaerts, A. Anti-cancer capacity of plasma-treated PBS: effect of chemical composition on cancer cell cytotoxicity. *Sci. Rep.* **2017**, *7*, 16478.
49. Bauer, G. Cold Atmospheric Plasma and Plasma-Activated Medium: Antitumor Cell Effects with Inherent Synergistic Potential. *Plasma Med.* **2019**, *9*, 57–88.
50. Girard, P.-M.; Arbabian, A.; Fleury, M.; Bauville, G.; Puech, V.; Dutreix, M.; Sousa, J.S. Synergistic Effect of H2O2 and NO2 in Cell Death Induced by Cold Atmospheric He Plasma. *Sci. Rep.* **2016**, *6*, 29098.

SUPPLEMENTARY INFORMATION - CHAPTER 2

Table S2-2: Chemical composition of AdvDMEM and Supplemented AdvDMEM cell culture media.

Composition (%)	AdvDMEM	Suplemented AdvDMEM
AlbuMax®II	Infinity	Infinity
Human Transferrin	Infinity	Infinity
Insulin Recombinant Full Chain	Infinity	Infinity
Sodium chloride	95.1	95.1
Sodium bicarbonate	2.3	2.3
D-glucose	1.4	1.4
Potassium chloride	0.3	0.3
Calcium chloride	0.1	0.1
Sodium phosphate monobasic	0.04	0.04
Sodium pyruvate	0.1	0.1
FBS	-	10
L-Glutamine	-	1
Penicillin/Streptomycin	-	1

CHAPTER 3

3. Production of Reactive Species in Alginate Hydrogels for Cold Atmospheric Plasma-based Therapies

ABSTRACT

In the last years, great advances have been made in therapies based in cold atmospheric plasmas (CAP). CAP generates reactive oxygen and nitrogen species (RONS) which can be transferred to liquids. These CAP conditioned liquids display the same biological efficacy (*i.e.* on killing cancer cells) as CAP themselves, opening the door for minimally invasive therapies. However, injection of a liquid in the body results in fast diffusion due to extracellular fluids and blood flow. Therefore, the development of efficient vehicles which allow local confinement and delivery of RONS to the diseased site is a fundamental requirement. In this chapter, we investigate the generation of RONS (H_2O_2, NO_2^-, and short-lived RONS) in alginate hydrogels by comparing two atmospheric pressure plasma jets: kINPen, a commercial device and a home-made helium needle, at a range of plasma treatment conditions (time, gas flow and distance to the sample). The physic-chemical properties of the hydrogels remain unchanged by the plasma treatment, while the hydrogel shows several-fold larger capacity for generation of RONS than a typical isotonic saline solution. Part of the RONS are quickly released to a receptor media, so special attention has to be put on the design of hydrogels with *in-situ* crosslinking. Remarkably, the hydrogels show capacity for sustained release of the RONS. The plasma-treated hydrogels remain fully biocompatible (due the fact that the species generated by plasma are previously washed away), indicating that no cytotoxic modifications have occurred on the polymer. Moreover, the RONS generated in alginate solutions showed cytotoxic potential towards bone cancer cells. These results open the door for the use of hydrogel-based biomaterials in CAP-associated therapies.

3.1.INTRODUCTION

Plasma is defined as a totally or partially ionized gas that contains a high number of reactive species, ions, electrons, metastable particles, etc. The development of plasma sources of small dimensions and able to operate at atmospheric pressure and at temperatures close to room temperature has fostered the development of a new field named *Plasma medicine* [1]. Atmospheric pressure plasma (APP) has been evaluated as an effective tool for sterilization [2], cancer treatment [3] or for enhancing wound healing [4]. APPs formed in air generate reactive oxygen and nitrogen species (RONS), which can be transferred to liquids through secondary reactions. Plasma-conditioned liquids (PCL) display different biological actions which have been mainly attributed to the generation of RONS such as hydrogen peroxides (H_2O_2), nitrites (NO_2^-), peroxynitrites, etc. These reactive species are known to be involved in a wide range of intracellular and intercellular processes [5]. Until now, major attention has been paid in *Plasma Medicine* to the monitoring of RONS induced in PCL used in indirect treatments [6], and some works have investigated their storage by freezing the PCL but this is not always possible [7]. However, transportation and diffusion from suitable biomaterials of these RONS for *in situ* therapy remains to be explored.

Hydrogels can be an asset for that aim, as they have characteristics such as biocompatibility, *in vivo* biodegradability and ductility that are key features in the design of advanced biomaterials [8,9]. These highly swollen 3D networks of macromolecules have emerged as powerful candidate biomaterials for the local delivery of a variety of drugs at physiologically relevant doses for prolonged periods of time. Our hypothesis is that due to their high water contents and porous network they could be suitably used as carrier for RONS generated in PCL, providing new alternatives for therapies based on cold plasmas. Hydrogels can be based on natural polymers (e.g. polysaccharides, gelatine and fibrin), synthetic polymers (e.g. ethylene oxide, vinyl alcohol or acrylic acid) or semi-synthetic polymers (mixture between both natural and synthetic polymers) [10]. Hydrogels obtained from natural polymers have many advantages including low toxicity and good biocompatibility

[11]. Alginate used in this chapter is obtained from brown algae and is typically used to produce hydrogels for a variety of applications in drug delivery and tissue engineering [12]. Alginate hydrogels can be prepared by simple gelation with divalent cations such as Ca^{2+} [13,14] so can be easily formed *in situ* in the body in contact with body fluids or in the lab in contact with Ca^{2+} containing solutions.

The purpose of this chapter is to evaluate and discuss the potential of employing alginate-based hydrogels as vehicles of RONS generated by atmospheric plasmas. Specifically, we analyse whether there are any chemical modifications in the structure of the alginate and its hydrogel-forming ability. In views of their possible therapeutic applications, their biological properties are investigated: biocompatibility of the plasma-treated polymer and cytotoxicity of the RONS generated therein.

3.2.MATERIALS & METHODS

3.2.1. Materials

Sodium alginate (Na-alginate MW: 10000-600000 g/mol) in powder form was purchased from Pancreac. Potassium chloride (KCl, Panreac), sodium chloride (NaCl, Sigma-Aldrich) and calcium chloride dehydrate ($CaCl_2.2H_2O$, Sigma-Aldrich) were used for the preparation of Ringer's saline solution. Phosphoric acid (85 %; MW: 98 g/mol, Panreac), sulphanilamide (M.W: 172.20 g/mol, Sigma-Aldrich) and N-(1-naphtyl)ethylenediamine (NEED, MW: 172.20 g/mol, Sigma-Aldrich) were used for synthesis of Griess reagent. Calcium chloride ($CaCl_2$, 96 % anhydrous, MW: 110, 98 g/mol), sodium nitrite ($NaNO_2$ MW: 69 g/mol) and sodium azide (NaN_3, MW: 65 g/mol), in powder form, were obtained from Sigma-Aldrich. Titanyl oxysulphate ($TiOSO_4$, MW: 159.90 g/mol; 27-31 % $_{wt}$ in H_2SO_4), hydrogen peroxide (H_2O_2, MW: 34.01 g/mol; 30 % $_{wt/wt}$ in H_2O), peroxidase from Horseradish type VI (HRP) (250 U/mg, Sigma-Aldrich) and 2',7'-Dichlorofluorescein diacetate (DCFH-DA) (≥ 97 %) were purchased from Sigma-Aldrich. Amplex Red reagent was provided by Invitrogen (Ref. A12222). Helium and argon gas were provided by Praxair, Spain.

Sarcoma osteogenic cells (SaOs-2, ATCC, USA) were expanded in McCoy's 5A culture medium (Sigma Aldrich). Foetal Bovine Serum (FBS) and Penicillin/Streptomycin (P/S) (50 U/ml and 50 µg/ml, respectively) were purchased from Invitrogen. Cells from passage between 24 and 32 were used in all experiments. Cell Proliferation Reagent WST-1 used for cell viability determination was purchased from Roche Diagnostics GmbH (Ref. 05015944001).

3.2.2. Preparation of alginate solutions and hydrogels

The alginate solutions were obtained by mixing the dry sodium-alginate powder with DI water in a SpeedMixer (DAC 150.1 FVZ-k, 3500 rpm) for 15 min at 0.5 % $_{w/v}$. Alginate solutions (or hydrosols), that refer to the physical state of the alginate before crosslinking of the polymer chains [15], were stored at 4 °C and used

within a lifespan of 2 weeks. The alginate hydrogels were obtained by ionic crosslinking of the hydrosol using a 150 µL of a 50 mM calcium chloride ($CaCl_2$) solution for 200 µL of alginate hydrosol for 5 min. Subsequent rinsing using 100 µL of DI water of the formed hydrogel was performed for 5 minutes before its use for release and cell culture experiments, to eliminate the excess of calcium coming from the crosslinking solution. Crosslinking and rinsing solution used for obtaining the hydrogel were kept for determination of [NO_2^-] and [H_2O_2], and the formed hydrogels were used for 72-hour release experiments. For cell experiments using alginate hydrogels, all the processes leading to the preparation of the formed hydrogel were carried out under sterile conditions. Alginate powder was sterilized by using a low pressure plasma (Diener, 100 W, O_2, rotary, 5 min)

3.2.3. Plasma treatments

In the research described in this chapter, two kinds of atmospheric plasma jet were used: a commercially available cold atmospheric plasma jet kINPen IND (NEOPLAS Tools, Germany) [6], operating with argon and an atmospheric pressure plasma jet (APPJ) using He as plasma gas in a jet design based on a single electrode as described elsewhere [16] (Figure 3.1 and 3.5 c). Gas flow was regulated between 1 and 2.5 L/min for kINPen and between 1 and 5 L/min for APPJ by using Ar and He Bronkhorst Mass View flow controllers (BRONKHORST, Netherlands), respectively.

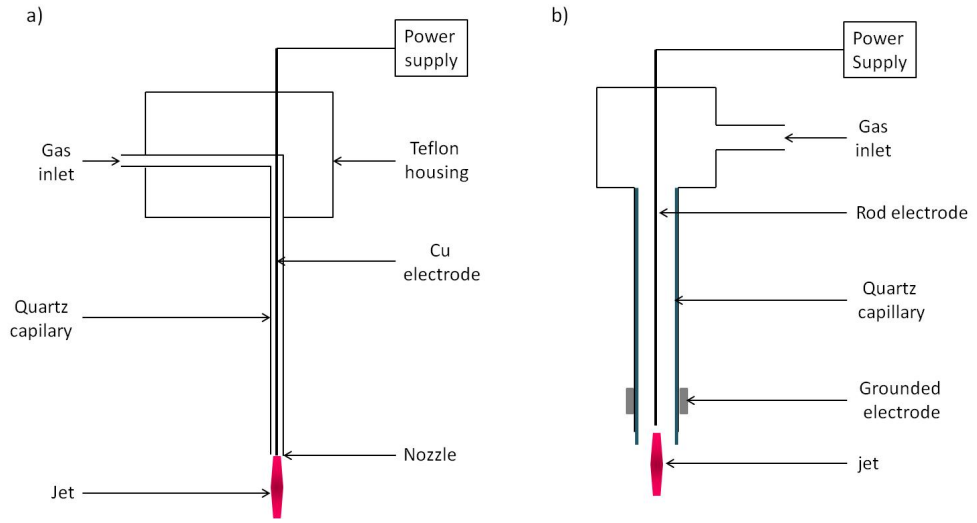

Figure 3.1: Schematic representation of a) APPJ and b) KinPen devices.

All plasma treatments of alginate for RONS quantification were performed on 200 µL of the alginate solution (before crosslinking) in 96-well plates, with a distance between the nozzle and the sample surface between 10 and 20 mm.

3.2.4. Detection of RONS in alginate hydrosols

Determination of NO_2^- concentration in plasma-treated alginate hydrosol was performed using Griess reagent [17–20]. The Griess reagent used was obtained by dissolving 1 % $_{w/v}$ of sulphanilamide, 0.1 % $_{w/v}$ of NEED and 5 % $_{w/v}$ of phosphoric acid in de-ionized water. 200 µL of Griess reagent were added on 200 µL of sample in 96 well-plates. The plates were incubated for 10 min at room temperature protected from the light. The absorbance was measured at λ_{abs} = 540 nm using a Synergy HTX Hybrid Multi Mode Microplate Reader (BioTek Instruments, Inc., USA). The $[NO_2^-]$ in each sample was determined from the absorbance values by using a calibration curve made from $NaNO_2$ dilutions in alginate hydrosols.

The concentration of hydrogen peroxide was determined by reaction of H_2O_2 with Amplex Red in presence of HRP enzyme that leads to the creation of resorufin, a fluorescent product (Figure 3.1 a). Amplex Red/HRP reagent consists in 100 µM

of Amplex Red and 0.25 U/mL HRP in DI water. Since the higher concentration of H_2O_2 able to be processed properly by this reagent is around 10 µM of H_2O_2, plasma-treated alginate hydrosols were diluted 200 times previously to the addition of the reagent. In this case, for hydrogen peroxide detection, 50 µL of the Amplex Red/HRP reagent was added to 200 µL of the 200x-diluted alginate sample in a 96-well plate and incubated for 30 min at 37 °C. Subsequent fluorescence measurements were performed by means of a Synergy HTX Hybrid Multi Mode Microplate Reader (BioTek Instruments, Inc., USA), with fluorescence filters centred at λ_{ex} = 560/20 nm and λ_{em} = 590/20 nm as excitation and emission wavelengths, respectively. Concentrations of H_2O_2 in alginate hydrosol generated by plasma treatment were obtained from the fluorescence values using a calibration curve made from 30 % hydrogen peroxide solution in alginate.

Presence of short-lived RONS was determined *in situ* in plasma-treated 0.5 % $_{w/v}$ alginate solution using 2',7' Dichlorodihydrofluorescein diacetate (DCFH-DA), which is a scavenger of short-lived RONS [21]. DCFH-DA is a non-fluorescent dye which is hydrolyzed into its polar, but non-fluorescent form DCFH on the action of $HO^{\bullet}$ radicals. Oxidation of DCFH by the action of reactive oxygen species (ROS) turns the molecule into its highly fluorescent form 2,7-Dichlorofluorescein (DCF) that can be detected by fluorescence [22] (Figure 3.2 b). Since 2',7'-DCFH is a non-specific probe and can react with various short-lived species, such as $OH^{\bullet}$, $HOO^{\bullet}$, $NO^{\bullet}$, H_2O_2, $ONOO^{\bullet}$ [18,22,23], and due to the short lifespan of these species, no calibration curve can be done and results are expressed in fluorescence intensity. DCFH was previously incorporated to alginate hydrosol before plasma treatments in proportion 1 µL of 2 mM 2,7-DCHF for 150 µL of alginate hydrosol. 200 µL of the alginate sample containing DCHF were placed in 96-well black plate for plasma treatment. After 30-min incubation at room temperature, fluorescence intensity was read with a Synergy HTX Hybrid Multi Mode Microplate Reader using λ_{ex}= 485/20 nm and λ_{em}= 528/20 nm as excitation and emission wavelength filters, respectively.

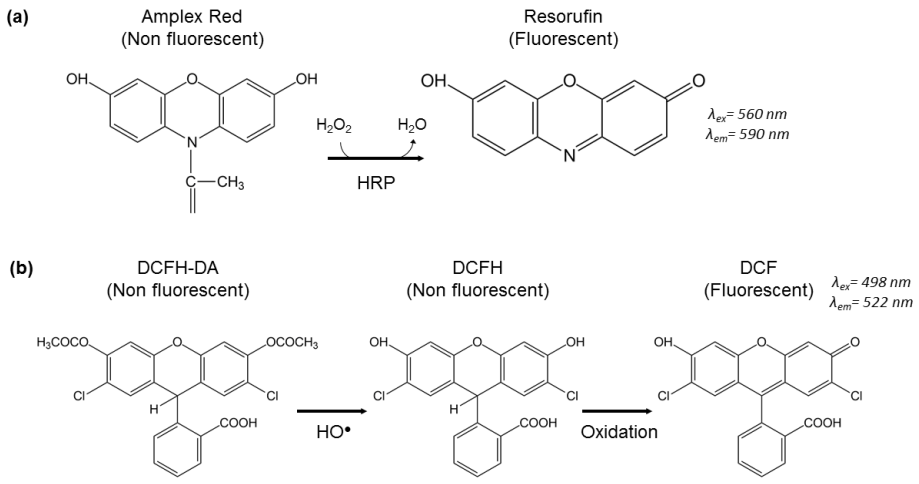

Figure 3.2 : Chemical reactions involved in the fluorescent probes used for the detection of H_2O_2 (a) and short-lived reactive species (b) in alginate hydrosol.

As control, 0.9 % Ringer's solution was used. Ringer's saline was prepared by dissolving 8.60 g/L NaCl, 0.30 g/L KCl and 0.33 g/L $CaCl_2.2H_2O$ in DI water, filtered by using 0.22-µm pore size MILLEXGP filter unit (Merck Millipore Ltd., Ireland).

3.2.5. pH monitoring

2 mL of 0.5 % $_{w/v}$ alginate were placed in a 24 well-plates and treated using kINPen and APPJ (10 mm, 1 L/min). pH was measured by using a PC80 Multiparameter instrument (XS Instruments, Italy) with a Crison 50 14 electrode (Crison, Spain).

3.2.6. FTIR-ATR

FTIR-ATR spectra of freeze-dried alginate hydrogels were recorded using a Nicolet 6700 spectrometer (Thermo Scientific), equipped with a Universal ATR sampling device with a germanium crystal. Spectra were acquired at room temperature in transmission mode as a function of the λ ranged between 4 000 and

675 cm^{-1} with 64 scans at a resolution of 1 cm^{-1}. A background spectrum of air was scanned under the same instrumental conditions before each series of measurements.

3.2.7. SEM

Lyophilized 0.5 % $_{w/v}$ alginate hydrosols were C-coated using an EMITECH K950X Turbo Evaporator (Quorum Technologies Ltd., UK). All samples were imaged in a Phenom XL SEM (Phenom-World B.V., The Netherlands) under high vacuum at 5 kV and a 5 mm working distance.

3.2.8. Release of RONS

200 µL of 0.5 % $_{w/v}$ alginate hydrosol in 96-well plate were treated by kINPen for 90 s, 10 mm and 1 L/min and APPJ for 15 min, 10 mm and 1 L/min. Since lower amount of NO_2^- are generated in alginate with APPJ than kINPen, a longer plasma treatment time for APPJ has been performed to be able to reasonably detect [NO_2^-] with absorbance values within the plate-reader working range. 200 µL of untreated and plasma-treated hydrosols were cross-linked in a 96-well plate by using 50 mM $CaCl_2$ solution for 5 min. Afterward, formed alginate hydrogels were transferred to another well with 100 µL distilled water for rinsing of the excess of calcium chloride solution for 5 min. Plasma treatments and crosslinking process for RONS release experiments were carried out in the same conditions used for cell culture experiments to be able to relate the release of RONS from the alginate hydrosol with the biological effects.

Formed alginate hydrogels were transferred to CORNING Transwell polyester membrane cell culture insert (Sigma-Aldrich), with a 6.5 mm diameter and a 0.4 µm pore size and placed in suspension in 1 mL volume of cell culture media in 24-well plates. For the monitoring of the release kinetics of RONS from the alginate hydrogels 100 µL of the cell culture medium used as release media were withdrawn at determined time points for subsequent quantification of NO_2^- and H_2O_2. 100 µL of fresh medium was replaced after each sample collection. Final volumes of release

media have been measured at the end of release experiment to take into account the volume correction in the concentration calculations of NO_2^- and H_2O_2. NO_2^- and H_2O_2 were quantified as described in the previous section.

3.2.9. In vitro cell experiments

3.2.9.1. Cell culture

Sarcoma Osteogenic (SaOs-2) were used to study the cytotoxicity of the alginate hydrogels. The cell culture medium consisted of McCoy's 5A with 10 % FBS and 1 % P/S. Cells were grown in 75 cm^2 cell culture flasks at 37 °C in a 5 % CO_2 incubator and upon reaching 80 % confluence. SaOs-2 were detached from the flask using trypsin (Invitrogen, Thermofisher) and 10000 cells/well were seeded into 24-well plates with 1 mL volume of culture medium. After 6 h-adhesion, plasma-treated sterile alginate hydrogels, previously prepared in sterile conditions, were introduced into a CORNING Transwell polyester membrane cell culture insert and placed in suspension in the well, to evaluate the effect of kINPen and APPJ plasma treatment of the alginate hydrogels on the SaOs-2 cell viability. As positive control, the same number of cells was placed without adding alginate. The cells were grown at 37 °C in a 5 % CO_2 incubator for another 72 h.

3.2.9.2. Cell viability

Influence of plasma-treated 0.5 % $_{w/v}$ alginate hydrogels on SaOs-2 cell viability was evaluated for kINPen and APPJ (10 mm, 1 L/min) for 90 and 180 s of plasma treatments. Plasma-treated alginate solutions were also studied for 180 s APPJ and kINPen plasma treatment. Cell viability was evaluated at 0, 24 and 72 hours. Cell culture media was replaced by preparation consisting of 250 µL of Cell Proliferation Reagent WST-1 in McCoy's culture medium (1:10) and incubated for 1 hour at 37 °C. Afterward, 100 µL of the supernatant were transferred to another well for absorbance measurement at 440 nm. To evaluate the effects untreated and

plasma-treated alginate hydrogels on SaOs-2 cell viability, normalization of the values was made with respect to the well containing cells only.

3.2.10. Statistics

All the experiments were done on triplicate. Statistical differences were determined using one-way ANOVA with Tukey's post-hoc tests using Minitab 18 software (Minitab Inc., USA). Statistical significance was considered when $p < 0.05$. Data are presented as mean ± standard deviation.

3.3.RESULTS

3.3.1. CAP produces high amount of RONS in alginate

CAP treatments of several concentrations of alginate (between 0.2 and 2 % $_{w/v}$) produced nitrites (NO_2^-) and hydrogen peroxides (H_2O_2) in all cases. However, plasma treatment of high concentrations of alginate revealed a hampered diffusion of the reactive species (Figure S3.9). Since this lack of homogeneity in the diffusion of the reagent influenced the precise detection of RONS, the solution of 0.5 % $_{w/w}$ alginate was selected for further work.

Figure 3.3 presents the quantification of nitrites, hydrogen peroxide and short-lived species generated by plasma as a function of gas flow and distance to the sample in 0.5 % $_{w/v}$ alginate or Ringer's saline, used as control, for 90 s plasma treatment time.

Plasma treatment of alginate allowed much higher generation of RONS (NO_2^- , H_2O_2 and short-lived species) than those obtained in Ringer's saline. In particular, the amounts of NO_2^- generated by APPJ in Ringer at gas flows above 2 L/min are very low and barely visible (Figure 3.3 a ii). For both kINPen and APPJ-treated alginate, a higher loading of NO_2^- was achieved for short distance to the sample and low gas flows (Figure 3.3 a). Higher concentrations of nitrites were generated using kINPen for all studied conditions.

The effects of plasma jet distance and gas flow on alginate followed a different trend when H_2O_2 was concerned (Figure 3.3 b). Increasing gas flow rates led to higher concentration of H_2O_2 in alginate, and short distances were still more suitable to generate higher amount of species. The amount of peroxides generated in Ringer's was several-fold lower than in alginate, and the effects of gas flow or distance were minimized. kINPen at 10 mm distance reached the highest concentrations of H_2O_2, but longer distances produced less peroxides than APPJ. Regarding APPJ, similar H_2O_2 concentrations were obtained between 2 and 5 L/min disregard the distance between the liquid and the jet. The maximum amount of H_2O_2

in alginate generated by APPJ was obtained using 15 mm nozzle distance and gas flow between 2 and 4 L/min.

kINPen treatment of 0.5 % $_{w/v}$ alginate and Ringer's saline highlighted that short distance enhances the generation of short-lived species (Figure 3.3 c). However, no significant differences were observed with the variation of gas flow for the alginate. The most efficient treatment of alginate with regard to the production of short-lived species was with kINPen at 10 mm distance and 1 L/min.

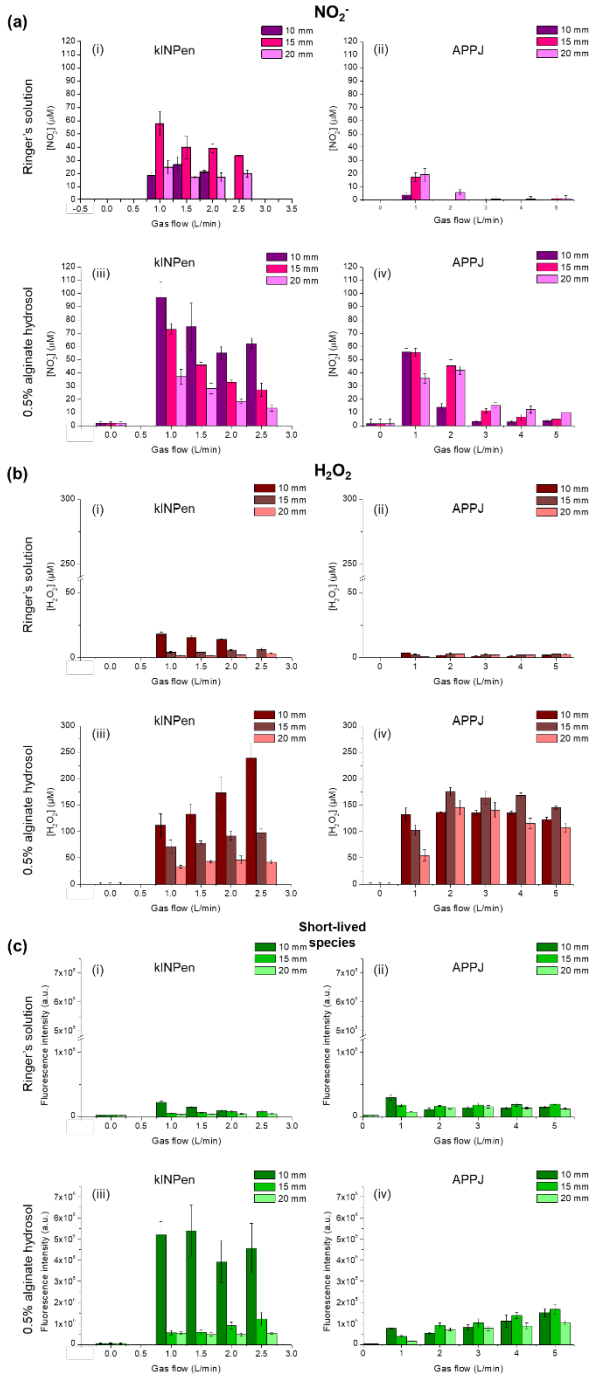

Figure 3.3: Influence of kINPen (Ar gas) (left) or APPJ (He gas) (right) distance to the sample and gas flow on the generation of NO_2^- (a), H_2O_2 (b) and short-lived species (c) in Ringer's saline and in 0.5 % $_{w/v}$ alginate solutions. Treatment time was fixed at 90 s.

These results with plasma-treated alginate contrast with those obtained for plasma-activated Ringer's solution in which APPJ treatment was more effective than kINPen in similar conditions. As observed with the long-lived species recorded (NO_2^- and H_2O_2), the capacity for generating RONS was much higher in alginate than in plasma-activated Ringer's saline, *i.e.* with up to 25 times higher concentrations of short-lived species for kINPen treatment of alginate with respect to physiological solution.

Plasma treatment time progressively increased the concentration of RONS ($[NO_2^-]$, $[H_2O_2]$ and short-lived species) in 0.5 % $_{w/v}$ alginate with both plasma jets (Figure 3.4 a). While the generation of H_2O_2 was relatively similar between kINPen and APPJ, it was observed that, independently of plasma treatment time, kINPen generated more NO_2^- than APPJ. However, important differences were recorded among both sources with regard to generation of short-lived RONS: kINPen being much more effective than APPJ from short treatment times.

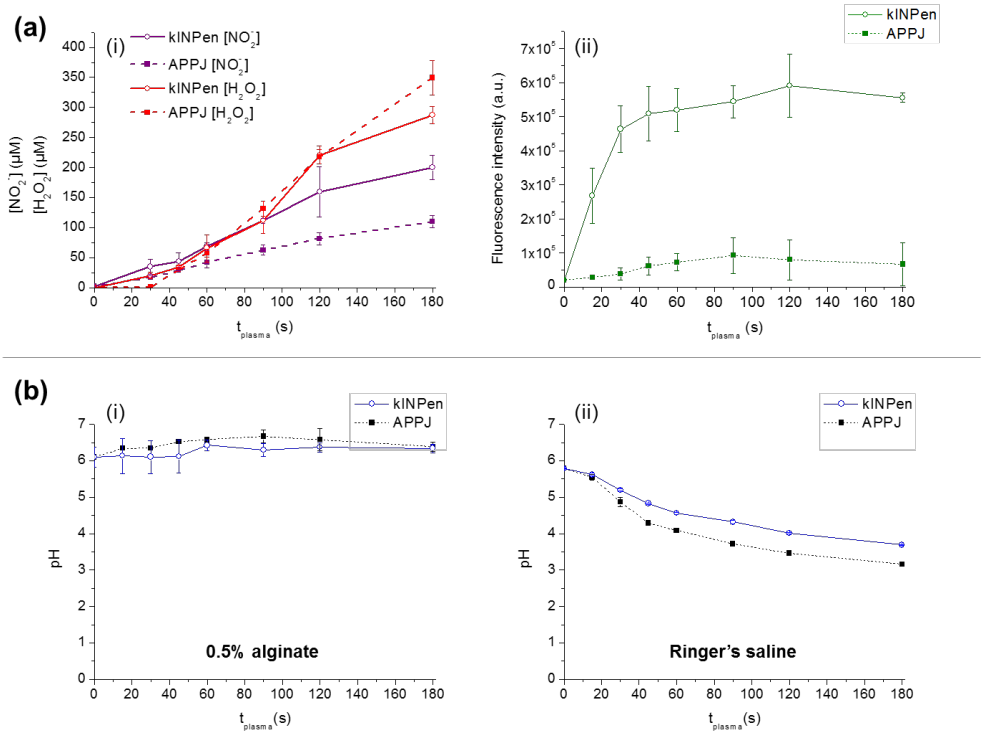

Figure 3.4: Influence of plasma treatment time on the generation of NO_2^-, H_2O_2 (i) and short-lived species (ii) in 0.5 % $_{w/v}$ alginate using kINPen or APPJ at 1 L/min and 10 mm distance (a). pH evolution as function of plasma treatment time of 0.5 % $_{w/v}$ alginate (i) and Ringer's saline (ii) (b).

3.3.2. CAP does not affect physic-chemical properties of alginate

In this section it is described how 2 mL of 0.5 % $_{w/v}$ alginate were treated with either kINPen or APPJ under selected conditions (10 mm, 1 L/min) (pictures shown in Figure 3.5 c). The pH of plasma-treated alginate with any of both plasma jets remained unchanged with treatment time (Figure 3.4 b). This contrasts to the pH of Ringer's saline that decreased down to pH between 3.2 and 3.7 after 3 min of treatment.

Typical porous structures of lyophilized alginate (Figure 3.5 a) were observed by Scanning Electron Microscopy (SEM) and no differences were found after the plasma treatment. Similarly, Fourier Transform Infrared (FTIR-ATR)

spectra of the 0.5 % $_{w/v}$ alginate (Figure 3.5 b) revealed no significant shifts between the different plasma jets studied (*i.e.* less than 5 cm^{-1}). According to the literature, FTIR-ATR spectra of the sodium alginate presents seven characteristic bands from 2000 to 650 cm^{-1} region of the FTIR spectra [24,25] which remain unaltered with plasma treatment either using kINPen or plasma needle, indicating that plasma jet treatment of the solution did neither affect the main chemical bonds of the polymer network nor the ability of the solution to form a hydrogel (Figure 3.5 d). Only a minor change in intensity is found in the broad −OH stretching band within the 3400–3200 cm^{-1} range (not shown). This peak corresponds to a convolution envelope including both FTIR bands from water molecules (usually appearing between 3700-3100 cm^{-1}) [26] and the bands that correspond to the hydroxyl groups from the hydrogel. Since this peak can be highly dependent on the freeze-drying process of the samples, this hampers drawing conclusions from the peaks appearing in this range.

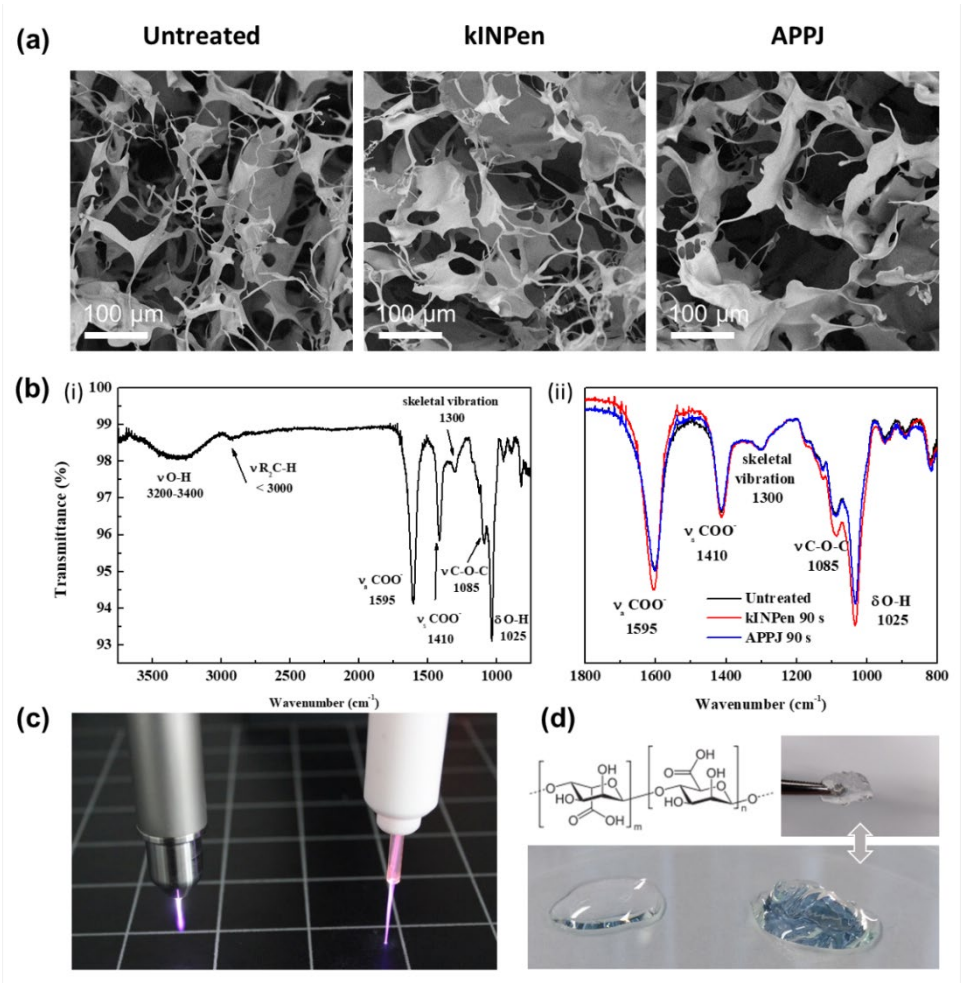

Figure 3.5: SEM micrographs (a) and FTIR-ATR spectra (b) of untreated (i), kINPen- and APPJ-treated 0.5 % $_{w/v}$ alginate for 90 s, at 10 mm distance and 1 L/min. Digital picture of kINPen and APPJ in operation (c). Chemical structure of alginate and digital pictures of the alginate solution (left side) and of the cross-linked alginate hydrogel (right side) (d).

3.3.3. Crosslinking is a critical step

Since our final aim was to evaluate the ability of hydrogels to act as reservoirs for RONS generated by plasma, crosslinking of the alginate was an essential step. Thus, the 0.5 % $_{w/v}$ alginate solutions were plasma-treated, cross-linked for 5 min in a $CaCl_2$ solution, and then rinsed to eliminate excess of crosslinker that could be toxic for further cell testing.

A significant part of the RONS generated by plasma in the alginate was released during the crosslinking process (Figure 3.6). Most NO_2^- was lost from plasma-treated alginate during its crosslinking (51.8 % for kINPen and 66.7 % for APPJ) and the rinsing process (14.8 % and 25.8 %, respectively). Thus, these steps left the alginate hydrogel with only 33.4 % for kINPen and 7.5 % for APPJ of the initial NO_2^- plasma-loading, which corresponds to 32.4 µM and 25.2 µM respectively.

In the case of H_2O_2, a lower fraction was lost during the whole crosslinking process (crosslinking + rinsing). A final percentage of 42.8 % and 39.3 % (in kINPen- and APPJ-treated alginate, respectively) remained in the hydrogel with respect to the initial loading, corresponding to final amounts of peroxides of 47.9 µM and 115.8 µM. These can be considered as the initial amount of nitrites and peroxides loaded in the alginate hydrogel at the beginning of the release experiments presented in Figure 3.7.

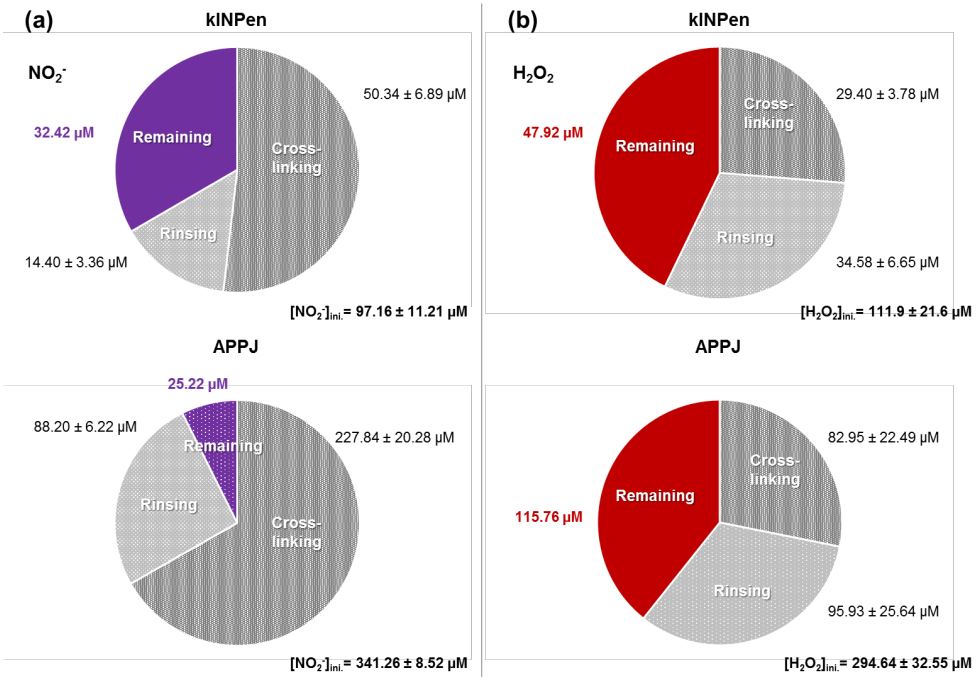

Figure 3.6: Total concentration of NO_2^- (a) and H_2O_2 (b) released during crosslinking and rinsing processes of the alginate hydrogel previously treated by kINPen for 90 s and APPJ for 15 min (10 mm, 1 L/min). The proportion of RONS remaining in the hydrogel after crosslinking and rinsing are highlighted in violet for NO_2^- and red for H_2O_2.

3.3.4. CAP-treated hydrogels are not cytotoxic

The diffusion of species remaining in the plasma-treated alginate hydrogels after the crosslinking process to the cell culture medium (Figure 3.7) was evaluated either in Transwell experiments or in direct contact with the medium.

Figure 3.7 a and 3.7 b show the respective NO_2^- and H_2O_2 release kinetics from plasma-treated alginate hydrogel to the cell culture medium during 72 h, using the hydrogel in direct immersion (i) or using an insert (Transwell experiments) (ii). Direct immersion of the alginate hydrogel led to higher release amount of NO_2^- from the hydrogel than Transwell experiments. Plasma-treated hydrogel presented a maximum release of nitrites of 30.01 ± 8.05 µM for kINPen and 22.68 ± 2.77 µM

for APPJ after 72 hours for direct immersion of the hydrogel, which corresponds to a 92.6 % and 89.9 % of the initial loading of NO_2^-.

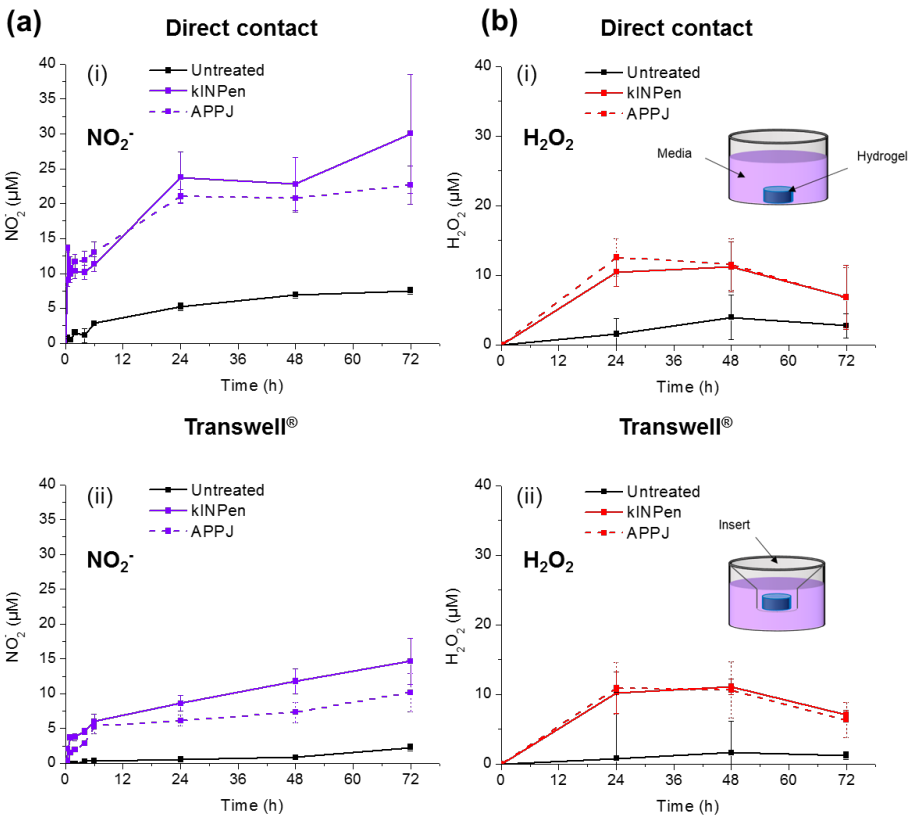

Figure 3.7: Cumulative release profiles of NO_2^- (a) and H_2O_2 (b) from the RONS-loaded 0.5 % $_{w/v}$ alginate hydrogels to cell culture media. The alginate hydrogels had been treated by kINPen or APPJ for 90 s or 15 min, respectively (at 10 mm, 1 L/min), crosslinked and rinsed. Release was evaluated either in direct contact (i) or in Transwell (ii).

Half NO_2^- release was recorded (14.65 ± 3.29 µM and 10.19 ± 2.75 µM, respectively) when placing the hydrogel in an insert (this corresponds to 45.2 % and a 40.4 % of the initial concentration of nitrites in the hydrogel), in kINPen and in APPJ respectively.

Regarding H_2O_2 release from the plasma-treated alginate (Figure 3.7 b), low amount of hydrogen peroxides was observed either in Transwell or in direct contact, with higher values of H_2O_2 in the release media around 10 µM.

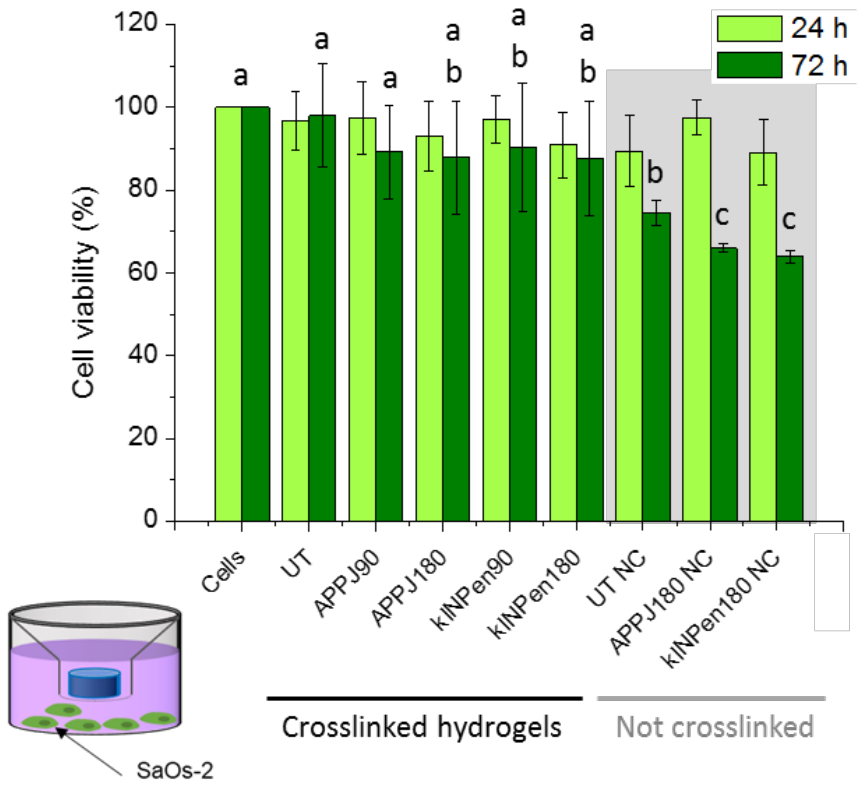

Figure 3.8: SaOS-2 cell viability of untreated (UT), APPJ- and kINPen-treated alginate hydrogels for 24- and 72-hour Transwell cell culture at treatment times of 90 and 180s. Cell viability using non-crosslinked alginate solutions (NC) is presented on grey background. a,b,c indicate statistically significant differences.

The effect of the release of RONS from the plasma-treated alginate was studied on Sarcoma osteogenic cells (SaOS-2) and results are presented in Figure 3.8. No significant differences were observed in SaOs-2 cell viability between untreated and plasma-treated crosslinked hydrogels placed in Transwell with respect to control, either for 24 or 72 hours. After crosslinking the hydrogels had undergone washing process, so few RONS remained in the material. Therefore, the lack of toxicity in the crosslinked hydrogels indicates that the plasma treatment of the alginate did not induce cytotoxic alterations in the alginate chains. In contrast, non-crosslinked alginate solutions presented a decrease of cell viability after 72 hours with respect to control, with cell viability of 76.0 % for UT NC and 65.9 % and 63.9 % for APPJ180 NC and kINPen180 NC, respectively.

3.4.DISCUSSION

In this chapter alginate hydrogels have been shown to be suitable vehicles for RONS produced by atmospheric pressure plasma jets. It is widely admitted that the CAP-generated RONS are basic anti-cancer factors supressing cancer cell proliferation in *in vitro* cell cultures [27–32] and are also essential in the treatment of chronic wounds [33]. Here, two atmospheric pressure plasma jets are compared: a single-electrode jet working with helium and the kINPen, a widely extended plasma jet working with argon.

It is known that a variety of RONS can be formed by CAP in water or saline solutions such as Phosphate Buffer Saline (PBS) [34–38] and, as recorded here, in Ringer's saline. Many parameters affect the generation of RONS in solutions, the differences in chemical composition of the treated solution being critical to that aim [6]. Three species were quantified here: H_2O_2, $NO_2^-$and short-lived species (Figure 3.3 a, b & c, I & ii), their concentration increasing with treatment time (Figure 3.4 a) with both plasma jets, APPJ and kINPen. As reviewed by Jablonowski et al. [33], RONS in the liquid phase can either be generated by direct interaction at the plasma/liquid interface [17,29], via transfer of the reactive species from the gas phase into the liquid [39,40], or by secondary or tertiary reactions in the bulk liquid [2].

It can be observed that the concentration of RONS generated in alginate was several-fold higher than in Ringer's saline, ranging between 2 (NO_2^-), 10 (H_2O_2) and 25 (short-lived RONS) -fold higher for kINPen and slightly lower for the He APPJ needle. This can be explained by the following: Nitrites are formed in plasma treated liquids through the dissolution of nitrogen oxides formed in the gas phase of the plasma jet. In general, in acidic conditions, nitrous acid (which is one of the major sources of NO_2^-) is not stable and decomposes into nitrogen dioxide, which may react with $OH^\bullet$ to form peroxinitrous acid.

Another reaction that is promoted in acidic solution takes place between NO_2^- and H_2O_2 (reaction 1) and is another source of peroxynitrites [6,18,41,42].

$$NO_2^- + H_2O_2 + H^+ \rightarrow ONOOH + H_2O \qquad (1)$$

Peroxinitrous acid is not stable at acidic pH and converts to NO_3^-, as shown by Bruggeman et al. [17].

As Ringer's saline is progressively acidified by the CAP treatment (Figure 3.4 b) - due to the formation of nitrites - these reactions can take place and decrease the amount of H_2O_2 and NO_2^- in the liquid (Figure 3.3). On the contrary, the close to neutral pH found in the alginate solutions (Figure 3.4 b), avoids this reaction taking place and may allow for the accumulation of much higher concentrations of these RONS. This hypothesis is confirmed by CAP treatment of a buffered solution (PBS) at the same pH of 6.5 as alginate (Figure S3.10). It can be observed that the concentrations of RONS generated by CAP treatment in PBS are similar with those obtained in alginate.

The screening of the plasma treatment conditions pointed out that the amount of the different reactive species (NO_2^-, H_2O_2 and short-lived species) can be easily tuned, a crucial feature to be able to control the dose of RONS. For instance, as observed in other works [43], on increasing the gas flow rate, after a certain point the concentration of NO_2^- decreases for both plasma jets (Figure 3.3 a). This can possibly be ascribed to the fluid dynamics in the gas phase which play a major role in the species that can reach the liquid surface and thus, on the generation of RONS in liquids. It has been reported that at low flow rates the jet effluent follows a laminar mode that allows the mixing of air with the noble gas generating the discharge (and thus generation of more RONS in the gas phase) [1,18,29,35]. Contrarily, at higher gas flows, the effluent enters a turbulent mode that impairs mixing of air and decreases the amount of certain RONS generated [29]. For a deeper understanding of the reactions taking place in liquids, Verlackt et al. [35], presented a 2D fluid dynamics model for the interaction between kINPen and a liquid (water). Despite the 0.5 % $_{w/v}$ alginate being more viscous than water, the plasma gas phase fluid dynamics may be extrapolated and the same descriptions valid at this point, since to our knowledge no modelling with hydrogels has been reported until now.

Alginate solutions are studied in this chapter given their ability to crosslink *in vivo* with Ca^{2+} ions from the body and form stable hydrogels which can allow drug delivery of RONS with a minimally invasive strategy. The higher concentrations of RONS generated by CAP in alginate, which displayed no apparent changes in the structure of the polymer (Figure 3.5) were progressively released to a surrounding medium (Figure 3.7). However, to simulate the crosslinking in the laboratory and obtaining the hydrogel, it is necessary to add a $CaCl_2$ solution to the alginate solution. This leads to an important loss of the initial amount of RONS by diffusion to the crosslinking solution (Figure 3.6). Although the loss of RONS in the crosslinking process could partly be limited during crosslinking by reducing the volume and increasing the concentration of $CaCl_2$ of the crosslinking solution, this leak of RONS is inevitable if working *in vitro.* The final values of RONS in the final hydrogel are between 7 % and 34 % of the initial amounts generated by CAP in the alginate hydrosol, depending on the reactive species and the initial plasma treatment performed. In particular, the final amount remaining in the alginate hydrogel for further release of NO_2^- was 32.4 µM for 90 s kINPen treatment and 25.2 µM for 15 min APPJ treatment (10 mm, 1 L/min); concentration of H_2O_2 was of 47.9 µM and 115.8 µM, respectively. These amounts of RONS are still higher in hydrogel compared to Ringer's saline (Figure 3.3), which is an advantage to the use of alginate with respect to saline solution. Furthermore, for *in vivo* application, as crosslinking would take place in the body with the Ca^{2+} in body fluids, all RONS would be available for local delivery.

Release experiments showed final nitrite release of 30.0 µM for kINPen and 22.7 µM for APPJ-treated alginate hydrogel after 72 h, in direct contact with cell culture medium, corresponding to release percentages of 92.4 % and 89.9 % of the initial concentration, respectively. The final NO_2^- concentrations go down to 14.7 µM and 10.2 µM, respectively, when the plasma-treated hydrogels were placed in suspension in the cell culture media using an insert (same configuration between the release and cytotoxicity experiments). Regarding H_2O_2, the highest amount (~ 10 µM) was obtained after 24 h of release for both plasma devices. A decreasing trend

of H_2O_2 concentration was observed in the release media from 48 to 72 hours, that may be attributed to an ageing of H_2O_2, as observed in cell culture media [44].

The viability of SaOS-2 was not affected when cells were cultured in indirect contact with untreated and plasma-treated crosslinked hydrogels for both kinds of plasma treatments (Figure 3.8). Despite the high loading of RONS in the alginate solutions achieved by plasma treatment, the low amount of RONS remaining after crosslinking (Figure 3.6 and Figure 3.7) does not affect cell viability, which agrees with previous works [6,45]. As most RONS were washed away by the crosslinking + washing process, this allowed to ascertain that the biomaterial itself remains fully biocompatible after the plasma treatment (no significant differences were observed in crosslinked alginate between treatments or with respect to controls, Figure 3.8).

To evaluate the biological efficacy of the plasma-generated RONS within the alginate, non crosslinked (NC) polymer solutions were employed (Figure 3.8, marked in grey shade). A slight decrease in cell viability was observed for the untreated alginate solution (UT NC) that could be attributed to calcium sequestration from the cell culture media by the alginate. The plasma-generated RONS lead to a further decrease of cell viability from the untreated (UT NC) to the plasma-treated alginate solutions. Cell viability after 72 hours decreased to 65.9 % for APPJ180 NC and 63.9 % for kINPen180 NC, respectively. This decrease on SaOS-2 cell viability can be ascribed to the concentration of H_2O_2 released to the media from the plasma-treated alginate solutions, and available for interaction with cells was of 39.79 ± 3.49 μM for APPJ180 NC and 37.68 ± 2.96 μM for kINPen180 NC.

The decrease in cell viability obtained with these levels of RONS is in line with previous works [45], where APPJ plasma treatment of cell culture medium resulted in a progressive decrease of the viability of SaOS-2 with the increase of RONS concentration in culture media. In that work, cell viability was found between 92 and 20 % for APPJ treatment times of 10-30 min. The higher cytotoxicity in that work [45] has to be directly related with the higher amount of RONS present in the McCoy's cell culture medium (ie. H_2O_2: 98 μM for 10 min APPJ treatment to 290

μM for 30 min APPJ treatment) with respect to the amounts found here. Despite here only NO_2^-, H_2O_2 and short-lived ROS were detected, many studies have described the anti-carcinogenic effects of plasma by many other reactive species such as O_2^-, OH^*, NO, O, NO_3^-, NO_2^- and $ONOO^-$ [29], and other works [34,46] investigated artificially supplementing liquids with the same concentrations of H_2O_2 and/or NO_2^- and did not observe the same effects as with plasma, confirming the hypothesis that the complex of RONS generated by plasma is necessary for its biological action.

Thus, generating reactive species by cold atmospheric plasmas in alginate-based biomaterials and their release opens great perspectives in the design of new implantable biomaterials for plasma therapies. These results have important implications in many biomedical applications of alginate hydrogels, including tissue engineering and drug delivery. An optimization is certainly required to obtain cross-linked hydrogels with sufficient concentration of RONS.

3.5.CONCLUSION

In this chapter two atmospheric pressure plasma jet devices were compared in the generation of RONS under different plasma settings conditions. Optimal plasma conditions show higher generation of RONS in alginate solution than in saline solution. Plasma treatment did not affect the alginate chemical structure with no cytotoxic modifications into the polymer backbone as the biocompatibility was conserved.

A fast RONS release was obtained from alginate hydrogels. Moreover, the RONS released from the plasma-treated alginate show cytotoxic activity towards bone cancer cells.

Results obtained in this chapter open new perspectives for the use of hydrogel-based biomaterials as RONS carrier for plasma-based therapies.

REFERENCES

1. Reuter, S.; von Woedtke, T.; Weltmann, K.-D. The kINPen—a review on physics and chemistry of the atmospheric pressure plasma jet and its applications. *J. Phys. D. Appl. Phys.* **2018**, *51*, 233001.
2. Hoffmann, C.; Berganza, C.; Zhang, J. Cold Atmospheric Plasma: Methods of production and application in dentistry and oncology. *Med. Gas Res.* 2013, *3*.
3. Dubuc, A.; Monsarrat, P.; Virard, F.; Merbahi, N.; Sarrette, J.P.; Laurencin-Dalicieux, S.; Cousty, S. Use of cold-atmospheric plasma in oncology: a concise systematic review. *Ther. Adv. Med. Oncol.* **2018**, *10*.
4. Hartwig, S.; Doll, C.; Voss, J.O.; Hertel, M.; Preissner, S.; Raguse, J.D. Treatment of Wound Healing Disorders of Radial Forearm Free Flap Donor Sites Using Cold Atmospheric Plasma: A Proof of Concept. *J. Oral Maxillofac. Surg.* **2017**, *75*, 429–435.
5. Rutkowski, R.; Pancewicz, S.A.; Rutkowski, K.; Rutkowska, J. Reactive oxygen and nitrogen species in inflammatory process. *Pol. Merkur. Lek.* **2007**, *23*, 131–136.
6. Khlyustova, A.; Labay, C.; Machala, Z.; Ginebra, M.-P.; Canal, C. Important parameters in plasma jets for the production of RONS in liquids for plasma medicine: A brief review. *Front. Chem. Sci. Eng.* **2019**, *13*, 238–252.
7. Shen, J.; Tian, Y.; Li, Y.; Ma, R.; Zhang, Q.; Zhang, J.; Reports, J.F.-S.; 2016, U. Bactericidal Effects against S. aureus and Physicochemical Properties of Plasma Activated Water stored at different temperatures. *Nature*.
8. Drury, J.L.; Mooney, D.J. Hydrogels for tissue engineering: scaffold design variables and applications. *Biomaterials* **2003**, *24*, 4337–4351.
9. Tan, H.; Marra, K.G. Injectable, Biodegradable Hydrogels for Tissue Engineering Applications. *Materials (Basel).* **2010**, *3*, 1746–1767.
10. Omidian, H.; Park, K. Hydrogels. In *Fundamentals and Applications of Controlled Release Drug Delivery*; 2012; pp. 75–105.
11. Nguyen, M.K.; Lee, D.S. Injectable Biodegradable Hydrogels. *Macromol. Biosci.* **2010**, *10*, 563–579.
12. Rowley, J.A.; Madlambayan, G.; Mooney, D.J. *Alginate hydrogels as synthetic extracellular matrix materials*; 1999; Vol. 20;.
13. Mørch, Ý.A.; Donati, I.; Strand, B.L.; Skjåk-Bræk, G. Effect of Ca2+, Ba2+, and Sr2+ on alginate microbeads. *Biomacromolecules* **2006**, *7*, 1471–1480.

14. Lee, K.Y.; Mooney, D.J. Alginate: Properties and biomedical applications. *Prog. Polym. Sci.* **2012**, *37*, 106–126.
15. Omidian, H.; Park, K. Introduction to Hydrogels. In *Biomedical Applications of Hydrogels Handbook*; 2010; pp. 1–16.
16. Zaplotnik, R.; Bišćan, M.; Kregar, Z.; Cvelbar, U.; Mozetič, M.; Milošević, S. Influence of a sample surface on single electrode atmospheric plasma jet parameters. *Spectrochim. Acta - Part B At. Spectrosc.* **2015**, *103–104*, 124–130.
17. Bruggeman, P.J.; Kushner, M.J.; Locke, B.R.; Gardeniers, J.G.E.; Graham, W.G.; Graves, D.B.; Hofman-Caris, R.C.H.M.; Maric, D.; Reid, J.P.; Ceriani, E.; et al. Plasma–liquid interactions: a review and roadmap. *Plasma Sources Sci. Technol.* **2016**, *25*, 053002.
18. Machala, Z.; Tarabova, B.; Hensel, K.; Spetlikova, E.; Sikurova, L.; Lukes, P. Formation of ROS and RNS in Water Electro-Sprayed through Transient Spark Discharge in Air and their Bactericidal Effects. *Plasma Process. Polym.* **2013**, *10*, 649–659.
19. Giustarini, D.; Rossi, R.; Milzani, A.; Dalle-Donne, I. Nitrite and Nitrate Measurement by Griess Reagent in Human Plasma: Evaluation of Interferences and Standardization. *Methods Enzymol.* **2008**, *440*, 361–380.
20. Guevara, I.; Iwanejko, J.; Dembińska-Kieć, A.; Pankiewicz, J.; Wanat, A.; Anna, P.; Gołąbek, I.; Bartuś, S.; Malczewska-Malec, M.; Szczudlik, A. Determination of nitrite/nitrate in human biological material by the simple Griess reaction. *Clin. Chim. Acta* **1998**, *274*, 177–188.
21. Gomes, A.; Fernandes, E.; and, J.L.-J. of biochemical; 2005, undefined Fluorescence probes used for detection of reactive oxygen species. *Elsevier*.
22. Rajneesh, .; Pathak, J.; Chatterjee, A.; Singh, S.; Sinha, R. Detection of Reactive Oxygen Species (ROS) in Cyanobacteria Using the Oxidant-sensing Probe 2',7'-Dichlorodihydrofluorescein Diacetate (DCFH-DA). *Bio-Protocol* **2017**, *7*.
23. Rastogi, R.P.; Singh, S.P.; Häder, D.P.; Sinha, R.P. Detection of reactive oxygen species (ROS) by the oxidant-sensing probe 2',7'-dichlorodihydrofluorescein diacetate in the cyanobacterium Anabaena variabilis PCC 7937. *Biochem. Biophys. Res. Commun.* **2010**, *397*, 603–607.
24. Daemi, H.; Barikani, M. Synthesis and characterization of calcium alginate nanoparticles, sodium homopolymannuronate salt and its calcium nanoparticles. *Sci.*

Iran. **2012**, *19*, 2023–2028.

25. Li, P.; Dai, Y.N.; Zhang, J.P.; Wang, A.Q.; Wei, Q. Chitosan-alginate nanoparticles as a novel drug delivery system for nifedipine. *Int. J. Biomed. Sci.* **2008**, *4*, 221–228.
26. Enev, V.; Sedláček, P.; Jarábková, S.; Velcer, T.; Pekař, M. ATR-FTIR spectroscopy and thermogravimetry characterization of water in polyelectrolyte-surfactant hydrogels. *Colloids Surfaces A Physicochem. Eng. Asp.* **2019**, *575*, 1–9.
27. Yan, D.; Sherman, J.H.; Keidar, M. Cold atmospheric plasma, a novel promising anti-cancer treatment modality. *Oncotarget* **2017**, *8*, 15977–15995.
28. Yan, D.; Cui, H.; Zhu, W.; Talbot, A.; Zhang, L.G.; Sherman, J.H.; Keidar, M. The Strong Cell-based Hydrogen Peroxide Generation Triggered by Cold Atmospheric Plasma. *Sci. Rep.* **2017**, *7*, 10831.
29. Lu, X.; Naidis, G.V.; Laroussi, M.; Reuter, S.; Graves, D.B.; Ostrikov, K. Reactive species in non-equilibrium atmospheric-pressure plasmas: Generation, transport, and biological effects. *Phys. Rep.* **2016**, *630*, 1–84.
30. Hirst, A.M.; Frame, F.M.; Arya, M.; Maitland, N.J.; O'Connell, D. Low temperature plasmas as emerging cancer therapeutics: the state of play and thoughts for the future. *Tumor Biol.* **2016**, *37*, 7021–7031.
31. Keidar, M. Plasma for cancer treatment. *Plasma Sources Sci. Technol.* **2015**, *24*, 033001.
32. Yan, D.; Talbot, A.; Nourmohammadi, N.; Sherman, J.H.; Cheng, X.; Keidar, M. Toward understanding the selective anticancer capacity of cold atmospheric plasma—A model based on aquaporins (Review). *Biointerphases* **2015**, *10*, 040801.
33. Jablonowski, H.; Santos Sousa, J.; Weltmann, K.D.; Wende, K.; Reuter, S. Quantification of the ozone and singlet delta oxygen produced in gas and liquid phases by a non-thermal atmospheric plasma with relevance for medical treatment. *Sci. Rep.* **2018**, *8*.
34. Van Boxem, W.; Van der Paal, J.; Gorbanev, Y.; Vanuytsel, S.; Smits, E.; Dewilde, S.; Bogaerts, A. Anti-cancer capacity of plasma-treated PBS: effect of chemical composition on cancer cell cytotoxicity. *Sci. Rep.* **2017**, *7*, 16478.
35. Verlackt, C.C.W.; Van Boxem, W.; Bogaerts, A. Transport and accumulation of plasma generated species in aqueous solution. *Phys. Chem. Chem. Phys.* **2018**, *20*, 6845–6859.
36. Tanaka, H.; Nakamura, K.; Mizuno, M.; Ishikawa, K.; Takeda, K.; Kajiyama, H.;

Utsumi, F.; Kikkawa, F.; Hori, M. Non-thermal atmospheric pressure plasma activates lactate in Ringer's solution for anti-tumor effects. *Sci. Rep.* **2016**, *6*, 36282.

37. Chauvin, J.; Judée, F.; Yousfi, M.; Vicendo, P.; Merbahi, N. Analysis of reactive oxygen and nitrogen species generated in three liquid media by low temperature helium plasma jet. *Sci. Rep.* **2017**, *7*, 4562.
38. Gorbanev, Y.; Privat-Maldonado, A.; Bogaerts, A. Analysis of Short-Lived Reactive Species in Plasma-Air-Water Systems: The Dos and the Do Nots. *Anal. Chem.* **2018**, *90*, 13151–13158.
39. Attri, P.; Kim, Y.H.; Park, D.H.; Park, J.H.; Hong, Y.J.; Uhm, H.S.; Kim, K.N.; Fridman, A.; Choi, E.H. Generation mechanism of hydroxyl radical species and its lifetime prediction during the plasma-initiated ultraviolet (UV) photolysis. *Sci. Rep.* **2015**, *5*.
40. Winter, J.; Tresp, H.; Hammer, M.U.; Iseni, S.; Kupsch, S.; Schmidt-Bleker, A.; Wende, K.; Dünnbier, M.; Masur, K.; Weltmann, K.D.; et al. Tracking plasma generated H2O2 from gas into liquid phase and revealing its dominant impact on human skin cells. *J. Phys. D. Appl. Phys.* **2014**, *47*.
41. Bosi, F.J.; Tampieri, F.; Marotta, E.; Bertani, R.; Pavarin, D.; Paradisi, C. Characterization and comparative evaluation of two atmospheric plasma sources for water treatment. *Plasma Process. Polym.* **2018**, *15*, 1700130.
42. Lukes, P.; Dolezalova, E.; Sisrova, I.; Clupek, M. Aqueous-phase chemistry and bactericidal effects from an air discharge plasma in contact with water: evidence for the formation of peroxynitrite through a pseudo-second-order post-discharge reaction of H_2O_2 and HNO_2. *Plasma Sources Sci. Technol.* **2014**, *23*, 015019.
43. Jeong Baek, E.; Min Joh, H.; Ja Kim, S.; Chung, T.H. Effects of the electrical parameters and gas flow rate on the generation of reactive species in liquids exposed to atmospheric pressure plasma jets. *J. Appl. Phys* **2016**, *23*, 13301.
44. Yan, D.; Nourmohammadi, N.; Bian, K.; Murad, F.; Sherman, J.H.; Keidar, M. Stabilizing the cold plasma-stimulated medium by regulating medium's composition. *Sci. Rep.* **2016**, *6*.
45. Canal, C.; Fontelo, R.; Hamouda, I.; Guillem-Marti, J.; Cvelbar, U.; Ginebra, M.-P. Plasma-induced selectivity in bone cancer cells death. *Free Radic. Biol. Med.* **2017**, *110*.
46. Tornin, J.; Mateu-Sanz, M.; Rodríguez, A.; Labay, C.; Rodríguez, R.; Canal, C.

Pyruvate Plays a Main Role in the Antitumoral Selectivity of Cold Atmospheric Plasma in Osteosarcoma. *Sci. Rep.* **2019**, *9*.

SUPPLEMENTARY INFORMATION – CHAPTER 3

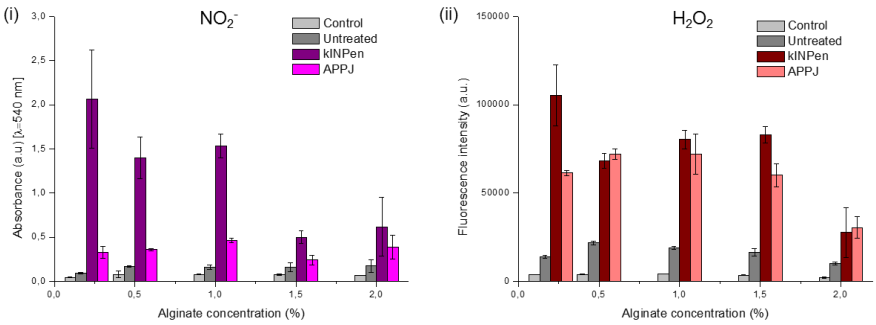

Figure S3.9: Influence of kINPen and APPJ plasma treatment (90 s, 10 mm, 1 L/min) on different concentrations of alginate solutions: detection of nitrites (i) and hydrogen peroxides (ii). Control in grey refers to an untreated sample.

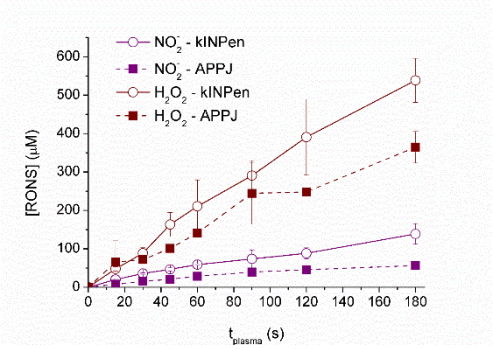

Figure S3.10: Influence of treatment time with APPJ or kINPen on the concentration of NO_2^- and H_2O_2 in PBS (pH 6.5) at 1 L/min gas flow and 10 mm nozzle distance.

CHAPTER 4

4. Generation of Reactive Species from Atmospheric Pressure Plasma Jet in Methacrylated Gelatine Hydrogel

ABSTRACT

Methacrylated gelatin hydrogels, as versatile gelatin-based polymers, have been widely studied for tissue engineering and drug delivery applications. Cold atmospheric pressure plasma jets show great capabilities in the generation of reactive oxygen and nitrogen species leading to a biological response, and the combination between plasma and polymers in solution is of interest in the biomedical field. In this chapter we report the effects of plasma treatment on methacrylated gelatin solutions. Reactive species such as H_2O_2 and NO_2^- were quantified using fluorescent and colorimetric probes, respectively. The chemical structure of methacrylated gelatin and its possible modifications due to plasma treatment were studied by ^{1}H-NMR spectroscopy and rheology. The results obtained showed an increase of the concentrations of H_2O_2 and NO_2^- in methacrylated gelatin solutions following plasma treatment. After treatment, NO_2^- ions are stable over time in methacrylated gelatin solutions, while H_2O_2 decays with a half-life time of 1.2 h. Release experiments in PBS showed a burst release within the first hour of H_2O_2 and NO_2^- up to 130 and 30 µM respectively from plasma-treated methacrylated gelatin hydrogels. No changes in the chemical structure were observed in the semi-synthetic polymer backbone. The viscoelastic properties were modified after plasma treatment as more brittle hydrogels were obtained comparing to untreated methacrylated gelatin hydrogel. The encouraging results of this work show that plasma-treated methacrylated gelatin hydrogel can be used for the storage and delivery of reactive species for future biomedical applications.

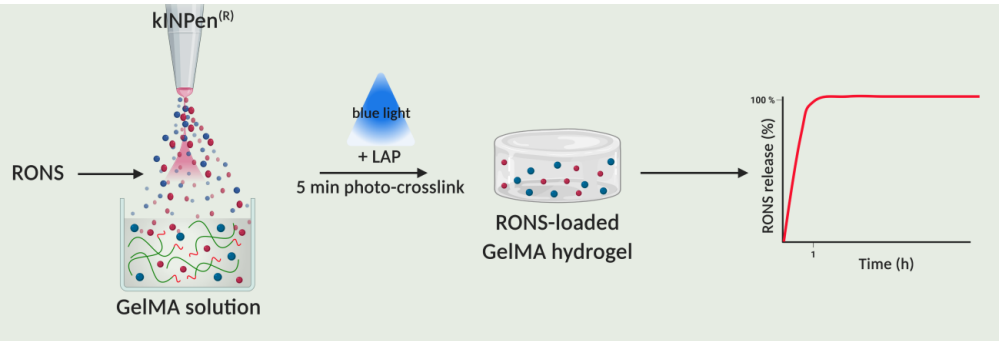

Figure 4.1: Representative scheme of Chapter 4; Plasma treatment of GelMA polymer solution followed by photo-crosslinking using blue light and release of reactive species from the plasma-treated hydrogel.

4.1.INTRODUCTION

Cold atmospheric pressure plasmas (CAP) are gaining great interest in research today [1–3]. Their applications in wound healing and cancer therapies are particularly attractive [4–6]. In fact, CAP devices working at atmospheric pressure are able to generate a substantial amount of reactive species at room temperature. This property makes them able to treat various samples such as living and biological tissues without degrading the surrounding environment. Many of the biological effects of plasma therapies are essentially based on the generation of reactive species [7–9]. It is reported that H_2O_2 and NO_2^- generated by plasma are two of the main long-lived species which seem to play a synergistic effect on the anti-cancer capacity [10,11]. In this context, a lot of research is focused on the generation of plasma-conditioned liquids that can allow minimally invasive therapies showing similar anti-cancer effects than the direct plasma treatment both *in vitro* and *in vivo* [12–17].

A possible approach for the generation and delivery of reactive species could be the use of biopolymer solutions. In fact, certain polymers can easily undergo crosslinking under adequate stimuli to lead to a stable self-standing hydrogel [18,19]. Hydrogels are great candidates in bio medical applications, since they are able to swell and retain a huge amount of water without losing their three-dimensional polymer network [20]. Among the variety of biocompatible polymers, methacrylated gelatin (GelMA) is actually one of the most popular hydrogels. GelMA is an attractive photo-curable material which is made from chemically modified gelatin with methacrylate groups [21]. GelMA presents a facile synthesis method, has a good stability, is cytocompatible and is commercially available [22–25]. GelMA is able to form a stable chemical gel in presence of a water soluble and biocompatible photo-initiator upon exposure to blue light [26–28]. One of the major advantages of photo-crosslinkable hydrogels is their allowance to be injected and cross-linked *in situ* in a minimally invasive manner [29–33]. The resultant hydrogel retains its physical form at body temperature and its structural stability. GelMA

hydrogels have been widely investigated in several applications in the biomedical field [34–40].

Atmospheric Pressure Plasma Jet (APPJ) treatment of polymer solutions or hydrogels for biomedical applications is starting to gain importance. Recently, polymer solutions treated by CAP showed better printability in electro-spinning for potential application in tissue engineering [41–43]. In the area of *Plasma Medicine*, gelatin or agarose hydrogels were employed as model to mimic the skin. Szili et al., investigated the transport and delivery of reactive species from APPJ through the hydrogels to understand the interactions between APPJ and the skin during *in vivo* treatments [44–46]. In Chapter 3, we treated alginate solutions using different APPJ devices. We recorded higher amounts of H_2O_2 and NO_2^- in alginate solutions subjected to APPJ treatment. We observed that the chemical structure of the alginate backbone was not altered by APPJ treatment. Moreover, a good biocompatibility towards bone cells was obtained. These recent advances in the treatment of polymer solution by APPJ devices open new doors for biomedical applications. Further investigations on the interactions of APPJ with polymer solutions and hydrogels are still needed for a better understanding of the phenomena taking place, for the design of new APPJ -based therapies.

In this context, we study here the effects of APPJ treatment on GelMA solutions. We aim to investigate the potential of a semi-synthetic hydrogel under APPJ treatment in the generation and storage of RONS for further use in biomedical applications. The usual methods for detection of RONS employed with liquids will be applied and adapted here to GelMA solutions. The chemical structure of the polymer as well as the hydrogel mechanical properties will be characterized following APPJ treatments.

4.2.MATERIALS & METHODS

4.2.1. Materials

Gelatin (bovine skin, type B, gel strength 225 g bloom), methacrylic anhydride (purity 94 %, MW: 154.16 g/mol, liquid), lithium phenyl-2,4,6-trimethylbenzoylphosphinate (LAP, purity > 95 %, M.W.: 294.21 g/mol, powder form), dialysis membrane (12-14 kDa), sulphanilamide (purity ≥ 99%, M.W.: 172.20 g/mol, powder form), N-(1-naphtyl) ethylenediamine (NED) (purity > 98 %, M.W.: 259.17 g/mol; powder form), sodium nitrite ($NaNO_2$) (purity of 99.999 %, M.W: 69.00 g/mol; powder form), Amplex^{TM} Red reagent (M.W.: 257.25 g/mol, powder form), horseradish peroxidase enzyme type VI (HRP) and hydrogen peroxide (30 % $_{w/w}$ in H_2O, M.W.: 34.01 g/mol, liquid form) were purchased from Sigma Aldrich. Ethanol (96 % purity) and phosphoric acid (85 %, M.W.: 98 g/mol, liquid form) were purchased from Panreac. Phosphate Buffered Saline (PBS) tablets were purchased from Gibco Life technologies. All the reagents used for detection of reactive species were prepared using MilliQ water (Millipore, Merck). All reagents were used as received in their chemical grade. Argon (Ar, 5.0) for plasma treatment was purchased from Praxair, Spain.

All the following measurements were performed in triplicate and the experimental results are reported as a mean ± standard deviation.

4.2.2. Chemical modification of gelatin

Methacrylated-gelatin (GelMA) was obtained as previously described [22]. Briefly, 10 g of gelatine were dissolved in 100 mL of Milli-Q water at 50 ºC and reacted with 1 mL of methacrylic anhydride during 90 min under high stirring. The solution was then diluted 1:3 in distilled water (Di-H_2O) and dialysed against Di-H_2O during 7 days at 40 ºC. The solutions were then sterilized by filtration with a 0.22 µm filter under sterile hood before freeze-drying and were stored at -20 ºC until use. Degree of substitution (DS) about 66 % was obtained as described in section

4.2.3. The GelMA foam obtained was then dissolved in PBS and heated at 37 °C in a water bath for further use.

4.2.3. ^{1}H-NMR spectroscopy

Proton nuclear magnetic resonance (^{1}H-NMR) with a Bruker Avance 400 MHz spectrometer was employed to characterize and to confirm the methacryloyl-functionalisation of the GelMA. The samples were dissolved in deuterated water (D_2O) at 2 % w/w before CAP treatment. Plasma treatment was performed as described in section 2.4. Samples were heated until complete homogenization before recording the spectra at room temperature. The NMR-spectra were normalized to the peak of valine, leucine and isoleucine (which appear at 0.9 – 1.1 ppm) by fixing the integral of this peak to 18 protons and lysine methylene signals (2.8 – 3.1 ppm) compared with the methacrylate groups (5.0 – 6.5 ppm) [47]. The Degree of Substitution (DS) of the synthesized GelMA was obtained following the equation (1):

$$\text{DS (\%)} = \frac{\int CH\ Methacrylates}{\int CH2\ Lysine} \times 100 \qquad (1)$$

4.2.4. Plasma treatment

kINPen IND® (NEOPLAS Tools, Germany) [48], a commercially available atmospheric pressure plasma jet was employed for the plasma treatment. kINPen was operating under argon gas flow at 1 L/min with a distance between the nozzle and the sample surface of 10 mm (Figure 4.2 a). Volumes of 1 mL of samples were treated in 24-well plates during 0, 2, 4, 6, 8 and 10 min at room temperature. PBS and GelMA solutions at 2 and 15 % $_{w/w}$ were treated by plasma.

The pH of the solutions was measured immediately after CAP treatment using an MM 41 Crison multimeter with 50 28 probe (Crison, Spain). No change in the pH (around 6.0) was observed after plasma treatment.

4.2.5. Optical emission spectroscopy

Optical emission spectra were acquired using a F600-UVVIS-SR instrument (StellarNet, Tampa, FL, USA) equipped a QP600-2SR-Ocean Optics optical fibre. The head of the optical fibre was positioned perpendicular to the plasma plume, keeping a fixed horizontal distance of 0.5 mm during all the experiments. Only the vertical distance between the plasma nozzle and the optical fibre was modified during the experiments. During the experiments, the plasma source was operated with the same parameters described in section 2.4 except for the volume of solution that was 1.9 mL in 48-well plates in order to have the entire plasma plume outside the well. Acquisition parameters were: range 185-840 nm, resolution 0.5 nm, integration time 200 ms and number of scans 9.

4.2.6. Hydrogel preparation

GelMA at a concentration of 15 % $_{w/w}$ was dissolved in PBS with either the photo-initiator (PI) LAP at 0.05 % $_{w/v}$. GelMA hydrogels were obtained by dispensing GelMA solution in the presence of the PI in a mould. Visible blue light (Figure 4.2 b) was exposed during 5 min (LED light curing machine LY-C240, λ = 420-480 nm, I = 100 mW/cm²) and the hydrogels maintained 10 min in the mold before use (Figure 4.2 c).

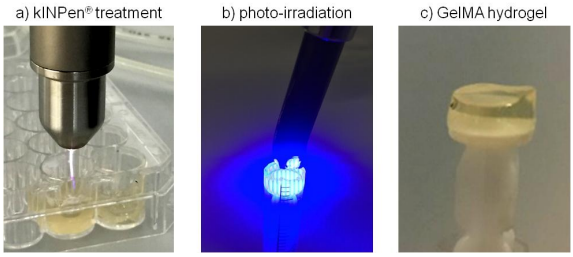

Figure 4.2: Pictures of a) plasma treatment, b) photo-irradiation of the solution of GelMA and c) GelMA hydrogel obtained.

4.2.7. Detection and quantification of reactive species

Reactive species generated by kINPen in GelMA solutions at 2 % $_{w/w}$, and in PBS were quantified after the plasma treatment described in section 2.4 using chemical probes. Concentration of nitrites (NO_2^-) was determined by the Griess reaction method [49–51]. Griess reagent was obtained by dissolving sulphanilamide, NED and phosphoric acid in Di-H_2O to obtain 1 % $_{w/v}$, 0.1 % $_{w/v}$ and 5 % $_{w/v}$ respectively. Plasma-treated samples were diluted by a factor of 4 to obtain a total volume of 100 µL in 96-well plates. Then 100 µL of Griess reagent were added and the plates were incubated for 10 min at room temperature protected from light. The absorbance was measured at λ_{abs} = 540 nm using a Synergy Hybrid Multi Mode Microplate Reader (Biotek, USA). Calibration curve was prepared by dissolving $NaNO_2$ in the corresponding medium.

Concentration of hydrogen peroxides (H_2O_2) was evaluated by fluorescence spectroscopy using Amplex™ Red Reagent (AR) and horseradish peroxidase (HRP) enzyme, following the supplier's protocol [52,53]. H_2O_2 generation with kINPen was measured through the detection of resorufin, a fluorescent compound, final product of the reaction of H_2O_2 with AR and HRP. Samples were diluted 200 times in the same media after the plasma treatment described in section 2.4. 50 µL of the AR and HRP mixture were added (25 µL and 5 µL respectively of AR and HRP in 4.970 mL of MilliQ water) to the diluted sample in black 96-wellplates. The samples were incubated in the dark at 37 ºC during 30 min. Fluorescence intensity was measured using λ_{exc} = 560/20 nm and λ_{em} = 590/20 nm in the Synergy Hybrid Multi Mode Microplate Reader (Biotek, USA). A calibration curve was prepared diluting a 30 % $_{w/v}$ hydrogen peroxide solution in the corresponding medium.

Generation and diffusion of nitrite ions was monitored real-time by mixing in a 24-well plate 0.5 mL of GelMA solution (2 and 15 % $_{w/w}$) or PBS and 0.5 mL of Griess reagent. The solutions were treated by plasma for 5 minutes using the parameters reported in section 4.2.4 and videos were recorded during the treatment using a high-resolution camera.

The stability of the reactive species generated in GelMA solutions and in PBS was quantified as a function of the incubation time at 37 ºC for the 10 min CAP-treated samples. [NO_2^-] and [H_2O_2] were quantified using the corresponding protocols as described in this section 4.2.7.

The rate of formation of each reactive species was determined from the slope of the fitting of the concentrations *vs*. treatment time.

4.2.8. Release of reactive species

The *in vitro* release profile of NO_2^- and H_2O_2 in PBS 1x, was assessed from untreated and plasma-treated GelMA hydrogels. Plasma treatment conditions were those described in section 2.4 for a plasma treatment time of 10 min. Hydrogels were prepared as described in section 2.6 by dispensing 200 µL of GelMA in the presence of the PI in a cylindrical mould of 8x5 mm. Hydrogels were then introduced in 48-well plates and 1 mL of PBS was added on the top. The plates were incubated at 37 ºC in the dark. The concentration of reactive species was determined at fixed time points (0, 5, 10, 15, 30, 60, 240 min). 50 µL and 20 µL of the supernatant PBS were withdrawn for the NO_2^- and H_2O_2 quantification respectively. 50 µL of Griess reagent was added for the NO_2^- quantification and was done as previously described in section 2.7. For the H_2O_2 detection, the 20 µL samples were diluted in 180 µL of PBS and 50 µL of AR mixture added before applying same protocol described in section 4.2.7. 70 µL of PBS at 37 °C was added after each withdrawal to avoid altering the total volume. The collected data were then corrected, taking into account the evaporation and all the dilution steps. For NO_2^- quantification, the absorption spectra were recorded between 400 and 700 nm and the absorbance at 540 nm was used after proper baseline subtraction. The initial rate of release was calculated from the slope of the fitted curve.

4.2.9. Rheology

Rheological measurements were done with a stress-control rheometer HR-2 Discovery Hybrid Rheometer (HR-2 DHR, TA Instruments, UK) equipped with a Peltier element for temperature control using plate-plate (PP) geometry (PP: 20 mm, gap: 1 mm). GelMA hydrogel was obtained as described in section 4.2.6 by photo-crosslinking 600 µL of GelMA at 15 % $_{w/w}$ in the presence of the PI in a 20x1 mm mould to fill the geometry. All the rheological measurements were done at 37 °C in the linear visco-elastic response regime (f = 1 Hz and 1 % of deformation). Storage (G') and loss (G") modulus were measured from 100 to 0.1 rad/s at 1 % of deformation and from 1 to 1 000 % of deformation at a frequency of 1 Hz.

4.3.RESULTS

4.3.1. Gas phase chemistry

The optical emission spectra of the plasma generated by the kINPen jet during the treatment of a 15 % $_{w/w}$ GelMA solution at different vertical distances between the plasma nozzle and the optical fibre are reported in Figure 4.3.

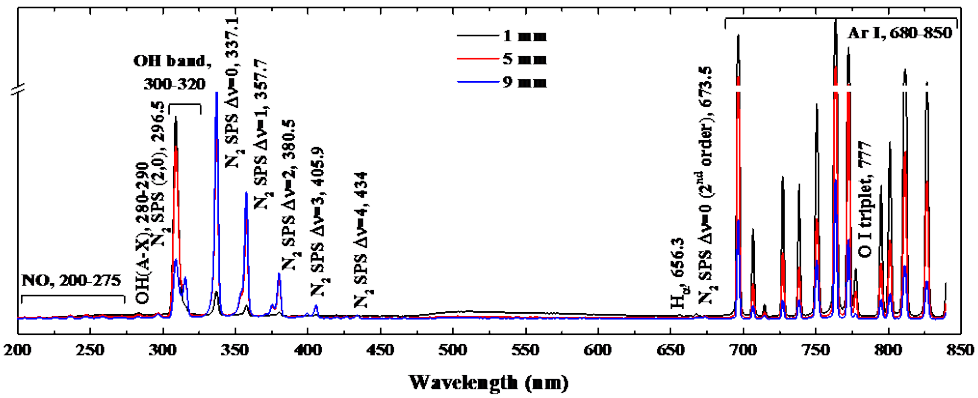

Figure 4.3: Optical emission spectra of the kINPen during the treatment of a 15 % $_{w/w}$ GelMA solution (Ar flow = 1 L/min, d = 10 mm, V = 1.9 mL) at different vertical distances (1 (black line), 5 (red line) and 9 mm (blue line)) between the plasma nozzle and the optical fibre. The main peaks are labelled.

The analysis of the spectra enabled to identify the emitting excited species in the gas phase: Ar, N_2, $NO^{\cdot}$, $^{\cdot}OH$, O and $^{\cdot}H$. The vertical distribution of the excited species along the plasma plume is based on the region where they are generated and their stability. Excited O and H atoms were evident mainly in proximity of the plasma nozzle, while the signals of excited nitrogen species (N_2 and NO) are more intense far from the nozzle, where the plasma effluent can mix effectively with ambient air. No signal deriving from the interaction of the plasma plume with the GelMA solution was detected, even when positioning the head of the optical fibre very close to the solution.

4.3.2. Diffusion of reactive species in GelMA solutions

The real-time generation and diffusion of nitrite ions in solution is tracked by treating with CAP jet the samples (MilliQ water, PBS, 2 % and 15 % GelMA solutions) containing Griess reagent (Figure 4.4). Nitrite ions are formed and accumulate within the interface of the liquid in contact with plasma, in all samples, during the first seconds of treatment. In MilliQ water and PBS, after 20-30 s of treatment, nitrites start to be transferred gradually in the bulk solution and occupy all the well volume uniformly in about 90 s. Differently, in GelMA solutions at 2 and 15 % $_{w/w}$, transfer of nitrites is not uniform. Small channels, evident in Figure 4.4 at 30-40 s of treatment, facilitate the transfer of nitrites from the top layer to the bottom of the well, leaving most of the central part colourless.

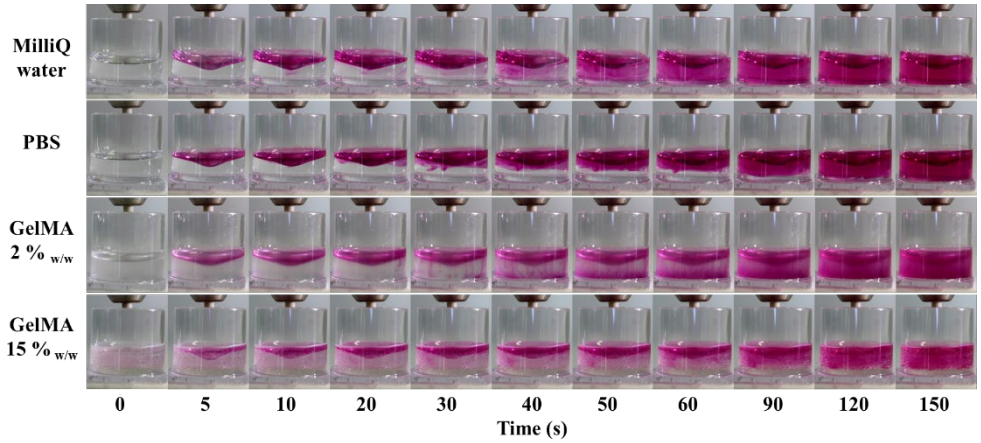

Figure 4.4: Generation and diffusion of nitrites generated by APPJ jet treatment in MilliQ water, PBS and GelMA solution (2 and 15 % $_{w/w}$) as function of treatment time.

When mixing together GelMA solutions and Griess reagent, the formation of small bubbles was observed and the solution turned pinkish, even in control samples (thus, in absence of nitrites from plasma). This effect is more pronounced when GelMA was in high concentration (15 % $_{w/w}$) and is evident in the last row of Figure 4.4. This is likely due to the formation of some diazo compounds that

decompose liberating gaseous nitrogen and generating a pink product different from the one that is usually produced during a Griess test. This can interfere with the quantification of NO_2^- in concentrated GelMA solution. For that reason, the quantification of reactive species will be investigated at lower polymer concentrations (2 % $_{w/w}$) in order to avoid these interferences.

4.3.3. Generation and stability of reactive species in GelMA solution

Two major long-lived species generated from CAP jet were quantified in GelMA solutions at 2 % $_{w/w}$ and in PBS according to the methods described in sections 4.2.4 and 4.2.7. The concentrations of H_2O_2 and NO_2^- linearly increase following CAP treatment time for all the solutions studied (Figure 4.5 a and b). After 10 min of CAP treatment, 700 ± 140 µM of H_2O_2 is generated in GelMA at 2 % $_{w/w}$ with a rate of production of 57 ± 4 µM/min. In PBS, the rate of H_2O_2 generation is lower (51 ± 1 µM/min) leading to 500 ± 15 µM in solution after 10 min of CAP treatment (Figure 4.5 a). For NO_2^- ions (Figure 4.5 b), higher concentration is generated in GelMA at 2 % $_{w/w}$ (530 ± 70 µM) than in PBS (200 ± 40 µM) after 10 min of CAP treatment. The rate of NO_2^- production in PBS is 3 times lower (21 ± 1 µM/min) than in GelMA solution (65 ± 3 µM/min). In general, higher amount of NO_2^- ions are generated in GelMA solution than in PBS.

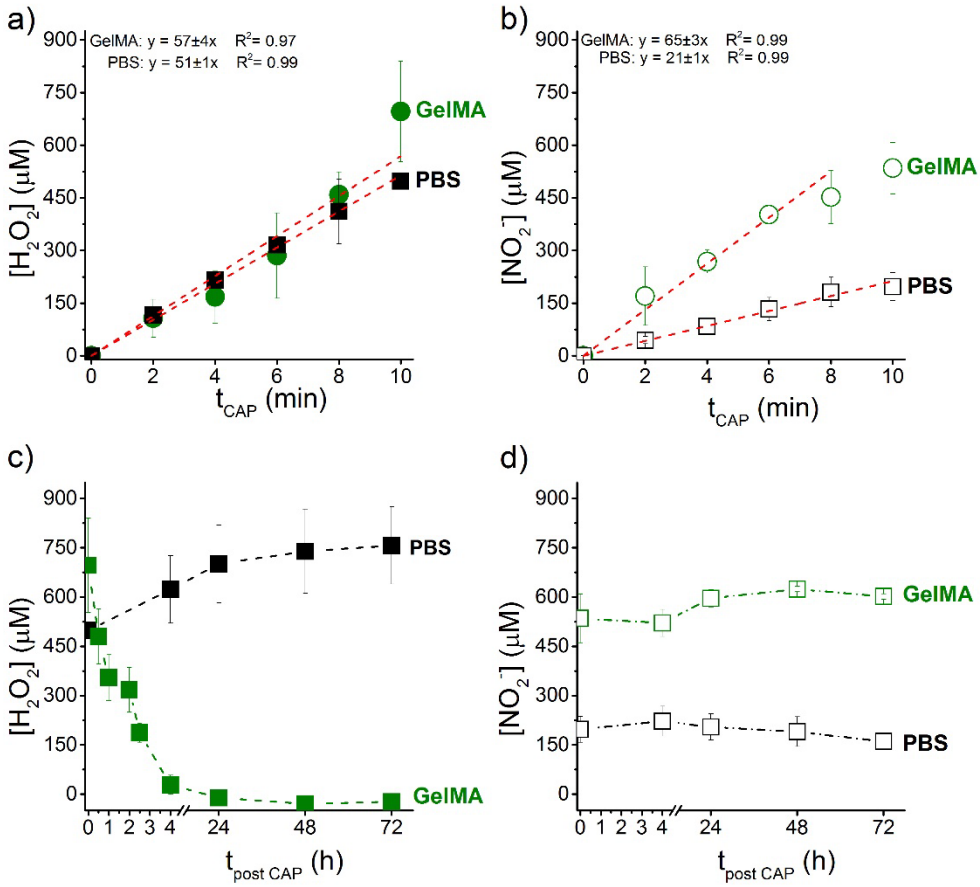

Figure 4.5: Generation of a) H_2O_2 and b) NO_2^- in GelMA at 2 % $_{w/w}$ (green circles) and in PBS (black squares) during APPJ treatment. Stability of c) H_2O_2 and d) NO_2^- in GelMA at 2 % $_{w/w}$ (green squares) and in PBS (black squares) generated during 10 min of CAP treatment and incubated at 37 °C for different times.

The stability at 37 ºC of H_2O_2 and NO_2^- is recorded in GelMA at 2 % $_{w/w}$ and compared to PBS, both treated for 10 min of CAP jet treatment (Figure 4.5 c and d). H_2O_2 decreases exponentially and the half-life time of H_2O_2 in GelMA 2 % $_{w/w}$ is estimated at 1.20 h. In PBS, H_2O_2 slightly increases and remains stable (700 ± 30 µM) during 72-hour incubation time (Figure 4-5 c). NO_2^- ions are relatively stable in GelMA at 2 % $_{w/w}$ and in PBS, constant values of (600 ± 9) µM and (180 ± 12) µM are respectively recorded (Figure 4.5 d).

4.3.4. Release of reactive species from GelMA hydrogels

The release of H_2O_2 and NO_2^- from 15 % $_{w/w}$ GelMA hydrogels was recorded in PBS at 37 °C as receptor media (Figure 4.6). A fast release of both reactive species is observed in the plasma treated hydrogel. An initial burst release of H_2O_2 was obtained with a rate of (13.6 ± 3) µM/min in plasma-treated GelMA hydrogel. The plateau was reached with H_2O_2 values of (130.0 ± 2.2) µM. Same release profile was observed for the NO_2^-, leading to a plateau value of (30.0 ± 2.4) µM. The initial rate of release of NO_2^- was of (2.9 ± 0.6) µM/min. Untreated GelMA hydrogel employed as control did not show any release of reactive species.

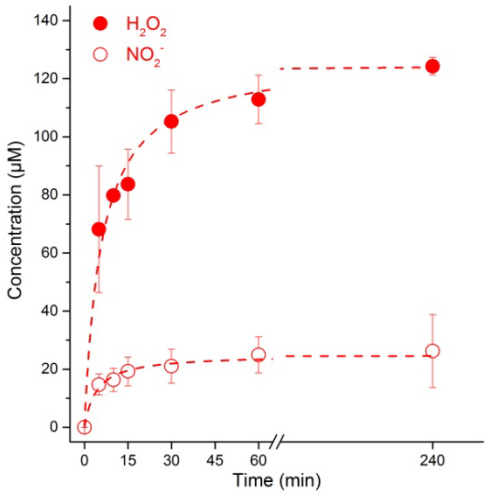

Figure 4.6: Release of a) H_2O_2 (filled circles) and b) NO_2^- (empty circles) from 10 min plasma-treated GelMA hydrogel to PBS release media.

4.3.5. Effects of CAP on the chemical structure of GelMA

The chemical structure of GelMA was investigated at 2 % $_{w/w}$ using proton nuclear magnetic resonance (^{1}H-NMR) in D_2O after 10 min of CAP jet treatment (Figure 4.7). The peaks on ^{1}H-NMR spectra can be assigned as follows: methyl residues of valine, leucine, and isoleucine are at 1.15 ppm (1). Then peaks of methylene residues of threonine appear at 1.45 ppm (2), alanine at 1.62 ppm (3), lysine + methyl proton of methacrylic anhydride at 1.91 ppm (4), and arginine at 2.3 ppm (5). Methylene resonance of aspartate at 2.65 ppm (6), lysine at 2.9 ppm (7), arginine at 3.21 ppm (8) and proline at 3.44 ppm (9) successively appear. Peaks 10 to 12 correspond to the methine residues of combined isoleucine + valine, threonine and aspartate respectively. The referred H_2O peak from D_2O traces is at 4.78 ppm, methacrylate groups at 5.4 and 5.6 ppm (13) and finally the aromatic proton at 7.4 ppm (14) [47,54]. Similar spectra were obtained before and after CAP jet treatment. There is no chemical modification in the backbone structure of the GelMA at 2 % $_{w/w}$. The same peaks and ratios appear in the same chemical shifts of the ^{1}H-NMR spectra for both untreated and CAP-treated GelMA. Moreover, no changes are recorded in the degree of substitution (DS) of the GelMA after 10 min of plasma treatment.

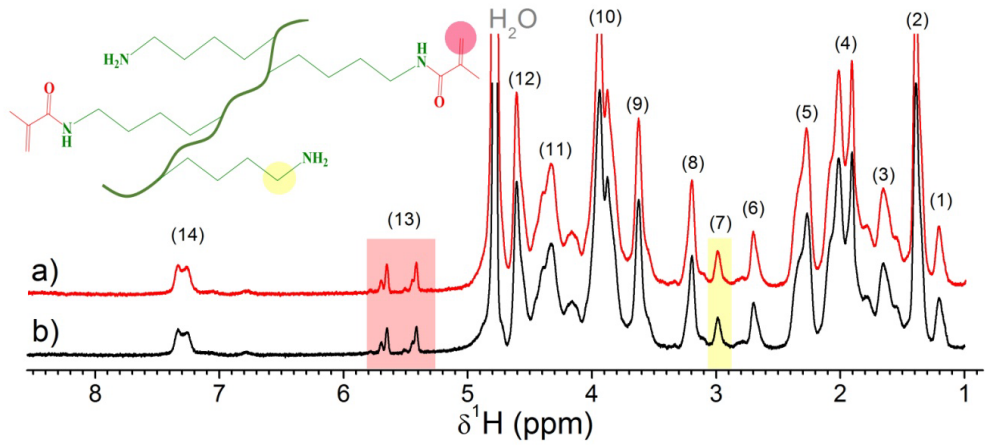

Figure 4.7: ^{1}H-NMR spectra of a) untreated and b) 10 min CAP treated GelMA at 2 % $_{w/w}$ in D_2O.

4.3.6. Effects of CAP on the rheological properties of the hydrogel

Viscoelastic properties of photo-crosslinked GelMA hydrogels were investigated by determination of the Storage (G') and Loss (G") modulus. To that end, GelMA at 15 $\%_{w/w}$ in the presence of lithium phenyl-2,4,6-trimethylbenzoylphosphinate (LAP) was exposed to blue light during 5 min and maintained 10 min in the mold to obtain a stable hydrogel. To ensure that hydrogels were stable after the crosslinking process, G' and G" modulus were monitored over time through oscillatory time sweep test (Figure 4.8 a). Results showed constant G' and G'' values over time in all samples, thus indicating that the studied hydrogels were stable, supporting that the crosslinking reaction was achieved. The G' modulus is directly related to the elastic properties of the samples tested giving information about their solid-like behavior. In contrast, the G" modulus provides information about the viscous properties of the samples and their liquid-like behavior. In this sense, in all the samples evaluated, G' values were higher than G'', which indicates that all hydrogels displayed solid-like behavior as a consequence of the solidification after the photo-crosslinking. Interestingly, differences between the 10 min CAP-treated and the non-treated hydrogels were detected. Higher G' and G" modulus for the CAP-treated were obtained (around 1.5 times), indicating higher solid-like behavior due to higher extent of cross-linking.

Afterwards, the viscoelastic properties were further investigated by performing oscillatory frequency sweep test at 37 °C (Figure 4.8 b & c). Results obtained show stable hydrogels at lower frequencies for both untreated and plasma-treated samples (G' > G''). When the frequency increases, untreated sample presents viscoelastic solid behavior while plasma-treated hydrogel breaks (G" > G') (Figure 4.8 b).

Regarding the strain sweep measurements, in the first place the crossover points of the G' and G'' curves were evaluated to determine the strain or deformation percentage at which the hydrogels reached the breakage. A lower strain at breakage (150 %) was obtained for the 10 min CAP-treated hydrogel than the untreated (250 %) (Figure 4.8 c). In this sense, the higher solid-like behavior of

CAP-treated hydrogel resulted in more brittle hydrogel than the untreated one, thus leading to lower strain percentage values of breakage.

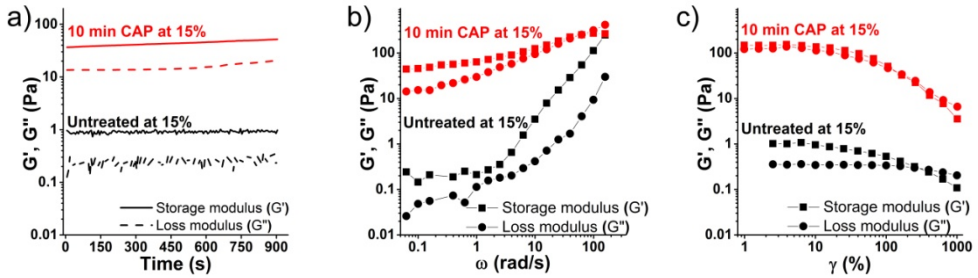

Figure 4.8: Storage (G') (squares) and loss (G") (circles) modulus of 10 min CAP jet-treated (red) and untreated (black) GelMA hydrogels in a) time sweep b) oscillation and c) deformation experiments at 37 ºC.

4.4.DISCUSSION

In this chapter we investigate the potential of GelMA hydrogels to act as vehicles of reactive species generated from a commercial APPJ (kINPen) for their potential application in the biomedical field. The effects of APPJ treatment were studied here on GelMA solutions, and then evaluated in the final hydrogel obtained.

First, the kINPen source employed here working with Argon as carrier gas generates several excited species in air (*i.e.* Ar, N_2, $NO^{\cdot}$, $^{\cdot}OH$, O and $^{\cdot}H$, Figure 4.3), as described in earlier works [48]. No modification in the OES spectra was recorded from the interaction of the jet with the GelMA solution. Closer to the liquid surface higher intensities of N_2 and NO are recorded in the gas phase, corresponding to the mixing of the jet with ambient air that at the gas flow of the experiment is in laminar flow regime. For OH radicals, earlier comparison of OH mapping distributions and the maximum densities in plasma jets suggested that the liquid conductivity has to be taken into account to calculate the OH production rate as one order of magnitude higher OH concentration was found in water than in saline solution [9], although this was not reflected in our OES measurements.

Here, the dynamics of formation and diffusion of NO_2^- were followed "live" thanks to Griess reagent (Figure 4.4). The different viscosity between the controls (MilliQ water and PBS) and the polymer solutions (GelMA at 2 % $_{w/w}$ or 15 % $_{w/w}$) revealed different dynamics of reactivity; In MilliQ water and PBS, nitrites were formed on the plasma-liquid interface, to finally diffuse, more easily in the case of water and in a more stratified manner for PBS. This is in agreement with modelling works by Tian and Kushner [55] and Lu [9] indicating the early formation of a layer of reactive nitrogen species. The nitrogen oxide chemistry in the water is initiated by gas-phase species diffusion into the water leading to several RONS through a cascade of reaction in the treated-media. As a result of the reactions of nitrogen oxide species from the gas phase with NO and NO_2, more and more HNO_2, HNO_3, and HOONO species are produced. All of the nitrogen oxide species from the gas phase diffuse into the water layer and are slowly converted into $HNOx_{aq}$ (e.g.,

HNO_{2aq}, HNO_{3aq} and $HOONO_{aq}$), in agreement with our experimental observations (Figure 4.4).

Conversely, in GelMA solutions at 2 and 15 % $_{w/w}$, a thin layer of nitrites was also formed on the interface of the polymer solution but; i. diffusion was slower than in water or PBS probably due to the increase of the viscosity of the solution and ii. non-uniform transfer of reactive species was recorded from 30-40 s of treatment, as small channels appeared to be preferential pathways for diffusion of NO_2^-. After 150 s of CAP jet treatment, homogenous distribution of reactive species was observed in GelMA solutions. Interferences were observed when the Griess reagent probe was introduced to GelMA solution at 15 % $_{w/w}$ leading to the formation of gases (Figure 4.4). For that reason, the quantification of the RONS generated by CAP jet were carried in GelMA solution at 2 % $_{w/w}$.

Besides, it is well-known that water becomes acidic following plasma treatment due to the generation of nitric acid [56], among others, the pH of GelMA solutions remain here unchanged after APPJ treatment. This buffering effect taking place with GelMA was previously observed in the plasma treatment of alginate in solution in chapter 3.

As RONS have the potential to play important roles in many biological processes, plasma-conditioned liquids and polymer solutions are of great interest today. Many works reported on the generation of RONS and their potential interaction in different liquids for cancer therapy [7,9,12,16,57–60]. Different works have observed a linear increase of RONS in liquids with plasma treatment time [56,61–63], as recorded here with both H_2O_2 and NO_2^- in PBS as well as in GelMA solution (Figure 4.5 a & b). The concentration of RONS generated in liquids or the polymer solution from APPJ depends on various factors with regard not only with the experimental setting of the plasma jet but also with the chemical composition of the treated media. Indeed, depending on the APPJ device employed and the working conditions used (gas flow, nozzle distance, surrounding temperature, treatment time, etc.), different amounts of RONS can be introduced [64]. The chemistry of the treated liquid also plays an important role in the generation and the stability of these

species. Chauvin et al., [61] compared the generation of H_2O_2 and NO_2^- in different media generated from a CAP jet. Authors also observed a linear dependence of H_2O_2 and NO_2^- concentrations in MilliQ water and in cell culture media following CAP jet exposure. They also reported that the amount of RONS generated was different depending on the chemical composition of the treated sample. In Chapter 3 we recorded higher amounts of H_2O_2 and NO_2^- in alginate solution at 0.5 % $_{w/v}$ than in control liquids. Using the same kINPen device in the same distance and flow conditions but with lower volume of treated solution (200 µL), comparable amount of H_2O_2 (110 µM) and NO_2^- (100 µM) are produced in solution at 90 s of treatment (Figure 3.3). A volume of 200 µL of gelatin solution at 2 % $_{w/v}$ was treated using the same kINPen plasma device in the same conditions of treatment in [65]. After 5 min of treatment, 11 times higher of H_2O_2 (2 250 µM) and twice higher of NO_2^- (600 µM) were generated in the gelatin solution in comparison to GelMA (200 µM and 300 µM for H_2O_2 and NO_2^- respectively) in the same experimental conditions used here for the treatment of GelMA (volume of 1 mL for 5 min of treatment). Moreover, authors observed higher amount of RONS introduced in gelatin than in water following plasma treatment, in parallel with our observations here with GelMA and PBS. The presence of chemical groups in the polymer solution probably enhances the reactions of the reactive species from the CAP jet, leading to stable long-live RONS. Studies already reported the chemical modifications induced by CAP jet on amino-acids leading to hydroxylation and nitration of the side chains at low concentrations [61,66]. Here, GelMA backbone is mainly composed of different amino-acids with carboxylic acid, thiol, hydroxyl and amino groups which potentially can react with the reactive species generated by the CAP jet source leading to higher concentrations of RONS in the liquid.

In order to further investigate if the proposed reactivity with the RONS generated by CAP in the liquid eventually affects the chemical structure of GelMA, ^{1}H-NMR spectra of untreated and 10 min CAP-treated GelMA solutions at 2 % $_{w/w}$ in D_2O were recorded (Figure 4.7). No changes in peak chemical shift or intensity were observed. The degree of substitution (DS) of the synthesized GelMA was

maintained. This confirms that the polymer structure of GelMA was not degraded by CAP jet treatment at this concentration. The 2 % $_{w/w}$ GelMA concentration is very high compared to the concentration of reactive species generated in the solution. Reactions that can potentially occur will be negligible on the polymer backbone.

The H_2O_2 and NO_2^- generated in PBS remain relatively stable with time at 37 °C up to 72 h (Figure 4.5 c & d). On the contrary, in GelMA solutions, H_2O_2 exponentially decreases to 0 µM of H_2O_2 in 24 h while NO_2^- remains stable over time up to 72 h. Similarly, in gelatin [64], 60 % of the generated NO_2^- remain in solution up to 72 h at 37 °C, and in contrast with our findings with GelMA, in gelatin H_2O_2 is found to be stable overtime (a slight decrease around 10 % is reported) [65]. In parallel, comparing to gelatin, GelMA presents highly reactive methacrylate groups, which may potentially react with the free RONS diminishing their available concentration in the liquid. This reflects that the stability of the reactive species highly depends on the plasma-treated sample chemistry. Furthermore, H_2O_2 is known to be relatively stable and degrades with time in certain conditions. We can speculate that here that one of the mechanisms related to degradation of H_2O_2, could be the reaction with the methacrylate side groups from the GelMA

The effects of the CAP jet treatment on the viscoelastic properties of GelMA hydrogels were studied by rheology at 37 °C to simulate their possible behaviour at body temperature (Figure 4.8). Stable hydrogels were obtained after exposure to blue light (Figure 4.8 a). The untreated photo-crosslinked GelMA hydrogel in our experimental conditions presents a solid viscoelastic behavior at high frequencies (Figure 4.8 b). In contrast, APPJ-treated GelMA solution during 10 min led to an increase of the storage (G') and the loss (G") modulus of the hydrogel. This result could be explained due to the complex interactions between APPJ and the GelMA solution. First, it is well reported that plasma treatment lead to water evaporation [62] which here is translated by an increase of the concentration. In fact, we recorded an 18 % of water evaporation after 10 min of kINPen treatment from the GelMA solution leading to a final concentration around 18 % $_{w/w}$. It is already

reported that by increasing the concentration of GelMA solution, more methacrylate groups can react leading to a higher cross-linking density per volume [22,47]. Billiet et al., [47] reported an increase by 3 fold of the G' modulus of GelMA hydrogels with the increase of the concentration from 15 to 20 % $_{w/v}$. An untreated hydrogel at 18 % $_{w/w}$ was compared to the plasma-treated one (Figure S4.9) in order to compare same concentrations. First, the untreated hydrogel at 18 % $_{w/w}$ presents higher modulus than the 10 min plasma-treated one (Figure S4.9 a). Secondly, both untreated at 18 % $_{w/w}$ and plasma-treated hydrogels have the same behaviour at low (stable solid behaviour with G' > G") and at high frequencies (they break, G" > G') (Figure S4.9 b). Moreover, the strain at break of APPJ-treated GelMA hydrogel was lower than those of the untreated GelMA hydrogel at 18 % $_{w/w}$ (Figure S4.9 c). Here, the resulting mechanical properties obtained are a combination between the evaporation and potential reactions that can occur during treatment. In fact, this result in lower crosslinking extends in the plasma-treated hydrogel which lead to a lower modulus that could be attributed to the degradation of the methacrylate's end groups by H_2O_2. Despite no chemical modification was observed in ^{1}H-NMR spectra, rheological experiments confirms the degradation of methacrylate groups following plasma treatment.

To investigate the ability of the CAP-treated GelMA solutions as effective vehicles for RONS, after treatment GelMA solutions at 15 % $_{w/w}$ were immediately photo-crosslinked to form a self-standing hydrogel, and immersed in PBS at 37 ºC as receptor media. A burst release of both H_2O_2 and NO_2^- from plasma-treated GelMA hydrogel was recorded within the first 5 min followed by a slower release rate was observed in PBS at 37 °C (Figure 4.6). Moreover, as the photo-crosslink of the sample was performed soon after plasma treatment, we assumed that H_2O_2 were not yet degraded (half-life time of 1.20 h). H_2O_2 generated in GelMA solution at 15 % $_{w/w}$ could be quantified by diluting the 10 min CAP jet-treated solution to 2 % $_{w/w}$ (in the presence of the PI, before photo-crosslinking) and a value of (300 ± 150) µM of H_2O_2 was recorded. A H_2O_2 release of 100 % was obtained from a 200 µL photo-crosslinked GelMA sample within the first 5 min. This result confirms that once

photo-crosslinking is achieved, H_2O_2 cannot react with methacrylate groups, which disappear in the reaction of polymerization. Regarding the NO_2^-, discussed earlier, as its quantification is not possible in the concentrated GelMA solution using the current method, it is not possible to calculate the percentage of release. However, as the release profile reaches the stationary stage and NO_2^- remains stable in solution, it may be assumed that all the NO_2^- generated in solution were also released. In that case, we may estimate that the NO_2^- generated in GelMA solution at 15 % $_{w/w}$ in our conditions could be around 150 µM. Similar release profiles were observed in alginate hydrogels, displaying a burst release of H_2O_2 and NO_2^- within the first 24 h (Chapter 3). In contrast to alginate where the crosslinking solutions washed away part of the RONS, as the crosslinking system of GelMA avoids the use of liquid crosslinkers, all species generated by APPJ remain in the hydrogel, so it allowed to release all the RONS generated in the GelMA solution.

Thus, according to the previous results obtained, the GelMA polymer solution investigated here may be injected and *in situ* crosslinked after CAP treatment for potential applications in *Plasma Medicine* area. The combination between hydrogels and RONS from CAP jets can offer promising opportunities in CAP-based therapies.

4.5.CONCLUSION

Here, the effects of plasma jet treatment with kINPen on GelMA solutions able to form hydrogels by crosslinking with blue light were investigated. Higher amounts of NO_2^- were generated in a 2 % GelMA solution than in PBS from the CAP jet that are stable at 37 ºC. In contrast, the H_2O_2 generated in similar concentrations than in PBS were unstable in GelMA solutions. Although the APPJ treatment did not degrade the polymer backbone of GelMA, it seems that the H_2O_2 generated quickly reacts with the methacrylate end groups leading to a lower extent of crosslinking. Lower modulus were obtained for the plasma-treated hydrogel at high concentrations (15 %) as a consequence of the chemical degradation induced by H_2O_2. Although it is not possible to determine the RONS generated in the GelMA solution at 15 % due to interferences with the measurement methods, it was observed that after photo-crosslinking of the kINPen-treated GelMA, there were indeed RONS that were released within a relatively short time at 37 °C to a release medium. The results obtained in this work seem promising on the use of hydrogels as vehicles of reactive species from APPJ and open new avenues for investigation.

REFERENCES

1. Pankaj, S.K.; Keener, K.M. Cold plasma: background, applications and current trends. *Curr. Opin. Food Sci.* **2017**, *16*, 49–52.
2. Laroussi, M.; Lu, X. Room-temperature atmospheric pressure plasma plume for biomedical applications. *Appl. Phys. Lett.* **2005**, *87*, 113902.
3. Tanaka, H.; Ishikawa, K.; Mizuno, M.; Toyokuni, S.; Kajiyama, H.; Kikkawa, F.; Metelmann, H.-R.; Hori, M. State of the art in medical applications using non-thermal atmospheric pressure plasma. *Rev. Mod. Plasma Phys.* **2017**, *1*, 3.
4. Yan, D.; Sherman, J.H.; Keidar, M. Cold atmospheric plasma, a novel promising anti-cancer treatment modality. *Oncotarget* **2017**, *8*, 15977–15995.
5. Dobrynin, D.; Fridman, G.; Friedman, G.; Fridman, A. Physical and biological mechanisms of direct plasma interaction with living tissue. *New J. Phys.* **2009**, *11*, 115020.
6. Haertel, B.; von Woedtke, T.; Weltmann, K.-D.; Lindequist, U. Non-thermal atmospheric-pressure plasma possible application in wound healing. *Biomol. Ther. (Seoul).* **2014**, *22*, 477–90.
7. Bauer, G.; Graves, D.B. Mechanisms of Selective Antitumor Action of Cold Atmospheric Plasma-Derived Reactive Oxygen and Nitrogen Species. *Plasma Process. Polym.* **2016**, *13*, 1157–1178.
8. Graves, D.B. Reactive Species from Cold Atmospheric Plasma: Implications for Cancer Therapy. *Plasma Process. Polym.* **2014**, *11*, 1120–1127.
9. Lu, X.; Naidis, G.V.; Laroussi, M.; Reuter, S.; Graves, D.B.; Ostrikov, K. Reactive species in non-equilibrium atmospheric-pressure plasmas: Generation, transport, and biological effects. *Phys. Rep.* **2016**, *630*, 1–84.
10. Girard, P.-M.; Arbabian, A.; Fleury, M.; Bauville, G.; Puech, V.; Dutreix, M.; Sousa, J.S. Synergistic Effect of H2O2 and NO2 in Cell Death Induced by Cold Atmospheric He Plasma. *Sci. Rep.* **2016**, *6*, 29098.
11. Bauer, G. The synergistic effect between hydrogen peroxide and nitrite, two long-lived molecular species from cold atmospheric plasma, triggers tumor cells to induce their own cell death. *Redox Biol.* **2019**, *26*, 101291.
12. Takeda, S.; Yamada, S.; Hattori, N.; Nakamura, K.; Tanaka, H.; Kajiyama, H.; Kanda, M.; Kobayashi, D.; Tanaka, C.; Fujii, T.; et al. Intraperitoneal Administration of Plasma-Activated Medium: Proposal of a Novel Treatment Option for Peritoneal

Metastasis From Gastric Cancer. *Ann. Surg. Oncol.* **2017**, *24*, 1188–1194.

13. Sato, Y.; Yamada, S.; Takeda, S.; Hattori, N.; Nakamura, K.; Tanaka, H.; Mizuno, M.; Hori, M.; Kodera, Y. Effect of Plasma-Activated Lactated Ringer's Solution on Pancreatic Cancer Cells In Vitro and In Vivo. *Ann. Surg. Oncol.* **2018**, *25*, 299–307.
14. Tanaka, H.; Nakamura, K.; Mizuno, M.; Ishikawa, K.; Takeda, K.; Kajiyama, H.; Utsumi, F.; Kikkawa, F.; Hori, M. Non-thermal atmospheric pressure plasma activates lactate in Ringer's solution for anti-tumor effects. *Sci. Rep.* **2016**, *6*, 36282.
15. Tanaka, H.; Mizuno, M.; Ishikawa, K.; Nakamura, K.; Kajiyama, H.; Kano, H.; Kikkawa, F.; Hori, M. Plasma-Activated Medium Selectively Kills Glioblastoma Brain Tumor Cells by Down-Regulating a Survival Signaling Molecule, AKT Kinase. *Plasma Med.* **2011**, *1*, 265–277.
16. Van Boxem, W.; Van der Paal, J.; Gorbanev, Y.; Vanuytsel, S.; Smits, E.; Dewilde, S.; Bogaerts, A. Anti-cancer capacity of plasma-treated PBS: effect of chemical composition on cancer cell cytotoxicity. *Sci. Rep.* **2017**, *7*, 16478.
17. Yan, D.; Sherman, J.H.; Keidar, M. The Application of the Cold Atmospheric Plasma-Activated Solutions in Cancer Treatment. *Anticancer. Agents Med. Chem.* **2017**, *17*.
18. Hoffman, A.S. Hydrogels for biomedical applications. *Adv. Drug Deliv. Rev.* **2012**, *64*, 18–23.
19. Omidian, H.; Park, K. Hydrogels. In *Fundamentals and Applications of Controlled Release Drug Delivery*; 2012; pp. 75–105.
20. Wang, Y. Programmable hydrogels. *Biomaterials* **2018**, *178*, 663–680.
21. Mazaki, T.; Shiozaki, Y.; Yamane, K.; Yoshida, A.; Nakamura, M.; Yoshida, Y.; Zhou, D.; Kitajima, T.; Tanaka, M.; Ito, Y.; et al. A novel, visible light-induced, rapidly cross-linkable gelatin scaffold for osteochondral tissue engineering. *Sci. Rep.* **2015**, *4*, 4457.
22. An I. Van Den Bulcke, †; Bogdan Bogdanov, †; Nadine De Rooze, †; Etienne H. Schacht, *; Maria Cornelissen, ‡ and; Berghmans§, H. Structural and Rheological Properties of Methacrylamide Modified Gelatin Hydrogels. **2000**.
23. Yue, K.; Trujillo-de Santiago, G.; Alvarez, M.M.; Tamayol, A.; Annabi, N.; Khademhosseini, A. Synthesis, properties, and biomedical applications of gelatin methacryloyl (GelMA) hydrogels. *Biomaterials* **2015**, *73*, 254–271.
24. Meinert, C.; Kaemmerer, E.; Martine, L.C.; Yue, K.; Levett, P.A.; Klein, T.J.; W

Melchels, F.P.; Loessner, D.; Khademhosseini, A.; Hutmacher, D.W. Functionalization, preparation and use of cell-laden gelatin methacryloyl–based hydrogels as modular tissue culture platforms. **2016**.

25. Klotz, B.J.; Gawlitta, D.; Rosenberg, A.J.W.P.; Malda, J.; Melchels, F.P.W. Gelatin-Methacryloyl Hydrogels: Towards Biofabrication-Based Tissue Repair. *Trends Biotechnol.* **2016**, *34*, 394–407.
26. Monteiro, N.; Thrivikraman, G.; Athirasala, A.; Tahayeri, A.; França, C.M.; Ferracane, J.L.; Bertassoni, L.E. Photopolymerization of cell-laden gelatin methacryloyl hydrogels using a dental curing light for regenerative dentistry. *Dent. Mater.* **2018**, *34*, 389–399.
27. Nguyen, A.K.; Goering, P.L.; Reipa, V.; Narayan, R.J. Toxicity and photosensitizing assessment of gelatin methacryloyl-based hydrogels photoinitiated with lithium phenyl-2,4,6-trimethylbenzoylphosphinate in human primary renal proximal tubule epithelial cells. *Biointerphases* **2019**, *14*, 021007.
28. Lim, K.S.; Klotz, B.J.; Lindberg, G.C.J.; Melchels, F.P.W.; Hooper, G.J.; Malda, J.; Gawlitta, D.; Woodfield, T.B.F. Visible Light Cross-Linking of Gelatin Hydrogels Offers an Enhanced Cell Microenvironment with Improved Light Penetration Depth. *Macromol. Biosci.* **2019**, 1900098.
29. Kadam, V.; Nicolai, T.; Nicol, E.; Benyahia, L. Structure and Rheology of Self-Assembled Telechelic Associative Polymers in Aqueous Solution before and after Photo-Cross-Linking. *Macromolecules* **2011**, *44*, 8225–8232.
30. Chen, G.; Kawazoe, N.; Ito, Y. Photo-Crosslinkable Hydrogels for Tissue Engineering Applications. In *Photochemistry for Biomedical Applications*; Springer Singapore: Singapore, 2018; pp. 277–300.
31. Fairbanks, B.D.; Schwartz, M.P.; Bowman, C.N.; Anseth, K.S. Photoinitiated polymerization of PEG-diacrylate with lithium phenyl-2,4,6-trimethylbenzoylphosphinate: polymerization rate and cytocompatibility. *Biomaterials* **2009**, *30*, 6702–6707.
32. Ifkovits, J.L.; Burdick, J.A. Review: Photopolymerizable and Degradable Biomaterials for Tissue Engineering Applications. *Tissue Eng.* **2007**, *13*, 2369–2385.
33. Killion, J.A.; Geever, L.M.; Devine, D.M.; Grehan, L.; Kennedy, J.E.; Higginbotham, C.L. Modulating the mechanical properties of photopolymerised polyethylene glycol–polypropylene glycol hydrogels for bone regeneration. *J. Mater.*

Sci. **2012**, *47*, 6577–6585.

34. Pahoff, S.; Meinert, C.; Bas, O.; Nguyen, L.; Klein, T.J.; Hutmacher, D.W. Effect of gelatin source and photoinitiator type on chondrocyte redifferentiation in gelatin methacryloyl-based tissue-engineered cartilage constructs. *J. Mater. Chem. B* **2019**, *7*, 1761–1772.
35. Lai, T.C.; Yu, J.; Tsai, W.B. Gelatin methacrylate/carboxybetaine methacrylate hydrogels with tunable crosslinking for controlled drug release. *J. Mater. Chem. B* **2016**, *4*, 2304–2313.
36. Huber, B.; Borchers, K.; Tovar, G.E.; Kluger, P.J. Methacrylated gelatin and mature adipocytes are promising components for adipose tissue engineering. *J. Biomater. Appl.* **2016**, *30*, 699–710.
37. Irmak, G.; Demirtaş, T.T.; Gümüşderelioğlu, M. Highly Methacrylated Gelatin Bioink for Bone Tissue Engineering. *ACS Biomater. Sci. Eng.* **2018**.
38. Luo, Z.; Sun, W.; Fang, J.; Lee, K.; Li, S.; Gu, Z.; Dokmeci, M.R.; Khademhosseini, A. Biodegradable Gelatin Methacryloyl Microneedles for Transdermal Drug Delivery. *Adv. Healthc. Mater.* **2019**, *8*, 1801054.
39. Dong, Z.; Yuan, Q.; Huang, K.; Xu, W.; Liu, G.; Gu, Z. Gelatin methacryloyl (GelMA)-based biomaterials for bone regeneration. *RSC Adv.* **2019**, *9*, 17737–17744.
40. Anada, T.; Pan, C.-C.; Stahl, A.; Mori, S.; Fukuda, J.; Suzuki, O.; Yang, Y.; Anada, T.; Pan, C.-C.; Stahl, A.M.; et al. Vascularized Bone-Mimetic Hydrogel Constructs by 3D Bioprinting to Promote Osteogenesis and Angiogenesis. *Int. J. Mol. Sci.* **2019**, *20*, 1096.
41. Grande, S.; Cools, P.; Asadian, M.; Van Guyse, J.; Onyshchenko, I.; Declercq, H.; Morent, R.; Hoogenboom, R.; De Geyter, N. Fabrication of PEOT/PBT Nanofibers by Atmospheric Pressure Plasma Jet Treatment of Electrospinning Solutions for Tissue Engineering. *Macromol. Biosci.* **2018**, 1800309.
42. Grande, S.; Van Guyse, J.; Nikiforov, A.Y.; Onyshchenko, I.; Asadian, M.; Morent, R.; Hoogenboom, R.; De Geyter, N. Atmospheric Pressure Plasma Jet Treatment of Poly-ε-caprolactone Polymer Solutions To Improve Electrospinning. *ACS Appl. Mater. Interfaces* **2017**, *9*, 33080–33090.
43. Shi, Q.; Vitchuli, N.; Nowak, J.; Lin, Z.; Guo, B.; Mccord, M.; Bourham, M.; Zhang, X. Atmospheric plasma treatment of pre-electrospinning polymer solution: A feasible method to improve electrospinnability. *J. Polym. Sci. Part B Polym. Phys.*

2011, *49*, 115–122.

44. Szili, E.J.; Oh, J.-S.; Hong, S.-H.; Hatta, A.; Short, R.D. Probing the transport of plasma-generated RONS in an agarose target as surrogate for real tissue: dependency on time, distance and material composition. *J. Phys. D. Appl. Phys.* **2015**, *48*, 202001.
45. Szili, E.J.; Hong, S.H.; Oh, J.S.; Gaur, N.; Short, R.D. Tracking the Penetration of Plasma Reactive Species in Tissue Models. *Trends Biotechnol.* **2017**.
46. Oh, J.-S.; Szili, E.J.; Gaur, N.; Hong, S.-H.; Furuta, H.; Kurita, H.; Mizuno, A.; Hatta, A.; Short, R.D. How to assess the plasma delivery of RONS into tissue fluid and tissue. *J. Phys. D. Appl. Phys.* **2016**, *49*.
47. Billiet, T.; Gasse, B. Van; Gevaert, E.; Cornelissen, M.; Martins, J.C.; Dubruel, P. Quantitative Contrasts in the Photopolymerization of Acrylamide and Methacrylamide-Functionalized Gelatin Hydrogel Building Blocks. *Macromol. Biosci.* **2013**, *13*, 1531–1545.
48. Reuter, S.; von Woedtke, T.; Weltmann, K.-D. The kINPen—a review on physics and chemistry of the atmospheric pressure plasma jet and its applications. *J. Phys. D. Appl. Phys.* **2018**, *51*, 233001.
49. Green, L.C.; Wagner, D.A.; Glogowski, J.; Skipper, P.L.; Wishnok, J.S.; Tannenbaum, S.R. Analysis of nitrate, nitrite, and [15N]nitrate in biological fluids. *Anal. Biochem.* **1982**, *126*, 131–138.
50. Giustarini, D.; Rossi, R.; Milzani, A.; Dalle-Donne, I. Nitrite and Nitrate Measurement by Griess Reagent in Human Plasma: Evaluation of Interferences and Standardization. *Methods Enzymol.* **2008**, *440*, 361–380.
51. Guevara, I.; Iwanejko, J.; Dembińska-Kieć, A.; Pankiewicz, J.; Wanat, A.; Anna, P.; Gołąbek, I.; Bartuś, S.; Malczewska-Malec, M.; Szczudlik, A. Determination of nitrite/nitrate in human biological material by the simple Griess reaction. *Clin. Chim. Acta* **1998**, *274*, 177–188.
52. Mishin, V.; Gray, J.P.; Heck, D.E.; Laskin, D.L.; Laskin, J.D. Application of the Amplex red/horseradish peroxidase assay to measure hydrogen peroxide generation by recombinant microsomal enzymes. *Free Radic. Biol. Med.* **2010**, *48*, 1485–1491.
53. Zhao, B.; Ranguelova, K.; Jiang, J.; Mason, R.P. Studies on the photosensitized reduction of resorufin and implications for the detection of oxidative stress with Amplex Red. *Free Radic. Biol. Med.* **2011**, *51*, 153–159.

54. Claaßen, C.; Claaßen, M.H.; Truffault, V.; Sewald, L.; Tovar, G.E.M.; Borchers, K.; Southan, A. Quantification of Substitution of Gelatin Methacryloyl: Best Practice and Current Pitfalls. *Biomacromolecules* **2018**, *19*, 42–52.

55. Tian, W.; Kushner, M.J. Atmospheric pressure dielectric barrier discharges interacting with liquid covered tissue. *J. Phys. D. Appl. Phys.* **2014**, *47*, 165201.

56. Labay, C.; Hamouda, I.; Tampieri, F.; Ginebra, M.P.; Canal, C. Production of reactive species in alginate hydrogels for cold atmospheric plasma-based therapies. *Sci. Rep.* **2019**, *9*.

57. Tian, W.; Kushner, M.J. Atmospheric pressure dielectric barrier discharges interacting with liquid covered tissue. *J. Phys. D. Appl. Phys.* **2014**, *47*, 165201.

58. Verlackt, C.C.W.; Van Boxem, W.; Bogaerts, A. Transport and accumulation of plasma generated species in aqueous solution. *Phys. Chem. Chem. Phys.* **2018**, *20*, 6845–6859.

59. Mateu-Sanz, M.; Tornín, J.; Brulin, B.; Khlyustova, A.; Ginebra, M.-P.; Layrolle, P.; Canal, C. Cold Plasma-Treated Ringer's Saline: A Weapon to Target Osteosarcoma. *Cancers (Basel).* **2020**, *12*, 227.

60. Tornin, J.; Mateu-Sanz, M.; Rodríguez, A.; Labay, C.; Rodríguez, R.; Canal, C. Pyruvate Plays a Main Role in the Antitumoral Selectivity of Cold Atmospheric Plasma in Osteosarcoma. *Sci. Rep.* **2019**, *9*.

61. Chauvin, J.; Judée, F.; Yousfi, M.; Vicendo, P.; Merbahi, N. Analysis of reactive oxygen and nitrogen species generated in three liquid media by low temperature helium plasma jet. *Sci. Rep.* **2017**, *7*, 4562.

62. Girard, F.; Badets, V.; Blanc, S.; Gazeli, K.; Marlin, L.; Authier, L.; Svarnas, P.; Sojic, N.; Clément, F.; Arbault, S. Formation of reactive nitrogen species including peroxynitrite in physiological buffer exposed to cold atmospheric plasma. *RSC Adv.* **2016**, *6*, 78457–78467.

63. Girard-Sahun, F.; Badets, V.; Lefrançois, P.; Sojic, N.; Clement, F.; Arbault, S. Reactive Oxygen Species Generated by Cold Atmospheric Plasmas in Aqueous Solution: Successful Electrochemical Monitoring in Situ under a High Voltage System. *Anal. Chem.* **2019**, *91*, 8002–8007.

64. Khlyustova, A.; Labay, C.; Machala, Z.; Ginebra, M.-P.; Canal, C. Important parameters in plasma jets for the production of RONS in liquids for plasma medicine: A brief review. *Front. Chem. Sci. Eng.* **2019**, *13*, 238–252.

65. Labay Cédric, Roldan Marcel, Tampieri Francesco, Stancampiano Augusto, Escot Bocanegra Pablo, Ginebra Maria Pau, C.C. Enhanced generation of reactive species in gelatin hydrogel solutions for selective cancer therapy. *Submitt. ACS Mater. Interfaces* **2020**.

66. Takai, E.; Kitamura, T.; Kuwabara, J.; Ikawa, S.; Yoshizawa, S.; Shiraki, K.; Kawasaki, H.; Arakawa, R.; Kitano, K. Chemical modification of amino acids by atmospheric-pressure cold plasma in aqueous solution. *J. Phys. D. Appl. Phys.* **2014**, *47*.

SUPPLEMENTARY INFORMATION – CHAPTER 4

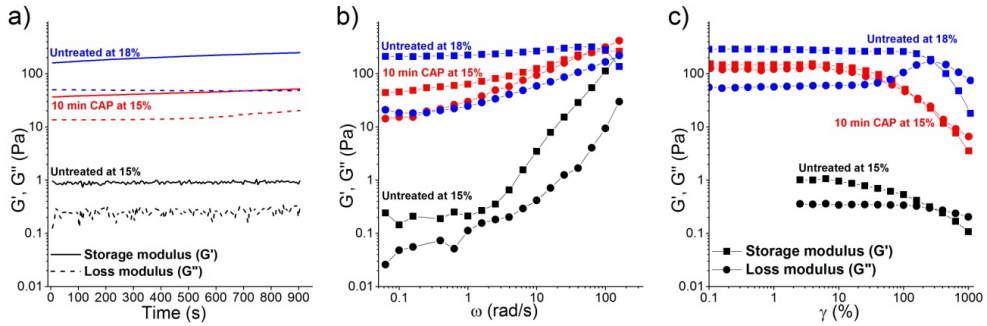

Figure S4.9: Loss (G') and storage (G") modulus a) in function of the time of untreated GelMA hydrogel at 15 % (black lines) and 18 % (blue lines) and of 10 min CAP-treated GelMA hydrogel at 15 % (red lines); b) in oscillation and in c) deformation experiments at 37 °C.

CHAPTER 5

5. Investigating the Atmospheric Pressure Plasma Jet Modification of a Photo-crosslinkable Hydrogel

ABSTRACT

Atmospheric pressure plasma jets (APPJ) have great potential in wound healing, bacterial disinfection and in cancer therapy. Recent studies pointed out that hydrogels can be used as screens during APPJ treatment, or even be used as reservoirs for reactive oxygen and nitrogen species generated by APPJ in liquids. Thus, novel applications are emerging for hydrogels which deserve fundamental exploration of the possible modifications undergone by the polymers in solution due to the reactivity with plasmas. In this chapter we investigate the possible modifications occurred by APPJ treatment of an amphiphilic poly(ethylene oxide)-based triblock copolymer (tPEO) photo-crosslinkable hydrogel. While APPJ treatments lead to a certain degradation of the self-assembly of the polymeric chains at low concentrations (< 2 g/L), at the higher concentrations required to form a hydrogel (> 2 g/L), the polymeric chains are unaffected by APPJ and the hydrogel forming ability is kept. APPJ treatments induced a pre-crosslinking of the network with an increase of the mechanical properties of the hydrogel. Overall, the small modifications induced in the polymer solutions open a platform for a variety of applications with great potential.

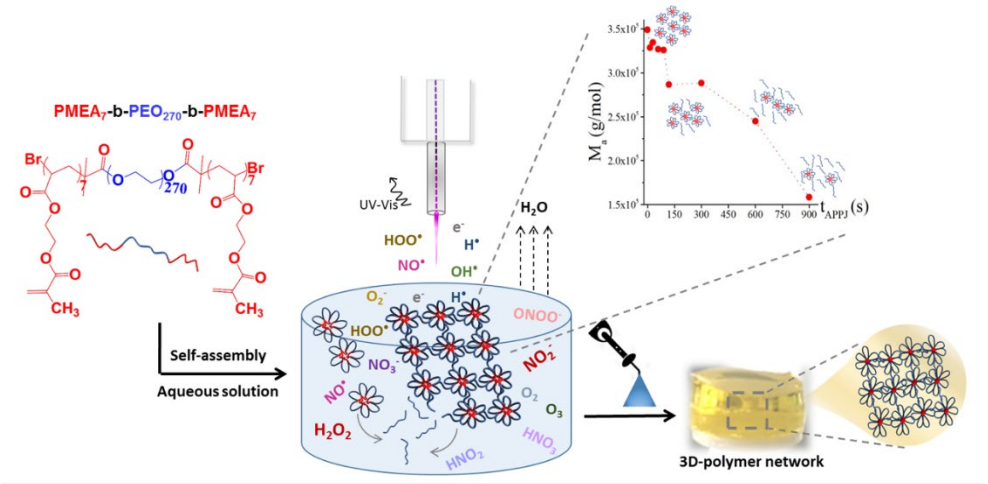

Figure 5.1 : Representative scheme of Chapter 5 experimental design and results obtained.

5.1. INTRODUCTION

Research dealing with cold plasma modification of polymers has traditionally employed polymers in the solid state to alter parameters such as adhesion, wettability, etc., usually employing low pressure plasma processes [1]. Chemical processes on the surface of polymers take place through all major plasma components, namely electrons, ions, excited particles, mainly radicals, atoms and UV radiation. The major primary products of treatment of polymer films with plasma are free radicals, non-saturated organic compounds, cross-links between polymer macromolecules, products of destruction of the polymer chains, and gas phase products. Most processes for the formation of radicals on the polymer surface under plasma treatment are due to electron impact and UV radiation and are related to breaking of R-H and C-C bonds in macromolecules. The main effects derived from these processes can be linked to functionalization and etching [2].

Nevertheless, with the development of Atmospheric Pressure Plasma Jets (APPJ) [3–11], which operate at near ambient temperature and atmospheric pressure a range of new possibilities has opened. For instance, in the last few years, APPJ treatment of polymeric solutions has been investigated to improve their printability by electro-spinning [12–14]. In Chapter 3, alginate solutions have shown the ability of generating reactive species following APPJ treatment and still form stable hydrogels, opening great perspectives in the design of new implantable biomaterials for plasma therapies. In parallel, agarose and gelatin semi-solid hydrogels have been investigated by Szili et al. [15–17] in order to mimic the effects of plasmas through the skin, and evaluate the transport of reactive oxygen and nitrogen species (RONS) from the plasma gas phase to investigate them as screens for certain species from APPJ during treatment of living tissues. Although the complete mechanisms involved in the biological effects of plasma treatment are not yet fully understood, APPJ devices present a safe, versatile and easy application without inducing heating to the treated living or non-living surfaces at short treatment times [10,18–20]. The efficiency of these plasma therapies is essentially related to the generation of RONS in biological tissues or liquids [21–23].

Thus, the variety of applications emerging in this area foster the interest for fundamental investigation of the effects of APPJ on polymer solutions.

In this sense, the plasma chemistry occurring in liquids is completely different to that described earlier occurring in solid surfaces; as reported in a recent review [24], the transfer of reactivity from the gas to the liquid phase has been highlighted as being of prime importance for biological effects. In fact, plasma treatment of aqueous solutions (water, saline solutions, or cell culture media) leads to their activation and non-equilibrium dissociation of water molecules. This results in the formation of short-lived species such as H atoms, OH* radicals, and hydrated (solvated) electrons (e_{solv}) [25]. Very quick reactions between these species lead to the formation of transient and more stable species such as O_3, H_2, O_2, H_2O_2 etc. Moreover, in the presence of air, reactive nitrogen species (NO^-, NO_2^-, NO_3^-, $ONOO^-$) are also formed in liquid medium. These nitrogen oxides subsequently react in water forming acids, which affect the conductivity and pH of the plasma-treated liquids, and further reactions may occur [26].

As mentioned earlier, natural polymers (alginate, agarose, gelatin) have been treated by APPJ in solution or in hydrated hydrogel state for a variety of applications. To the best of our knowledge, the effects derived from the reactions between the cocktail of reactive species generated by APPJ and polymeric solutions are challenging and still largely unexplored. However, assessing certain modifications in natural polymers can be rather challenging, so it is of interest to employ a synthetic polymer with hydrogel-forming ability, that can be used as a first model to investigate the potential changes and reactivity undergone through APPJ treatment.

Among potential polymers that can be employed to form hydrogels, poly(ethylene glycol) (PEG) (also called poly(ethylene oxide) (PEO)), a biocompatible synthetic polymer, has good properties for tissue engineering and drug delivery applications [27–31], so it might also be of interest for the novel applications highlighted earlier. By introducing methacrylate functional end groups in the polymer chains, through adequate chemical modification, the polymeric

solution can undergo photo-crosslinking in the presence of photo-initiators to form a self-standing hydrogel [32–36]. One of the major advantages of photo-crosslinked hydrogels is that they can be formed *in situ* in a minimally invasive manner.

A few years ago, a PEO-based self-associating amphiphilic triblock copolymer (tPEO) able form injectable and rapidly photo-cross-linkable hydrogels was developed from [32]. Associated to other macromolecules, this copolymer can lead to microporous hydrogels [37] or double network hydrogels of enhanced mechanical properties [38,39]. It was also shown to be non-cytotoxic and biocompatible leading to potential biomedical applications [40]. Therefore, we explore here the APPJ treatment of a photo-crosslinkable tPEO self-assembling polymer solution and analyze the potential modifications in the polymer (*i.e.* self-assembly in micelles) through different techniques, including the conservation of the ability of the hydrogel photo-crosslinking, its mechanical properties and chemical modifications.

5.2. MATERIALS & METHODS

5.2.1. Materials

Phosphate Buffered Saline (PBS) tablets were purchased from Gibco Life technologies. N-phenylglycine (NPG) (≥ 97 % purity, MW: 151.16 g/mol, powder form), triethanolamine (TEA) (purity ≥ 99.0 %, M.W.: 149.19 g/mol, liquid form), riboflavin (purity ≥ 98 %, M.W.: 376.36 g/mol, powder form), dimethyl sulfoxide (purity ≥ 99.7 %, M.W.: 78.13 g/mol, liquid form), sulphanilamide (purity ≥ 99 %, M.W.: 172.20 g/mol, powder form), N-(1-naphtyl) ethylenediamine (NED) (purity > 98 %, M.W.: 172.20 g/mol; powder form). Ethanol (99.8 % purity) and phosphoric acid (85 %, M.W.: 98 g/mol, liquid form) were purchased from Panreac. All reagents were used as received in their chemical grade except for NPG, which was purified by dissolving in water at 60 °C, filtered over 0.45 µm filter then freeze-dried before use. Gaseous He (He 5.0) for plasma treatments was purchased from PRAXAIR, Spain.

5.2.2. Polymer synthesis

Poly(2-methacryloyloxyethyl acrylate)-b-poly(ethylene oxide)-b-poly(2-methacryloyloxyethyl acrylate) ($PMEA_7$-b-PEO_{270}-b-$PMEA_7$) triblock copolymer (tPEO) was synthesized as reported elsewhere [41]. Each polymeric solution was prepared by dilution in PBS and homogenized overnight.

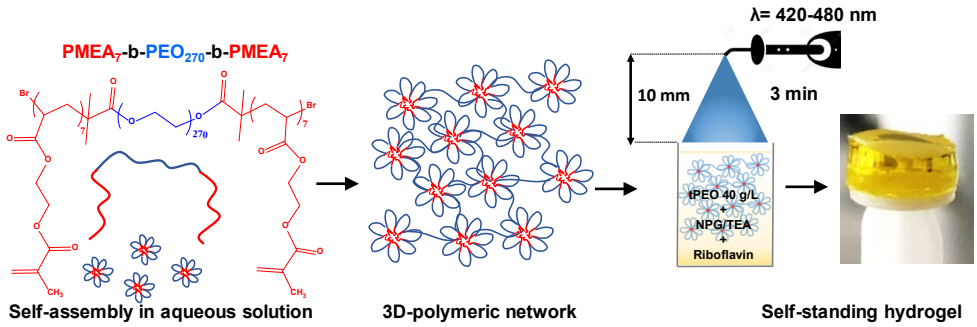

Figure 5.2: Chemical structure, self-assembly in aqueous solutions of tPEO and its photo-crosslinking at 40 g/L using blue light.

5.2.3. Hydrogel preparation

Hydrogels were prepared from a tPEO solution at 40 g/L in presence of N-phenylglycine (NPG), triethanolamine (TEA) and riboflavin as photo-initiating system (PIS) components. In a 10 mL glass bottle, 20 µL of purified NPG at 90 mg/mL in ethanol were introduced with 20 µL of TEA at 90 mg/mL in ethanol. Solvent was evaporated gently using compressed air before adding 2 mL of tPEO solution and stirring was performed overnight protected from light. Before crosslinking, 20 µL of riboflavin solution at a concentration of 28 mg/mL in dimethylsulfoxide were added. To obtain a photo-crosslinked hydrogel, 200 µL of sample were placed in a 48-well plate and irradiated during 3 min using blue light (LED light curing machine LY-C240, λ = 420-480 nm, I = 100 mW/cm²) (Figure 5.2).

5.2.4. Plasma treatment

An atmospheric pressure plasma jet (APPJ) using He as plasma carrier gas was employed, in a jet with a single electrode described elsewhere [42]. Plasma discharge was operating with sinusoidal waveform at 25 kHz with (U) ~ 2 kV and (I) ~ 3 mA. Helium flow was regulated at 1 L/min through a Bronkhorst MassView (Bronkhorst, Netherlands) mass flow controller.

To treat liquids and polymer solutions with plasma, 2 mL of the corresponding sample was introduced in a 24-mm diameter glass bottle and plasma treatments were performed from 15 to 900 s, using a gap of 10 mm between plasma nozzle and the surface of the sample (Figure 5.3). Due to water evaporation during plasma treatment, the concentration of the solution was recalculated after each APPJ treatment.

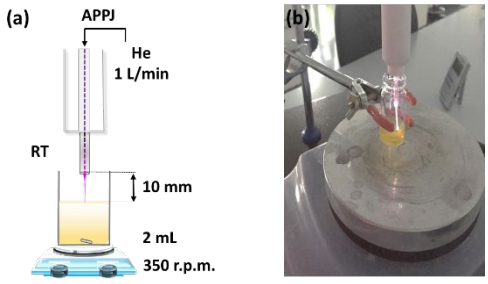

Figure 5.3: (a) Scheme of the experimental setup of plasma treatment of samples; (b) Picture of plasma treatment of tPEO solution during plasma treatment.

5.2.5. Light Scattering

Apparent molar masses (Ma) and hydrodynamic radius (R_{ha}) of tPEO self-assemblies in solution were assessed by static (SLS) and dynamic (DLS) light scattering. Data were recorded with a ALV-5000 multibit (ALV-GmbH, Germany), multitau, full digital correlator in combination with a Spectra-Physics laser (emitting vertically polarized light at k = 632.8 nm) and a thermostat bath controlled within ± 0.2 °C. Measurements were made at angles (θ) ranging between 20 and 150°. Before measurement, the polymer solutions were filtered using 0.2 µm inorganic membrane filter. Polymer concentration varied between 0.5 and 10 g/L and the refractive index increment of the copolymer in water was assumed to be that of pure PEO in water, *i.e.*, (dn/dC) = 0.135 mL/g. The average relaxation rate (Γ) was found to be q^2 independent (where q is the scattering vector) (equation (1)):

$$q = \frac{(\frac{4\pi n}{k})}{\sin(\theta/2)} \quad (1)$$

The cooperative diffusion coefficient (Dc) was calculated as in equation (2):

$$Dc = \frac{\Gamma}{q^2} \quad (2)$$

At sufficiently low concentrations, where interactions are negligible, the z-average apparent hydrodynamic radius (R_{ha}) of the solute can be calculated from the diffusion coefficient (Dc) using the Stokes-Einstein relation (equation (3):

$$R_{ha} = \frac{k_B \times T}{6 \times \pi \times \eta_s \times D_c} \quad (3)$$

Where k_B is the Boltzmann constant, T is the absolute temperature and η_s is the solvent viscosity.

The relative excess scattering intensity (Ir) was determined as the total intensity minus the solvent scattering divided by the scattering of toluene at 20 °C. Ir is related to the osmotic compressibility ($(d\pi/dC)^{-}1$) and the z average structure factor (S(q)) (equation (4)):

$$\text{Ir} = K \times C \times R \times T \times \left(\frac{d\pi}{dc}\right)^{-1} \times S(q) \quad (4)$$

With R the gas constant and T the absolute temperature. In dilute solutions Ir is related to the weight average molar mass (M_w) and the z-average structure factor (S(q)) (equation (5)):

$$\text{Ir} = K \times C \times M_W \times S(q) \quad (5)$$

With C the solute concentration and K an optical constant that depends on the refractive index increment. S(q) describes the dependence of Ir on the scattering wave vector. For the concentrations studied (0.5 to 10 g/L), interactions influence the scattering intensity and the result obtained by extrapolation to q = 0 represents an apparent value for the apparent molar mass (M_a).

The weight percentage of the remaining flower-like aggregates in solution after plasma treatment is calculated according to equation (6):

$$\text{C (\%)} = \frac{Ma\ (APPJ)}{Ma\ (untreated)} \times 100 \quad (6)$$

The concentration of self-assembled tPEO chains in solution after plasma treatment can be obtained following equation (7):

$$C_{\text{tPEO-APPJ (g/L)}} = \left(\frac{Ma\ (APPJ)}{Ma\ (untreated)}\right) \times C\ (tPEO\ initial)\ \text{(g/L)} \quad (7)$$

By this way, the concentration of the degraded flower-like aggregates can be deduced from equation (8):

$$C_{\text{degraded}}\ \text{(g/L)} = C_{\text{tPEO initial}} - C_{\text{tPEO-APPJ}}\ \text{(g/L)} \quad (8)$$

5.2.6. Rheology

Rheological measurements were done at 25 °C with a stress-control rheometer MCR301 (Anton Paar, Austria) using a cone-plate geometry (CP: 40 mm, gap: 1 mm). The measurements were done in the linear response regime (f = 1 Hz). For *in situ* photo-crosslinking, the sample was covered with mineral oil in order to avoid evaporation and the rheometer protected from light. A blue LED (Thorlabs – M450LP1) (λ_{max} = 450 nm) was equipped with a light guide (Ø = 5 mm) placed 5 cm below the glass plate. The samples were irradiated at ~ 0.1 W/cm^2 during 3 min.

5.2.7. 1H-NMR

Proton nuclear magnetic resonance (^{1}H NMR) with a Bruker Advance 400 MHz spectrometer was employed to characterize the triblock copolymer. The tPEO was dissolved in deuterated water at a concentration of 2 g/L and the ^{1}H NMR spectra was recorded at room temperature.

5.2.8. pH

The pH of the solutions was measured immediately after plasma treatment in 2 mL of solution using an MM 41 Crison multimeter with 50 28 probe (Crison, Spain).

5.2.9. Statistics

All the experiments were done on triplicate and data are presented as mean ± standard deviation.

5.3.RESULTS

An atmospheric pressure plasma jet was employed to treat a Poly(2-methacryloyloxyethyl acrylate)-b-poly(ethylene oxide)-b-poly(2-methacryloyloxyethyl acrylate) triblock copolymer (tPEO) solution at the suitable concentration necessary to allow obtaining a self-standing hydrogel (40 g/L), and compared to PBS as control. A linear evaporation was observed during APPJ treatments (Figure 5.4 a) leading to up to 15 % water evaporation after 15 min of APPJ treatment. The pH remained relatively stable in the polymer, with minor decrease of around 0.4 units of pH only, after APPJ treatments (Figure 5.4 b).

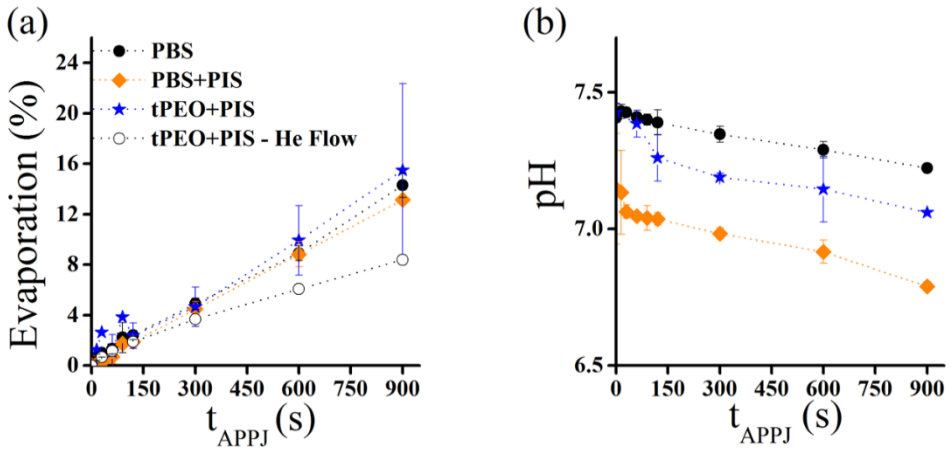

Figure 5.4: Effects of different APPJ treatment times on the tPEO polymer (complete, with the photo-initiator (PIS) crosslinker system) on (a): Evaporation and (b) pH. PBS was used as control and in (a) the polymer solution was subjected to gas flow alone without plasma treatment.

To investigate the effects of plasma on the triblock copolymer and photo-crosslinked hydrogels, different concentrations of tPEO were treated by APPJ. The evolutions of the apparent molar mass (M_a) and apparent hydrodynamic radius (R_{ha}) of the tPEO self-assemblies in aqueous solution were measured by static (SLS) and dynamic (DLS) light scattering respectively as a function of APPJ treatment time and concentration (Figure 5.5). The samples did not exhibit any angular dependence of the scattered intensity indicating that the scattering objects are small ($Rg < 20$ nm) (Figure S5.10). APPJ treatment of a solution of tPEO flower-like micelles (at $C = 0.5$ g/L) revealed a clear decrease of M_a after APPJ treatments up to 900 s (Figure 5.5 a). The influence of the polymer concentration on the self-assembly of the flower-like micelles was investigated up to $C = 10$ g/L at the longest APPJ treatment time studied here ($t = 900$ s). The M_a of each sample was measured just after APPJ treatment and 24 h later (Figure 5.5 b). No time evolution of the plasma-treated samples was observed after 24 h. As previously reported [32], increasing the concentration leads to the formation of larger aggregates due to bridging of micelles. APPJ treatment led to a decrease of M_a whatever the initial tPEO concentration. This phenomenon could be attributed to the degradation of tPEO micellar aggregates whose number or aggregation number (*i.e.* number of polymeric chains per micelle) decreases with the plasma treatment. Yet, the hydrodynamic radius (R_{ha}) of the aggregates slightly increases after 15 min of APPJ treatment (Figure 5.5 c). The total amount of degraded material being almost constant whatever the initial concentration, the degradation effect due to plasma is very important at low polymer concentration but negligible at high concentration (Figure 5.5 d).

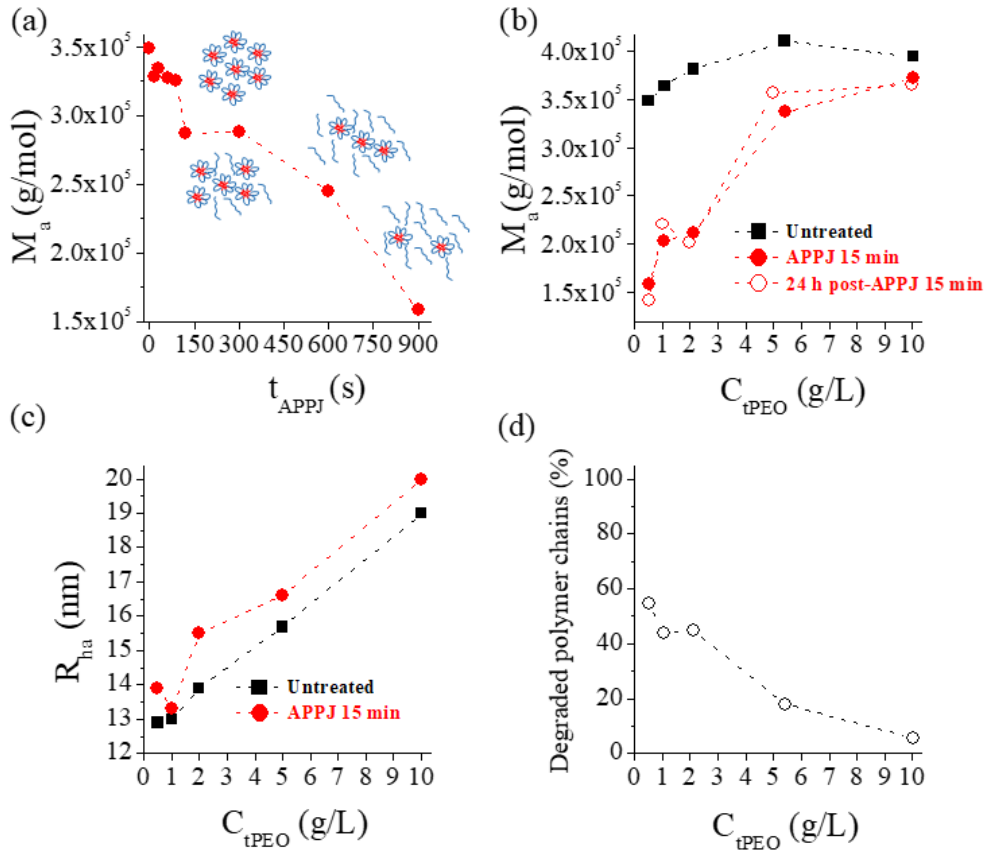

Figure 5.5: (a): Apparent molar mass (M_a) of tPEO at C = 0.5 g/L as a function of the APPJ treatment time. (b): M_a as a function of tPEO concentration before APPJ treatment (squares), after 15 min of APPJ (filled circles) and 24h later (empty circles). (c): Apparent hydrodynamic radius (R_{ha}) of the micelles as a function of tPEO concentration before APPJ treatment (squares) and after 15 min of APPJ (circles). (d): Percentage of the tPEO micellar aggregates degraded after 15 min of APPJ treatment as a function of the initial tPEO concentration.

The effects of APPJ on the properties of tPEO solutions were further investigated by rheology at concentrations were tPEO forms dynamic physical hydrogels [32]. The viscosity of the tPEO solution at C = 40 g/L (without photo-initiator system (PIS)) was evaluated at different APPJ treatment times (Figure 5.6 a). The untreated solution initially exhibited a Newtonian behavior up to a shear rate $\dot{\gamma}=100\ s^{-1}$ with a viscosity of η = 0.34 Pa.s. By increasing the APPJ treatment time, an increase of the viscosity was progressively observed.

As described earlier, there is an evaporation of 1 % /min in the tPEO solution due to the gas flow during APPJ treatment. Thus, the viscosity of a tPEO solution treated for 15 min was compared to an untreated tPEO solution at C = 47 g/L; concentration reached after 15 min of APPJ treatment. A slight decrease of the zero-shear viscosity of the APPJ-treated tPEO was observed compared to an untreated solution at 47 g/L. In parallel, the same comparison was made with tPEO solutions containing the PIS (Figure 5.6 b). A non-Newtonian fluid of high zero shear viscosity was obtained by treating the solution during 15 min by APPJ, in contrast to the untreated solutions at C = 40 g/L and C = 47 g/L.

Higher storage (G') and loss (G") moduli were obtained for the APPJ-treated solution compared to the untreated one (Figure 5.7 a). Moreover, at low frequency, the 15 min APPJ-treated sample tends to a very soft solid behavior (G' > G"). Figure 5.7 b represents the evolution of G' and G" during *in situ* photo-crosslinking of the hydrogel. After 30 s, samples were exposed to blue light during 3 min. Faster crosslinking and higher elastic modulus were observed for the APPJ-treated hydrogel. Figure 5.7 c shows the frequency dependence of the moduli for the photo-crosslinked hydrogels. Both untreated and APPJ-treated photo-cross-linked hydrogels exhibit a plateau for G'(ω) at low frequency indicating a soft solid behavior. However, the elastic modulus of the APPJ-treated hydrogel obtained after photo irradiation was twice as high as that of the untreated one indicating a higher extent of cross-linking. After APPJ treatment, photo-cross-linked hydrogels were more brittle than the untreated one as shown by their lower strain at breakage (Figure 5.7 d).

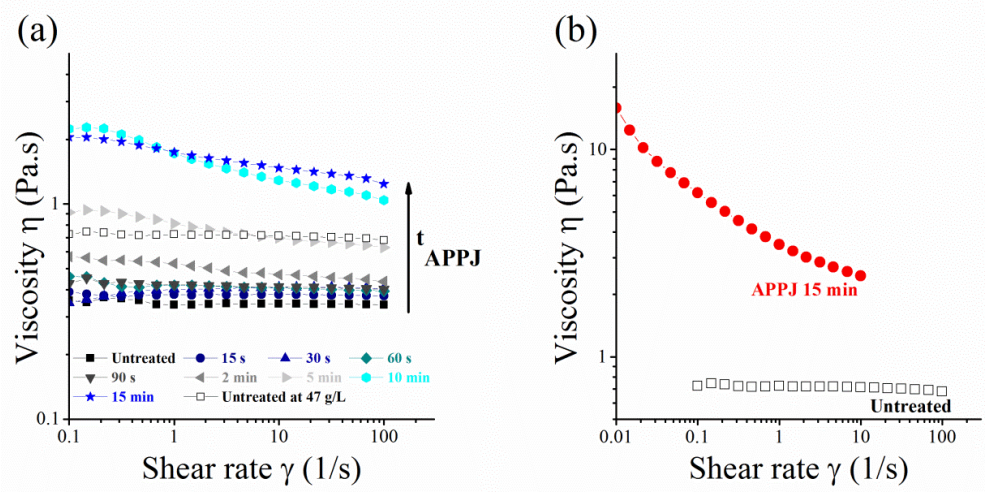

Figure 5.6: (a): Viscosity of tPEO solution at C = 40 g/L for different APPJ treatment times and an untreated at C = 47 g/L. (b) Viscosity of a 15 min APPJ-treated tPEO solution at C = 40 g/L (red dots) compared to untreated one at C = 47 g/L (empty black squares) in the presence of the PIS.

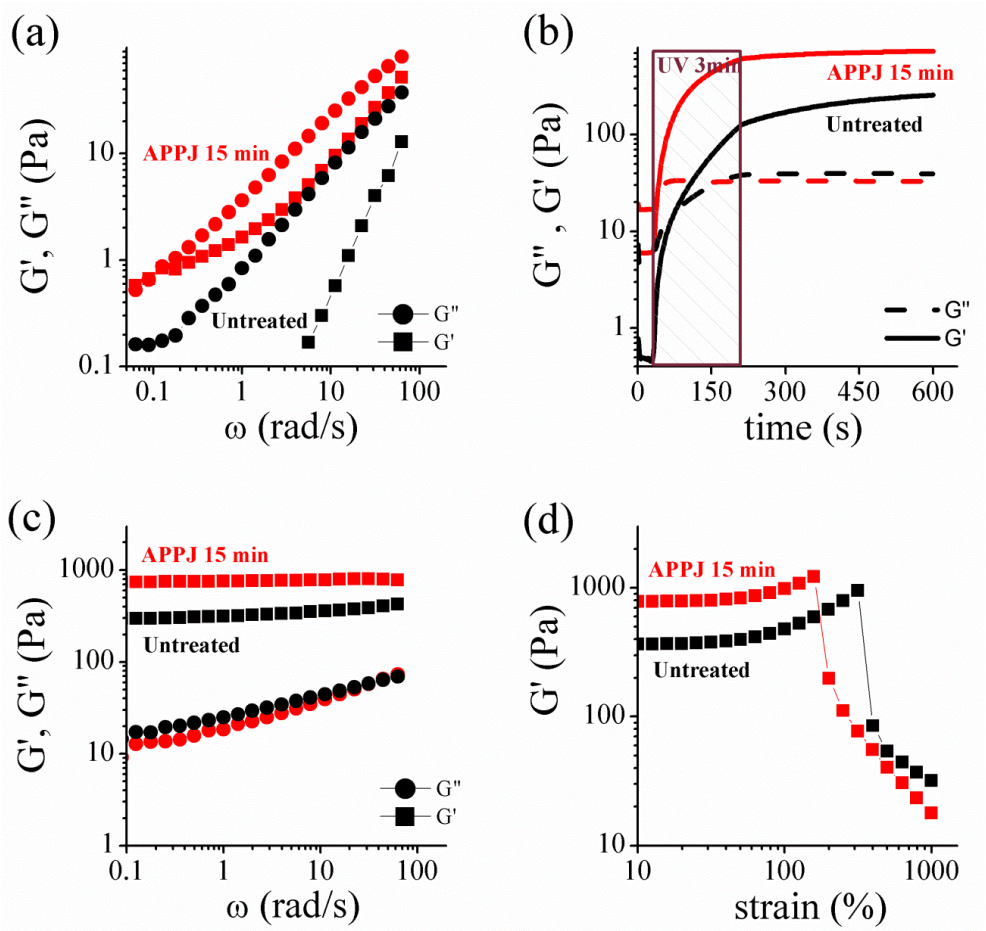

Figure 5.7: (a): Frequency dependence of the shear moduli of a 15 min APPJ-treated (red) and untreated tPEO at C = 47 g/L in the presence of the PIS (black). (b): Time evolution of the moduli of a 15 min APPJ-treated tPEO solution at C = 40 g/L (red) and an untreated tPEO solution at C = 47 g/L (black). Light irradiation was switched on after 30 s and stopped 3 min after (c): Frequency dependence of the shear moduli of a 15 min APPJ-treated tPEO hydrogel (red) compared to an untreated one (black) after photo-cross-linking. (d): Evolution of the storage modulus with strain for a 15 min APPJ-treated tPEO photo-cross-linked hydrogel at C = 40 g/L compared to an untreated one at C = 47 g/L (black).

To further investigate the structural changes in the structure of the tPEO, H^1 NMR experiments were performed at 2 g/L after 15 min of plasma treatment in D_2O (Figure 5.8).

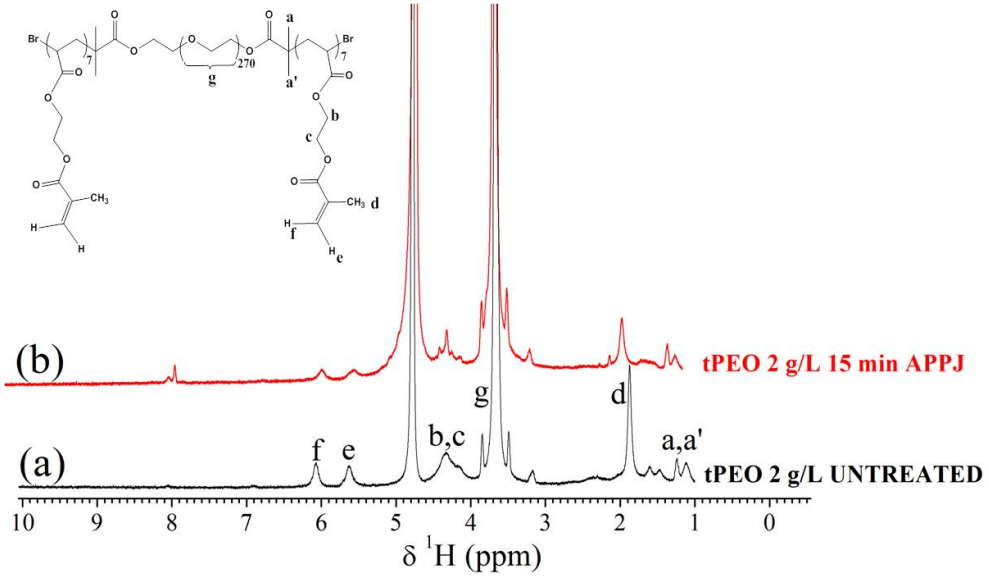

Figure 5.8: ^1H NMR spectra (400 MHz, in D_2O) of (a) untreated tPEO, (b) 15 min APPJ treated tPEO at 2 g/L in D_2O.

^1H NMR analysis shows degradation of some PEO chains and that the PMEA hydrophobic block is also affected by the plasma treatment. In fact, by setting the integration of the CH_2 peak of the PEO to 1080 (DP_n=270), it was observed that the integration of the characteristic signals of the PMEA block decrease by a factor of ~2. However, all the signals do not decrease at the same rate. The characteristic peaks of the methacrylate double bonds decrease more than the methyl signals (a, a') at 1.2 ppm. This indicates that plasma treatment also induces a cross-linking of the double bonds.

5.4.DISCUSSION

The effects of a He APPJ treatment were investigated here on tPEO solutions able to form hydrogels (Figure 5.2), with the aim of understanding the potential chemical and physical modifications of such kind of polymeric systems in solution.

The plasma gas chemistry of the APPJ employed here includes O• radicals, N_2 1st positive and N_2^+ 2nd negative and He, among other reactive species [43]. These species can react with the treated liquid (water, saline solutions or cell culture media) and after diffusion and cascade reactions they produce short-lived species able to recombine into chemically stable species, including nitrates, nitrites, hydrogen peroxides, among others; [44–49] [24], depending on the chemical composition of the treated-liquid [47,50,51]. Despite this, the effects of diffusion and reaction of these RONS in polymer chains in solution are a complex issue and largely unexplored.

The gas flow and distance to the solution employed here were selected according to previous works as they maximize the production of RONS in a liquid [52], and will thus allow to investigate any potential modifications in the polymer solution.

It is well established that evaporation occurs in liquids during plasma treatment. The evaporation depends on the plasma device employed and is mainly related to the gas flow which is directly applied on the surface of the liquid [53,54]. To confirm that, tPEO+PIS solutions were treated without plasma only using the He gas flow and a linear evaporation up to 9 % was recorded. This value is slightly below than that recorded after plasma treatment (about 15 %). It can therefore be assumed that the main contribution to evaporation is mainly due to the gas flow with an additional contribution derived from the plasma treatment itself. As there is very little heating of the polymer solution due to plasma treatment (only 4 ºC increase in 15 min plasma treatment was recorded), this is not a parameter expected to contribute significantly to evaporation. The linear increase of the evaporation observed in

Figure 5.4 a following plasma treatment was in agreement with observations in polymers dissolved in organic solvents for electrospinning applications [12,13].

It is well-known that the chemical composition of the plasma treated-liquids have a major impact on the generation of reactive species and therefore on its pH variations [54–56], most of the reported studies showing an acidification after plasma exposure [26,47,54,57–59]. This acidification has been widely described as being induced by the accumulation of the reactive species, especially NO_2^- and NO_3^- generated in solution from the APPJ. In the present chapter, pH of PBS, tPEO and PBS + PIS used for tPEO photo-crosslinking remained between 6.5 and 7.5 (Figure 5.4 b) and showed a very limited acidification. By avoiding the acidification of the solution, pH buffering prevents potential subsequent reactions of the two main species usually detected, H_2O_2 and NO_2^-, for example, to form peroxynitric acid (ONOOOH).

The effect of APPJ treatment on the self-assembly and rheological behaviour of tPEO solutions was investigated here by different techniques. The self-assembling colloidal nature of the selected polymer allowed using static (SLS) and dynamic (DLS) light scattering to quantify the evolution of size (R_{ha}) and apparent molar mass (M_a) of the amphiphilic tPEO self-assemblies in aqueous solution (Figure 5.5). On tPEO single micelle solutions (at C = 0.5 g/L), a decrease of the apparent molar mass with APPJ treatment time was observed. This decrease cannot be attributed to the solvent evaporation since concentrating the solution would lead to higher M_a. Two scenarios are thus possible: 1) The number of micelles remains constant but their molar mass decreases or 2) the average molar mass of the micelles remains constant but their number decreases. By analyzing the evolution of the micelles size (Figure 5.5 c), we observe that the size of the micelles has slightly increased after APPJ treatment. As the radius of star-like objects (including flower-like micelles) varies with the aggregation number (N_{agg}) as $R \sim N_{agg}^{1/5}$ [60], a decrease of N_{agg} should lead to a decrease of R_{ha}. So, it can be concluded that scenario 1 is not occurring. The conclusion is therefore that the micelles size is barely affected but the total number of micelles decreases by destruction of part of the block copolymer

chains under plasma treatment. The broken chains are not able to self-assemble anymore and remain as unimers in solution; their scattering intensity is thus negligible compared to the intensity scattered by the micelles. Simultaneously, part of the micelles reorganize to recover their equilibrium structure (with a constant N_{agg}) which barely depends on the concentration in diluted regime [32,41]. This observation can be done for all the tPEO concentrations studied. This scenario is illustrated in Figure 5.9.

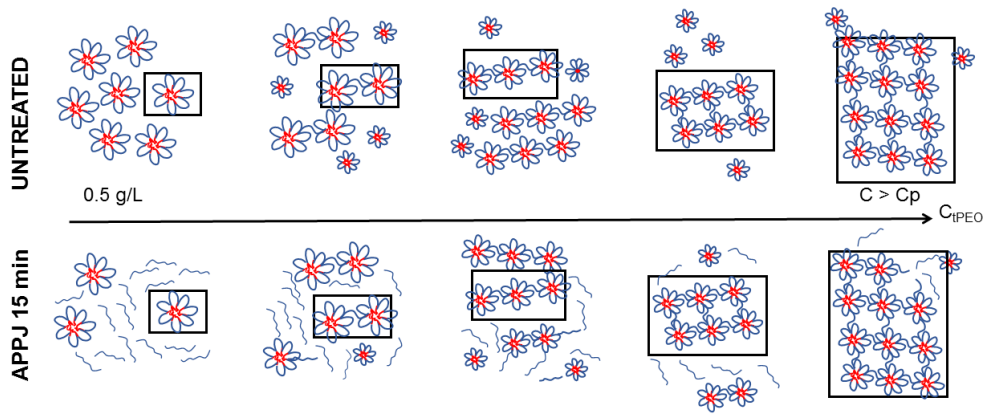

Figure 5.9: Schematic representation of the effect of concentration and plasma treatment on tPEO micellar solutions.

The slight increase of R_{ha} can be attributed to a partial covalent cross-linking of the micelles due to the reactive species or radicals generated by the plasma treatment. This observation is supported by H^1NMR where the decrease of the methacrylate peaks at δ = 5.6 and 6.1 ppm indicates a partial crosslinking of the PMEA group (Figure 5.8). This hypothesis was also confirmed by the rheological measurements made on concentrated tPEO solutions (Figure 5.7).

To produce photo-cross-linked hydrogels that can be handled, the polymer solution concentration must be far above the percolation concentration (Cp ≈ 20 g/L). A rheological study was thus made with a tPEO concentration of 40 g/L. A progressive increase of the tPEO solution viscosity was observed with increasing APPJ treatment time (Figure 5.6 a). Concomitantly, a non-Newtonian behavior appears from shear rates of 0.2-0.3 s^{-1}. As it was shown that water evaporation

occurred during the plasma treatment (Figure 5.4 a), the viscosity increase can partly be explained by the concentration of the tPEO solution. Anyhow, at the same time, the plasma treatment also degrades polymeric chains which are not able to self-assemble anymore and thus reduces the connectivity of the transient polymeric network. For instance, the hydrophilic PEO block might be slightly affected by APPJ treatment since the plasma-treated precursor alone shows some degradation of the main chains (only detectable at low concentration) (Figure S5.12) and a partial crosslinking (Figure S5.13 and Table S 5-1). Moreover, the signal appearing in APPJ-treated tPEO at $\delta = 8.15$ ppm that could be attributed to a small molecule such as formic acid [61] which could be derived from some potential reactions between the degraded tPEO and reactive species generated by APPJ in the polymer solution.

The chemical modifications of the PMEA hydrophobic block of the polymer by the plasma treatment (Figure 5.8), which lead to the irreversible cross-linking of a small fraction of the micellar aggregates, contribute to increase the viscosity of the solution. The evolution of the rheological behavior is thus a complex combination of these 3 factors: 1) solvent evaporation, 2) block copolymer chains degradation, 3) partial irreversible cross-linking. By comparing the rheological behaviour of the APPJ treated solution and a non-treated solution at C = 47 g/L (concentration reached after plasma treatment), it can be concluded that the irreversible cross-linking affects more the properties than polymeric chains degradation since the zero-shear viscosity of the APPJ-treated solution is higher than that of the tPEO solution at C = 47 g/L.

In the presence of PIS, APPJ-treated tPEO solution exhibits a non-Newtonian fluid behavior and a solid-like behavior appears at low frequency ($G' > G''$) (Figure 5.7 a and b). These results indicate that a very soft ($G' < 1$ Pa) and fragile hydrogel is formed by treating the polymeric solution by APPJ during 15 min. The hydrogel formed during this process is probably continuously broken by the shear applied to measure the viscosity which could explain the non-Newtonian behavior. It must be pointed out that the partial linkage of micellar aggregates induced by APPJ treatment in the absence of PIS does not lead to the formation of

soft hydrogel (Figure S5.11). The presence of the PIS in solution probably leads to the creation of higher amount of radicals in solution under APPJ treatment either because of the UV-VIS light emitted by the plasma or by the interaction between the plasma and the PIS. Nevertheless, the tPEO solution is still able to flow so it can potentially be injected. Furthermore, the photo-crosslinking is faster and more efficient indicating that the integrity of both the PIS and the polymeric micelles remain sufficiently high to allow for the formation of covalent hydrogels. As shown in Figure 5.7 c, this pre-cross-linking induced by APPJ treatment is beneficial to the material since the elastic modulus obtained after photo-cross-linking is twice as higher than that measured on untreated hydrogels after the same irradiation time. The counterpart to this higher extent of cross-linking is that the hydrogels formed are more fragile; they break at lower stretching rates (Figure 5.7 d). As the different applications of APPJ treated hydrogels investigated up to now [16,17,62] are not intended for load-bearing applications, this would not seem to be a restriction for future use.

5.5. CONCLUSION

The effects of atmospheric pressure plasma treatments of an amphiphilic poly (ethylene glycol)-based triblock copolymer solution were investigated here. In this chapter, plasma treatment led to the irreversible degradation of a small amount of the block copolymer chains, through their hydrophobic block. This treatment had a non-negligible effect on the self-assembled structures at low polymer concentrations but it only slightly modified the properties of the transient polymeric network at high concentration. In presence of a photo-initiating system, plasma treatment alone induced a slight cross-linking leading to a very weak and fragile hydrogel, which could be efficiently and rapidly covalently cross-linked under visible light irradiation. The pre-cross-linking induced by the plasma helped in enhancing mechanical properties than that obtained with untreated hydrogels. Overall, this chapter opens new perspectives for further applications in plasma-treated hydrogels for several biomedical applications.

REFERENCES

1. Canal, C.; Molina, R.; Bertran, E.; Erra, P. Wettability, ageing and recovery process of plasma-treated polyamide 6. *J. Adhes. Sci. Technol.* **2004**, *18*, 1077–1089.
2. Fridman, A. *Plasma Chemistry*; Press, C.U., Ed.; Cambridge.; New York, USA, 2008;
3. Stoffels, E.; Kieft, I.E.; Sladek, R.E.J.; Bedem, L.J.M. van den; Laan, E.P. van der; Steinbuch, M. Plasma needle for in vivo medical treatment: recent developments and perspectives. *Plasma Sources Sci. Technol.* **2006**, *15*, S169–S180.
4. Kolb, J.F.; Mohamed, A.-A.H.; Price, R.O.; Swanson, R.J.; Bowman, A.; Chiavarini, R.L.; Stacey, M.; Schoenbach, K.H. Cold atmospheric pressure air plasma jet for medical applications. *Appl. Phys. Lett.* **2008**, *92*, 241501.
5. Lu, X.; Xiong, Z.; Zhao, F.; Xian, Y.; Xiong, Q.; Gong, W.; Zou, C.; Jiang, Z.; Pan, Y. A simple atmospheric pressure room-temperature air plasma needle device for biomedical applications. *Appl. Phys. Lett.* **2009**, *95*, 181501.
6. Graves, D.B. Low temperature plasma biomedicine: A tutorial review. *Phys. Plasmas* **2014**, *21*, 080901.
7. Weltmann, K.-D.; Polak, M.; Masur, K.; von Woedtke, T.; Winter, J.; Reuter, S. Plasma Processes and Plasma Sources in Medicine. *Contrib. to Plasma Phys.* **2012**, *52*, 644–654.
8. Pankaj, S.K.; Keener, K.M. Cold plasma: background, applications and current trends. *Curr. Opin. Food Sci.* **2017**, *16*, 49–52.
9. Laroussi, M.; Lu, X. Room-temperature atmospheric pressure plasma plume for biomedical applications. *Appl. Phys. Lett.* **2005**, *87*, 113902.
10. Winter, J.; Brandenburg, R.; Weltmann, K.-D. Atmospheric pressure plasma jets: an overview of devices and new directions. *Plasma Sources Sci. Technol.* **2015**, *24*, 064001.
11. Tanaka, H.; Ishikawa, K.; Mizuno, M.; Toyokuni, S.; Kajiyama, H.; Kikkawa, F.; Metelmann, H.-R.; Hori, M. State of the art in medical applications using non-thermal atmospheric pressure plasma. *Rev. Mod. Plasma Phys.* **2017**, *1*, 3.
12. Grande, S.; Cools, P.; Asadian, M.; Van Guyse, J.; Onyshchenko, I.; Declercq, H.; Morent, R.; Hoogenboom, R.; De Geyter, N. Fabrication of PEOT/PBT Nanofibers by Atmospheric Pressure Plasma Jet Treatment of Electrospinning Solutions for Tissue Engineering. *Macromol. Biosci.* **2018**, 1800309.

13. Grande, S.; Van Guyse, J.; Nikiforov, A.Y.; Onyshchenko, I.; Asadian, M.; Morent, R.; Hoogenboom, R.; De Geyter, N. Atmospheric Pressure Plasma Jet Treatment of Poly-ε-caprolactone Polymer Solutions To Improve Electrospinning. *ACS Appl. Mater. Interfaces* **2017**, *9*, 33080–33090.
14. Shi, Q.; Vitchuli, N.; Nowak, J.; Lin, Z.; Guo, B.; Mccord, M.; Bourham, M.; Zhang, X. Atmospheric plasma treatment of pre-electrospinning polymer solution: A feasible method to improve electrospinnability. *J. Polym. Sci. Part B Polym. Phys.* **2011**, *49*, 115–122.
15. Szili, E.J.; Oh, J.-S.; Hong, S.-H.; Hatta, A.; Short, R.D. Probing the transport of plasma-generated RONS in an agarose target as surrogate for real tissue: dependency on time, distance and material composition. *J. Phys. D. Appl. Phys.* **2015**, *48*, 202001.
16. Szili, E.J.; Hong, S.H.; Oh, J.S.; Gaur, N.; Short, R.D. Tracking the Penetration of Plasma Reactive Species in Tissue Models. *Trends Biotechnol.* **2017**.
17. Oh, J.-S.; Szili, E.J.; Gaur, N.; Hong, S.-H.; Furuta, H.; Kurita, H.; Mizuno, A.; Hatta, A.; Short, R.D. How to assess the plasma delivery of RONS into tissue fluid and tissue. *J. Phys. D. Appl. Phys.* **2016**, *49*.
18. Metelmann, H.-R.; Seebauer, C.; Miller, V.; Fridman, A.; Bauer, G.; Graves, D.B.; Pouvesle, J.-M.; Rutkowski, R.; Schuster, M.; Bekeschus, S.; et al. Clinical Experience with Cold Plasma in the Treatment of Locally Advanced Head and Neck Cancer. *Clin. Plasma Med.* **2017**.
19. Weltmann, K.-D.; Polak, M.; Masur, K.; von Woedtke, T.; Winter, J.; Reuter, S. Plasma Processes and Plasma Sources in Medicine. *Contrib. to Plasma Phys.* **2012**, *52*, 644–654.
20. Weltmann, K.-D.; Kindel, E.; Brandenburg, R.; Meyer, C.; Bussiahn, R.; Wilke, C.; von Woedtke, T. Atmospheric Pressure Plasma Jet for Medical Therapy: Plasma Parameters and Risk Estimation. *Contrib. to Plasma Phys.* **2009**, *49*, 631–640.
21. Bauer, G.; Graves, D.B. Mechanisms of Selective Antitumor Action of Cold Atmospheric Plasma-Derived Reactive Oxygen and Nitrogen Species. *Plasma Process. Polym.* **2016**, *13*, 1157–1178.
22. Graves, D.B. Reactive Species from Cold Atmospheric Plasma: Implications for Cancer Therapy. *Plasma Process. Polym.* **2014**, *11*, 1120–1127.
23. Graves, D.B. Reactive Species from Cold Atmospheric Plasma: Implications for

Cancer Therapy. *Plasma Process. Polym.* **2014**, *11*, 1120–1127.

24. Khlyustova, A.; Labay, C.; Machala, Z.; Ginebra, M.-P.; Canal, C. Important parameters in plasma jets for the production of RONS in liquids for plasma medicine: A brief review. *Front. Chem. Sci. Eng.* **2019**, *13*, 238–252.
25. Tian, W.; Kushner, M.J. Atmospheric pressure dielectric barrier discharges interacting with liquid covered tissue. *J. Phys. D. Appl. Phys.* **2014**, *47*, 165201.
26. Bruggeman, P.J.; Kushner, M.J.; Locke, B.R.; Gardeniers, J.G.E.; Graham, W.G.; Graves, D.B.; Hofman-Caris, R.C.H.M.; Maric, D.; Reid, J.P.; Ceriani, E.; et al. Plasma–liquid interactions: a review and roadmap. *Plasma Sources Sci. Technol.* **2016**, *25*, 053002.
27. Lin, C.-C.; Anseth, K.S. PEG Hydrogels for the Controlled Release of Biomolecules in Regenerative Medicine. *Pharm. Res.* **2009**, *26*, 631–643.
28. Burdick, J.A.; Anseth, K.S. Photoencapsulation of osteoblasts in injectable RGD-modified PEG hydrogels for bone tissue engineering. *Biomaterials* **2002**, *23*, 4315–4323.
29. LeValley, P.J.; Tibbitt, M.W.; Noren, B.; Kharkar, P.; Kloxin, A.M.; Anseth, K.S.; Toner, M.; Oakey, J. Immunofunctional photodegradable poly(ethylene glycol) hydrogel surfaces for the capture and release of rare cells. *Colloids Surfaces B Biointerfaces* **2019**, *174*, 483–492.
30. Peppas, N.A.; Keys, K.B.; Torres-Lugo, M.; Lowman, A.M. Poly(ethylene glycol)-containing hydrogels in drug delivery. *J. Control. Release* **1999**, *62*, 81–87.
31. Colombo, P.; Bettini, R.; Peppas, N.A. Observation of swelling process and diffusion front position during swelling in hydroxypropyl methyl cellulose (HPMC) matrices containing a soluble drug. *J. Control. Release* **1999**, *61*, 83–91.
32. Kadam, V.; Nicolai, T.; Nicol, E.; Benyahia, L. Structure and Rheology of Self-Assembled Telechelic Associative Polymers in Aqueous Solution before and after Photo-Cross-Linking. *Macromolecules* **2011**, *44*, 8225–8232.
33. Chen, G.; Kawazoe, N.; Ito, Y. Photo-Crosslinkable Hydrogels for Tissue Engineering Applications. In *Photochemistry for Biomedical Applications*; Springer Singapore: Singapore, 2018; pp. 277–300.
34. Fairbanks, B.D.; Schwartz, M.P.; Bowman, C.N.; Anseth, K.S. Photoinitiated polymerization of PEG-diacrylate with lithium phenyl-2,4,6-trimethylbenzoylphosphinate: polymerization rate and cytocompatibility.

Biomaterials **2009**, *30*, 6702–6707.

35. Ifkovits, J.L.; Burdick, J.A. Review: Photopolymerizable and Degradable Biomaterials for Tissue Engineering Applications. *Tissue Eng.* **2007**, *13*, 2369–2385.
36. Killion, J.A.; Geever, L.M.; Devine, D.M.; Grehan, L.; Kennedy, J.E.; Higginbotham, C.L. Modulating the mechanical properties of photopolymerised polyethylene glycol–polypropylene glycol hydrogels for bone regeneration. *J. Mater. Sci.* **2012**, *47*, 6577–6585.
37. Klymenko, A.; Nicolai, T.; Chassenieux, C.; Colombani, O.; Nicol, E. Formation of porous hydrogels by self-assembly of photo-cross-linkable triblock copolymers in the presence of homopolymers. *Polymer (Guildf).* **2016**, *106*, 152–158.
38. Klymenko, A.; Nicolai, T.; Benyahia, L.; Chassenieux, C.; Colombani, O.; Nicol, E. Multiresponsive Hydrogels Formed by Interpenetrated Self-Assembled Polymer Networks. *Macromolecules* **2014**, *47*, 8386–8393.
39. Nicol, E.; Nicolai, T.; Zhao, J.; Narita, T. Photo-Cross-Linked Self-Assembled Poly(ethylene oxide)-Based Hydrogels Containing Hybrid Junctions with Dynamic and Permanent Cross-Links. *ACS Macro Lett.* **2018**, *7*, 683–687.
40. Argün, A.; Halgand, B.; Le Visage, C.; Guicheux, J.; Weiss, P.; Nicolai, T.; Nicol, E.. Dynamic/Covalent photo-cross-linkable microporous PEG hydrogels for 3D cell culture. *Prep.*
41. Kadam, V.S.; Nicol, E.; Gaillard, C. Synthesis of Flower-Like Poly(Ethylene Oxide) Based Macromolecular Architectures by Photo-Cross-Linking of Block Copolymers Self-Assemblies. *Macromolecules* **2012**, *45*, 410–419.
42. Zaplotnik, R.; Bišćan, M.; Kregar, Z.; Cvelbar, U.; Mozetič, M.; Milošević, S. Influence of a sample surface on single electrode atmospheric plasma jet parameters. *Spectrochim. Acta - Part B At. Spectrosc.* **2015**, *103–104*, 124–130.
43. Canal, C.; Fontelo, R.; Hamouda, I.; Guillem-Marti, J.; Cvelbar, U.; Ginebra, M.-P. Plasma-induced selectivity in bone cancer cells death. *Free Radic. Biol. Med.* **2017**, *110*.
44. Adachi, T.; Tanaka, H.; Nonomura, S.; Hara, H.; Kondo, S.I.; Hori, M. Plasma-activated medium induces A549 cell injury via a spiral apoptotic cascade involving the mitochondrial-nuclear network. *Free Radic. Biol. Med.* **2015**, *79*.
45. Mohades, S.; Laroussi, M.; Maruthamuthu, V. Moderate plasma activated media suppresses proliferation and migration of MDCK epithelial cells. *J. Phys. D. Appl.*

Phys. **2017**, *50*, 185205.

46. Yan, D.; Cui, H.; Zhu, W.; Talbot, A.; Zhang, L.G.; Sherman, J.H.; Keidar, M. The Strong Cell-based Hydrogen Peroxide Generation Triggered by Cold Atmospheric Plasma. *Sci. Rep.* **2017**, *7*, 10831.
47. Bruggeman, P.J.; Kushner, M.J.; Locke, B.R.; Gardeniers, J.G.E.; Graham, W.G.; Graves, D.B.; Hofman-Caris, R.C.H.M.; Maric, D.; Reid, J.P.; Ceriani, E.; et al. Plasma–liquid interactions: a review and roadmap. *Plasma Sources Sci. Technol.* **2016**, *25*, 053002.
48. Lin, A.; Gorbanev, Y.; De Backer, J.; Van Loenhout, J.; Van Boxem, W.; Lemière, F.; Cos, P.; Dewilde, S.; Smits, E.; Bogaerts, A. Non-Thermal Plasma as a Unique Delivery System of Short-Lived Reactive Oxygen and Nitrogen Species for Immunogenic Cell Death in Melanoma Cells. *Adv. Sci.* **2019**, *6*, 1802062.
49. Gorbanev, Y.; O'Connell, D.; Chechik, V. Non-Thermal Plasma in Contact with Water: The Origin of Species. *Chem. - A Eur. J.* **2016**, *22*.
50. Yan, D.; Cui, H.; Zhu, W.; Nourmohammadi, N.; Milberg, J.; Zhang, L.G.; Sherman, J.H.; Keidar, M. The Specific Vulnerabilities of Cancer Cells to the Cold Atmospheric Plasma-Stimulated Solutions. *Sci. Rep.* **2017**, *7*, 4479.
51. Norberg, S.A.; Tian, W.; Johnsen, E.; Kushner, M.J. Atmospheric pressure plasma jets interacting with liquid covered tissue: touching and not-touching the liquid. *J. Phys. D. Appl. Phys.* **2014**, *47*.
52. Tornin, J.; Mateu-Sanz, M.; Rodríguez, A.; Labay, C.; Rodríguez, R.; Canal, C. Pyruvate Plays a Main Role in the Antitumoral Selectivity of Cold Atmospheric Plasma in Osteosarcoma. *Sci. Rep.* **2019**, *9*.
53. Ikawa, S.; Kitano, K.; Hamaguchi, S. Effects of pH on Bacterial Inactivation in Aqueous Solutions due to Low-Temperature Atmospheric Pressure Plasma Application. *Plasma Process. Polym.* **2010**, *7*, 33–42.
54. Girard, F.; Badets, V.; Blanc, S.; Gazeli, K.; Marlin, L.; Authier, L.; Svarnas, P.; Sojic, N.; Clément, F.; Arbault, S. Formation of reactive nitrogen species including peroxynitrite in physiological buffer exposed to cold atmospheric plasma. *RSC Adv.* **2016**, *6*, 78457–78467.
55. Chauvin, J.; Judée, F.; Yousfi, M.; Vicendo, P.; Merbahi, N. Analysis of reactive oxygen and nitrogen species generated in three liquid media by low temperature helium plasma jet. *Sci. Rep.* **2017**, *7*, 4562.

56. Ikawa, S.; Kitano, K.; Hamaguchi, S. Effects of pH on Bacterial Inactivation in Aqueous Solutions due to Low-Temperature Atmospheric Pressure Plasma Application. *Plasma Process. Polym.* **2010**, *7*, 33–42.

57. Machala, Z.; Tarabova, B.; Hensel, K.; Spetlikova, E.; Sikurova, L.; Lukes, P. Formation of ROS and RNS in Water Electro-Sprayed through Transient Spark Discharge in Air and their Bactericidal Effects. *Plasma Process. Polym.* **2013**, *10*, 649–659.

58. Samukawa, S.; Hori, M.; Rauf, S.; Tachibana, K.; Bruggeman, P.; Kroesen, G.; Whitehead, J.C.; Murphy, A.B.; Gutsol, A.F.; Starikovskaia, S.; et al. The 2012 Plasma Roadmap. *J. Phys. D. Appl. Phys.* **2012**, *45*, 253001.

59. Adamovich, I.; Baalrud, S.D.; Bogaerts, A.; Bruggeman, P.J.; Cappelli, M.; Colombo, V.; Czarnetzki, U.; Ebert, U.; Eden, J.G.; Favia, P.; et al. The 2017 Plasma Roadmap: Low temperature plasma science and technology. *J. Phys. D. Appl. Phys.* **2017**, *50*, 323001.

60. Daoud, M.; Cotton, J.P. Star shaped polymers : a model for the conformation and its concentration dependence. *J. Phys.* **1982**, *43*, 531–538.

61. Yoshida, K.; Wakai, C.; Matubayasi, N.; Nakahara, M. NMR Spectroscopic Evidence for an Intermediate of Formic Acid in the Water−Gas−Shift Reaction. *J. Phys. Chem. A* **2004**, *108*, 7479–7482.

62. Endre, J.S.; James, W.B.; Robert, D.S. A â€˜tissue modelâ€™ to study the plasma delivery of reactive oxygen species. *J. Phys. D. Appl. Phys.* **2014**, *47*, 152002.

SUPPLEMENTARY INFORMATION - CHAPTER 5

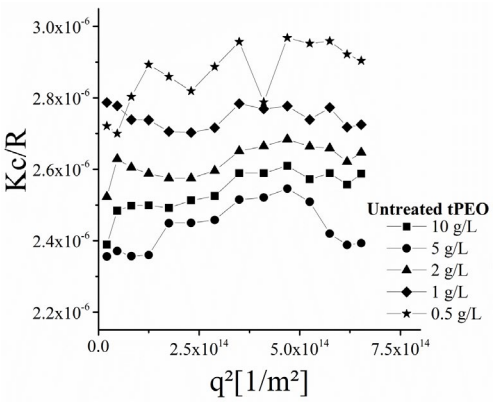

Figure S5.10: Angular dependence of the Kc/R ratio of the untreated tPEO solutions (concentrations indicated in the figure).

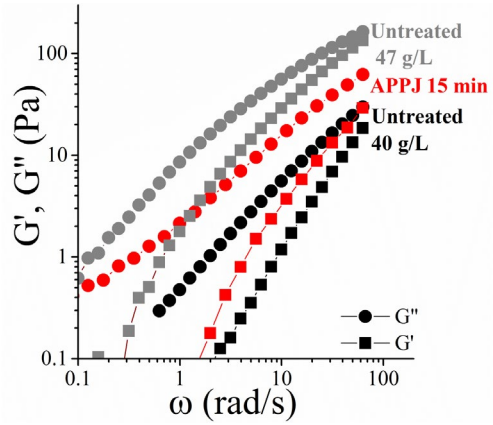

Figure S5.11: Storage (G') and Loss (G") modulus of untreated tPEO solutions at 40 g/L (black) and 47 g/L (gray) compared to a 15 min APPJ-treated tPEO solution (red).

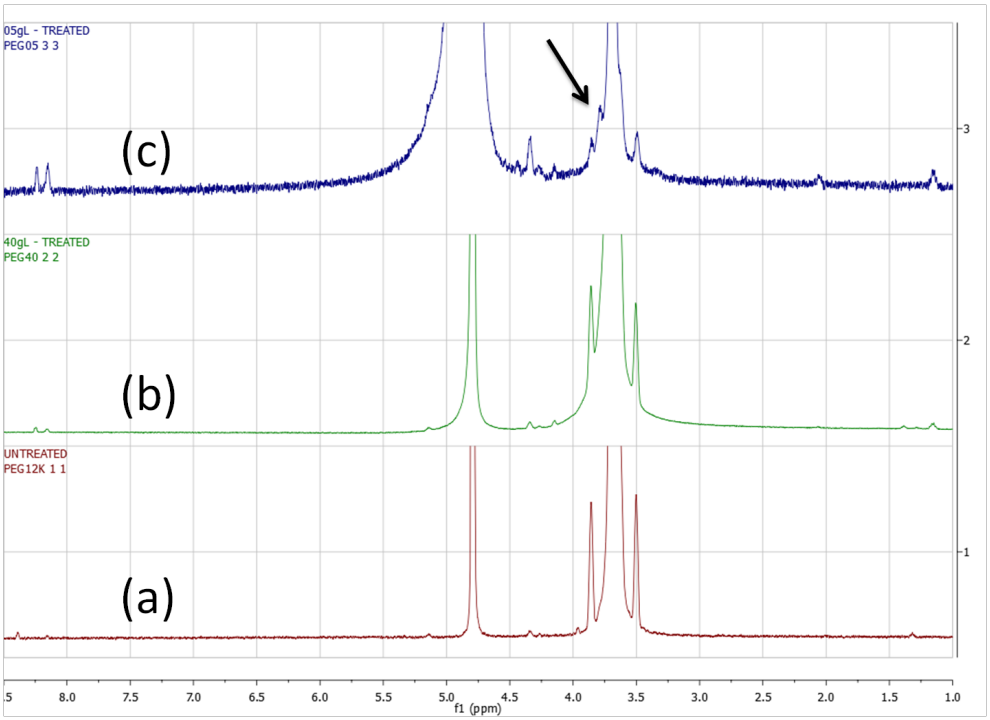

Figure S5.12: ^{1}H NMR spectra (400 MHz, in D_2O) of (a) untreated PEO_{12k}, (b) APPJ treated PEO_{12k} at 40 g/L and (c) APPJ treated PEO_{12k} at 0.5 g/L.

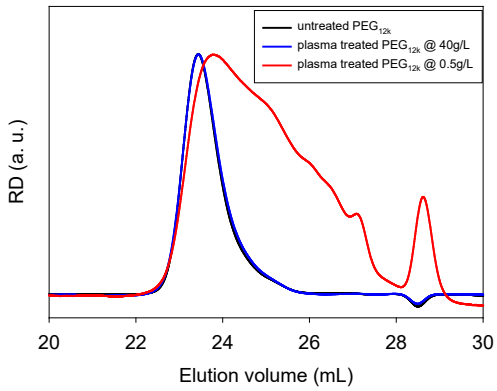

Figure S5.13: SEC traces in water of untreated PEO_{12k} (black), APPJ treated PEO_{12k} at 40 g/L (blue) and APPJ treated PEO_{12k} at 0.5 g/L (red).

Table S5-1: SEC analyses of untreated PEO_{12k} samples and 15 min APPJ treated.

Sample	M_n (g/mol)	M_w (g/mol)	Đ	insoluble fraction
Untreated PEO	11400	12800	1.12	0 %
PEO treated at 40 g/L	11900	13000	1.10	~1-2 %
PEO treated at 0.5 g/L	6200	10400	1.68	12 %

CONCLUSIONS

CONCLUSIONS

This PhD. Thesis has investigated the effects of atmospheric pressure plasma jet treatments in liquids and hydrogels for applications in bone cancer therapy and in general in the Plasma Medicine field. The main findings are summarized below:

- *Regarding the plasma treatment of liquids:*

- Two of the main reactive species generated from plasma jet sources (H_2O_2 and NO_2^-) were quantified in different liquid media (water, cell culture media and saline solutions). Higher concentrations of RONS were found in cell culture medium due to their complex composition, with **a plasma treatment time-dependent increase of H_2O_2 and NO_2^- concentrations** observed for all the liquids.

- Here, **cytotoxicity on cancer cell lines** has been established using SaOS-2 and MG63 cell lines. Cell survival decreased with the plasma treatment time, which is associated to the concentration of reactive species generated in the media following plasma treatment. Similar results were revealed both for direct or indirect plasma treatment. While direct plasma treatment of the cancer cell lines revealed a decrease of the cell viability down to 55 % for MG63 and 27 % for SaOS-2 for the longest plasma treatment time studied (1.5 min), indirect treatment of both cell lines with PCM revealed cell viability below 40 % after 72 hours by treating the cell culture media with plasma for 15 min.

- **Selectivity** was demonstrated towards bone cancer cell lines by comparing the biological effects on cancer cells with 2 healthy cell lines (hMSC & hOB). While cell viability of bone cancer cells decreased with the increase of plasma treatment time, either for direct or indirect treatment, healthy cell

lines maintained cell viability over 80 %, presenting including an enhanced cell proliferation in the case of direct treatment of hOBs. This opens a window of opportunity for a **minimally-invasive approach** for bone cancer therapy.

- *Regarding the plasma treatment of a natural polymer:*

- Higher production of H_2O_2 and NO_2^- was recorded in 0.5 % alginate solution than in plasma-treated water or Ringer's saline, and in general **kINPen achieved higher generation of RONS than the home-made APPJ,** in our experimental conditions. Despite the usual acidification of the plasma-treated liquid, **buffering effect** of the alginate was observed.

- **Most of the NO_2^- was released** from the plasma-treated alginate hydrogel to a release medium. Release percentages of H_2O_2 were lower and difficult to quantify, mainly due to the ageing that H_2O_2 is suffering in the release media.

- *In vitro* **crosslinking of the plasma-treated alginate solution** with a $CaCl_2$ solution associated washing away, and thus **an important loss of the generated RONS** into the polymer network. However, this will be avoided *in vivo* as alginate can crosslink with the Ca^{2+} available in the body.

- **Plasma-treated alginate** solution revealed a time-dependent **decrease of cell viability** in SaOS-2 cancer cells, with cytotoxicity around 40 % achieved at 72 hours for the longest plasma treatment time studied (3 min).

- *Plasma treatment of semi-synthetic polymer:*

- **GelMA solutions treated with kINPen showed** a linear increase of the H_2O_2 and NO_2^- concentration with high levels, in the range of 700 µM and 500 µM for H_2O_2 and NO_2^- , respectively, generated after 10 min of plasma treatment.

- The chemistry of GelMA determines the **stability of RONS in the solution;** In contrast to PBS where both H_2O_2 and NO_2^- are stable up to 72 h, H_2O_2 quickly degraded in GelMA solution within a time-lag of one hour at 37 °C while NO_2^- remained stable over time. This has been explained due to the reaction of H_2O_2 with the methacrylate end groups of GelMA**.** This reaction stops once the photo-crosslink is performed, and this seems to allow the entrapment a certain amount of reactive species within the GelMA hydrogel.

- The release of reactive species was performed from a plasma-treated photo-crosslinked GelMA hydrogel. **Fast release** of H_2O_2 and NO_2^- from plasma-treated GelMA hydrogels was obtained.

- **GelMA polymer backbone was not degraded by plasma treatment in solution** and the degree of substitution of GelMA employed was unaffected following plasma treatment, although the plasma treatment led to stiffer hydrogels.

- *Regarding the plasma treatment of synthetic polymer:*

- Fundamental investigations on the effects of the APPJ on flower-like micelles were carried through the tPOE triblock copolymer solution. Evaporation during the **plasma treatment led to increase the final polymer concentration,** up to 15 %.

- At low polymer concentration (< 2 g/L), tPOE polymer chains were degraded due to plasma treatment. An irreversible scission occurred between the hydrophobic (PMEA**)** and hydrophilic (POE) chains. **At high polymer concentrations, the 3D polymer network was not affected by plasma treatment and no chemical changes** were reported on the tPOE structure.

- **In the presence of the photo-initiator, a slight cross-linking of the tPOE network was induced following plasma treatment**, most likely due to the UV-radiation emitted during plasma treatment. The plasma-treated polymer solution remained injectable after plasma exposure.

- When applying photo-crosslink, **faster polymerization rates** were obtained for the plasma-treated tPOE than the untreated one due to the pre-crosslinking induced by plasma. Stiffer hydrogels with higher mechanical properties were obtained.

  - *Regarding the comparison between plasma-treated hydrogels and Plasma- conditioned liquids*

- In general, **higher amounts of RONS were generated in polymer solution with plasmas** than in biological liquids or water, with a clear dependency on the chemical composition of the polymer.

- While liquids (i.e saline solutions) commonly showed an acidification following plasma treatment, the **3 different polymer solutions studied allowed to maintain a neutral pH**, which is very interesting regarding their further integration in the design of plasma-treated hydrogel-based biomaterials.

- The use of biocompatible hydrogels opens great perspectives in the **design of hydrogel-based biomaterials aimed as RONS carrier**. Such approach aims to bring plasma-generated RONS to the diseased site, while **avoiding being washed away by the bloodstream,** that remains the main limitation for plasma-treated physiological liquids.

    - *Regarding the influence of the crosslinking process on the final loading of RONS inside the plasma-treated hydrogel*

- **Physical crosslinking** (employed for alginate) **of the polymer network revealed to be a limiting aspect regarding the final amount of RONS loaded into the polymer solution**, leading to a loss of the major part of the RONS generated by plasma during the crosslinking process in the release crosslinking media itself.

OUTCOMES DERIVED FROM THIS PHD. THESIS

PUBLICATIONS

1. Investigating the atmospheric pressure plasma jet modification of a photo-crosslinkable hydrogel, *Inès Hamouda, Cédric Labay, Maria-Pau Ginebra, Erwan Nicol, Cristina Canal,* **Polymer**, Vol. 192, **2020**, p. 122-308.

2. Production of reactive species on alginate hydrogels for cold atmospheric pressure plasma therapies, *Cédric Labay, Inès Hamouda, Francesco Tampieri, Maria Pau Ginebra, Cristina Canal,* **Scientific Reports**, Vol. 9, **2019**, p. 16160.

3. Liquids treated by atmospheric pressure plasma jet for bone cancer therapy, *Inès Hamouda, Jordi Guillem-Marti, Maria-Pau Ginebra, Cristina Canal,* **Biomecánica**, Vol. 25, **2017**, p. 7-15.

In preparation

1. Evolution in plasma treatment of polymers: Moving towards plasma medicine applications, *Inès Hamouda, Cédric Labay, Maria Pau Ginebra, Cristina Canal*, Submitted to **Progress in Polymer Science**

2. Selectivity of plasma jet treatment and of plasma-conditioned media on bone cancer cell lines, *Inès Hamouda, Cédric Labay, Maria-Pau Ginebra, Cristina Canal*, Submitted to **Applied Science**

3. Generation of reactive species from atmospheric pressure plasma jet in methacrylated gelatin hydrogel, *Inès Hamouda, Cédric Labay, Francesco Tampieri, Maria Pau Ginebra, Cristina Canal*, **In preparation**

CONFERENCES

1. I. Hamouda, C. Labay, M.P. Ginebra, E. Nicol, C. Canal. *Evaluation of a photo-crosslinked hydrogel as carrier of reactive species generated by plasma jets*, 6th International Workshop on Plasma for Cancer Treatment (IWPCT 2019), Antwerp (Belgium), April 1-3rd, **2019**. **Poster communication - Awarded**

2. I. Hamouda, C. Labay, M.P. Ginebra, C. Canal. *Modification of alginate based-hydrogel for therapeutical applications using cold atmospheric plasma,* 4th International Conference on Biomedical Polymers & Polymeric Biomaterials (ISBPPB 2018), Kraków (Poland), July 15-18th, **2018**. **Oral communication**

3. I. Hamouda, A. Gouhier, C. Labay, M.P Ginebra, C. Canal. *Generation of reactive species by plasma needle in different liquids,* 5th International Workshop on Plasma for Cancer Treatment (IWPCT 2018), Greifswald (Germany), March 20-21th, 2018. **Poster communication**

4. I. Hamouda, J. Guillem-Marti, M.P Ginebra, C. Canal. *Liquids treated by atmospheric pressure plasma jet for bone cancer therapy*. SIBB2017: XL Congreso de la Sociedad Iberica de Biomecanica y Biomateriales, Barcelona (Spain), November 10-11th, **2017**. **Oral Presentation – Awarded**

Awards

1. **Bob Baker Student Award** – for poster communication "*Evaluation of a photo-crosslinked hydrogel as carrier of reactive species generated by plasma jets"* in the 6th International Workshop on Plasma for Cancer Treatment (IWPCT) in Antwerp (Belgium), 2019.

2. **First prize** for the best oral presentation "*Liquids treated by atmospheric pressure plasma jet for bone cancer therapy"* in the SIBB2017: XL Congreso de la Sociedad Iberica de Biomecanica y Biomateriales in Barcelona (Spain), 2017.

Stage abroad

Internship from the 15th to the 30th of June 2018 at the IMMM – *Institut des Molécules et Matériaux du Mans* – at the Université du Mans, France.

PUBLICATIONS

4. Investigating the atmospheric pressure plasma jet modification of a photo-crosslinkable hydrogel, *Inès Hamouda, Cédric Labay, Maria-Pau Ginebra, Erwan Nicol, Cristina Canal,* **Polymer**, Vol. 192, **2020**, p. 122-308.

5. Production of reactive species on alginate hydrogels for cold atmospheric pressure plasma therapies, *Cédric Labay, Inès Hamouda, Francesco Tampieri, Maria Pau Ginebra, Cristina Canal,* **Scientific Reports**, Vol. 9, **2019**, p. 16160.

6. Liquids treated by atmospheric pressure plasma jet for bone cancer therapy, *Inès Hamouda, Jordi Guillem-Marti, Maria-Pau Ginebra, Cristina Canal,* **Biomecánica**, Vol. 25, **2017**, p. 7-15.

In preparation

4. Evolution in plasma treatment of polymers: Moving towards plasma medicine applications, *Inès Hamouda, Cédric Labay, Maria Pau Ginebra, Cristina Canal*, Submitted to **Progress in Polymer Science**

5. Selectivity of plasma jet treatment and of plasma-conditioned media on bone cancer cell lines, *Inès Hamouda, Cédric Labay, Maria-Pau Ginebra, Cristina Canal*, Submitted to **Applied Science**

6. Generation of reactive species from atmospheric pressure plasma jet in methacrylated gelatin hydrogel, *Inès Hamouda, Cédric Labay, Francesco Tampieri, Maria Pau Ginebra, Cristina Canal*, **In preparation**

CONFERENCES

5. I. Hamouda, C. Labay, M.P. Ginebra, E. Nicol, C. Canal. *Evaluation of a photo-crosslinked hydrogel as carrier of reactive species generated by plasma jets*, 6th International Workshop on Plasma for Cancer Treatment (IWPCT 2019), Antwerp (Belgium), April 1-3rd, **2019**. **Poster communication - Awarded**

6. I. Hamouda, C. Labay, M.P. Ginebra, C. Canal. *Modification of alginate based-hydrogel for therapeutical applications using cold atmospheric plasma,* 4th International Conference on Biomedical Polymers & Polymeric Biomaterials (ISBPPB 2018), Kraków (Poland), July 15-18th, **2018**. **Oral communication**

7. I. Hamouda, A. Gouhier, C. Labay, M.P Ginebra, C. Canal. *Generation of reactive species by plasma needle in different liquids,* 5th International Workshop on Plasma for Cancer Treatment (IWPCT 2018), Greifswald (Germany), March 20-21th, 2018. **Poster communication**

8. I. Hamouda, J. Guillem-Marti, M.P Ginebra, C. Canal. *Liquids treated by atmospheric pressure plasma jet for bone cancer therapy*. SIBB2017: XL Congreso de la Sociedad Iberica de Biomecanica y Biomateriales, Barcelona (Spain), November 10-11th, **2017**. **Oral Presentation – Awarded**

Awards

3. **Bob Baker Student Award** – for poster communication "*Evaluation of a photo-crosslinked hydrogel as carrier of reactive species generated by plasma jets"* in the 6th International Workshop on Plasma for Cancer Treatment (IWPCT) in Antwerp (Belgium), 2019.

4. **First prize** for the best oral presentation "*Liquids treated by atmospheric pressure plasma jet for bone cancer therapy"* in the SIBB2017: XL Congreso de la Sociedad Iberica de Biomecanica y Biomateriales in Barcelona (Spain), 2017.

Stage abroad

Internship from the 15th to the 30th of June 2018 at the IMMM – *Institut des Molécules et Matériaux du Mans* – at the Université du Mans, France.

LIST OF FIGURES

LIST OF FIGURES

LIST OF TABLES

LIST OF TABLES